Albert-Ludwigs-University, Freiburg

Master Thesis

Using a non-linear reservoir model to quantify the lateral outflow from a raised bog near Vancouver, Canada

Author:
Johannes Exler

Supervisors:
Prof. Dr. Markus Weiler (Albert-Ludwigs-University, Freiburg)
Prof. Dr. R.D. Moore (University of British Columbia)

July 2015

Declaration of Authorship

I, Johannes Exler, hereby declare the originality of this thesis. I confirm that the presented work is my own, that all work of others is quoted properly and that I have acknowledged all main sources of my help.

Date: _____ Signed: _____

ALBERT-LUDWIGS-UNIVERSITY, FREIBURG

Abstract

Faculty of Environment and Natural Resources
Chair of Hydrology

Master of Science

Using a non-linear reservoir model to quantify the lateral outflow from a raised bog near Vancouver, Canada

by Johannes Exler

This study investigates the runoff processes occurring in the lagg of Burns Bog, a raised bog in British Columbia, Canada, with an area of 3000 hectares. Field measurements were conducted between August 22 and December 10, 2014. Ground level was identified as important control on low and high water tables. During the end of the summer when the water table was at a mean of -90.5 cm below ground, seepage was the only observed runoff process. During the transition from October 12 to October 25, the water table rose at a mean rate of 4.4 $cm\ day^{-1}$. The mean water level after the transition was -20.6 cm below the soil surface. Lateral subsurface flow and pipeflow developed shortly after the transition and were, together with seepage, modeled by a non-linear reservoir approach, which included a threshold. Results suggest the initialization of lateral flow and pipeflow, when the water table is within -35 to -45 cm to the soil surface. The Nash-Sutcliffe-Efficiencies of the lateral flow model were always above 0.9, pipeflow showed less dependency on the water table with a Nash-Sutcliffe-Efficiency of only 0.38 and the seepage efficiency was negative at -0.21. During conditions with high water tables, this work identifies subsurface lateral flow as most dominant runoff process with relative contributions between 81-92.5% of total runoff. Pipeflow adds between 5-13% to the overall outflow and seepage contributes 2.5-6%. During dry conditions, however, seepage generates 100% of the drainage. A mixing model quantified the bog water portion in the drainage ditch to be 70-80%, when normal conditions are given.

Keywords: Raised bog, drainage ditch, lagg, lateral outflow, non-linear reservoir model, threshold

Abstract — German

Diese Arbeit befasst sich mit den auftretenden Abflussprozessen im Lagg des Burns Bog, in der kanadischen Provinz British Columbia. Das Hochmoor besitzt eine Fläche von 3000 Hektar. Die Feldmessungen wurden zwischen dem 22. August und 10. Dezember 2014 durchgeführt, wobei während der Untersuchung die Geländehöhe als wichtiger Einfluss- und Kontrollfaktor für den Grundwasserspiegel identifiziert wurde. Seepage war der einzige Abflussprozess, als am Sommerende der Wasserspiegel bei -90.5 cm unter der Bodenoberfläche lag. Nach der Übergangszeit vom 12. Oktober bis 25. Oktober, während dieser der Grundwasserspiegel mit einer mittleren Rate von 4,4 $cm\ Tag^{-1}$ stieg, lag die mittlere Grundwasserhöhe bei -20.6 cm unter der Bodenoberfläche. Kurz nach der Übergangsphase entwickelten sich lateraler Abfluss nahe der Bodenoberfläche, sowie Pipeflow. Ein nichtlineares Speichermodel wurde um einen Schwellenwert erweitert, um Seepage, lateralen Abfluss und Pipeflow zu modellieren. Laut der Modellergebnisse treten lateraler Abfluss und Pipeflow ab einer Wasserspiegelhöhe von -35 cm bis -45 cm unter der Bodenoberfläche auf. Der laterale Abfluss konnte mit Nash-Sutcliffe-Efficiencies von über 0,9 sehr gut dargestellt werden, wohingegen das Pipeflow-Model nur eine Nash-Sutcliffe-Efficiency von 0,38 aufweist; der Seepage-Prozess erreicht nur eine negative Efficiency von -0,21. Mit einem Anteil von 81-92,5% wurde lateraler Abfluss als dominanter Abflussprozess während Zeiträumen mit hohen Wasserspiegeln identifiziert. Pipeflow ist mit 5-13% ebenfalls wichtig, nur Seepage spielt mit 2,5-6% Abflussanteil eine untergeordnete Rolle. In Trockenzeiten wenn der Wasserspiegel niedrig genug ist, ist Seepage hingegen der einzig auftretende Prozess und generiert somit 100% des Abflusses. Ein einfaches Mischmodel ergab außerdem, dass während der nassen Jahreszeit der Anteil an Wasser aus dem Hochmoor im angrenzenden Graben zwischen 70-80% liegt, sofern normale Bedingungen gegeben sind.

Stichworte: Hochmoor, Drainagegraben, Lagg, Lateraler Ausfluss, Nichtlineares Speichermodell, Schwellenwert

Acknowledgements

First and foremost I would like to thank Professor Markus Weiler, Albert-Ludwigs-University Freiburg. Due to his advice and contacts I experienced an exchange year that actually changed my life. He put me in touch with Professor Dan Moore, University of British Columbia, my current co-supervisor and future Ph.D. advisor. I am very grateful for the mentorship by Professor Dan Moore, who was extraordinarily supportive throughout my stay at the University of British Columbia. I would like to thank the staff at Metro Vancouver, especially Markus Merkens, for logistical and financial support during my field campaign. Dr. Sarah Howie provided much appreciated expertise in the field, as well as essential parts of the field equipment. Rick Ketler was a great help when technical advice was required. Without the field great assistance of Caroline Chestnutt and Pascal Armborst, I would not have been able to accomplish all field measurements, thank you. Finally my gratitude goes to Katrin Schmid, Larissa Goh and Mike Zima for linguistic advice and assistance.

Contents

List of Figures

List of Tables

Abbreviations

a.s.l	**a**bove **s**ea **l**evel
EC	**E**lectrical **C**onductivity
nse	**N**ash-**S**utcliffe-**E**fficiency
mbe	**M**ean **B**ias **E**rror
mae	**M**ean **A**bsolute **E**rror
rmse	**R**oot **M**ean **S**quare **E**rror

Symbols

t	specific point in time	-
$x(t)$	observed water table	mm
$y(t)$	predicted water table	mm
$d(t)$	difference $x(t)$ and $y(t)$	mm
$C(t)$	linearly varying shift	mm
K	saturated hydraulic conductivity	ms^{-1}
r	inner radius of piezometer casing	m
R	outer radius of piezometer casing	m
L	screen length of piezometer	m
T_0	required time to recharge 37% of initial water level	s
Q	volumetric discharge	m^3s^{-1}, Ld^{-1}
A	cross-sectional area	m^2
δh	hydraulic head difference	m
δh	distance between head measurements	m
g	hydraulic gradient	-
$_t$	specific point in time	-
$_i$	specific well location	-
z_{gi}	ground elevation at location $_i$	cm
z_{si}	silt depth at location $_i$	cm
h_{it}	water level heigth at location $_i$, at time $_t$	cm
α_{it}	vertical separation water table and ground surface	cm
β_{it}	vertical separation water table and silt layer	cm
h	stratum index	-
$\bar{x}_h$	estimator of true stratum mean	-
x_{hi}	estimator of true value of ith unit in hth stratum	-

n_h	number of randomly selected units of stratum h	-
W_h	weight of stratum (relative size)	-
$\bar{x}_{st}$	unbiased estimator of true mean	-
S	storage (here water table)	cm
a	fitting parameter, slope	-
b	fitting parameter, curvature	-
c	fitting parameter, threshold	-
$frac_b$	fraction of bog water in ditch	-
$cond_d$	electrical conductivity ditch	[μS cm^{-1}]
$cond_b$	electrical conductivity bog	[μS cm^{-1}]
$cond_s$	electrical conductivity soil deposit	[μS cm^{-1}]

Chapter 1

Introduction

1.1 Background

1.1.1 General

According to Clymo [1984], about 2% of Earth's surface is covered by peatlands. It is estimated that the total area exceeds 400 million hectares and that the carbon storage adds up to between one third and one half of the world's carbon pool [Holden, 2005a]. In Canada, peatlands occupy around 12% of its surface, which is equally to approximately 1.1 million km^2 [NWWG, 1988]. Most Canadian peatlands developed after the Pleistocene glaciers retreated. In southern Canada, it took even longer for peatlands to establish, because of the dry and warm Altithermal period (8,000 to 6,000 years ago), which restricted peat formation further [Tarnocai et al., 2005]. Once suitable conditions took place, including evenly distributed precipitation throughout the year and a lower potential evapotranspiration than the annual total precipitation [Schouten, 2002], two major processes enabled bogs to develop, namely terrestrialization (the filling of shallow lakes) or paludification (the blanketing of adjacent ecosystems by bog vegetation expansion) [Whitfield et al., 2009]. Many raised bogs worldwide had been subject to man-made disturbance like peat mining and drainage. Without human intervention most disturbed bogs will not regenerate by themselves [Price et al., 2003]. The restoration of peatland includes the re-establishment of high water tables, which is done by ditch blocking in many cases [Armstrong et al., 2009]. The recolonization of the area with Sphagnum moss is also widely-used [Holden, 2005a]. In 2011, Wallage and Holden

[2011] found that ditch blocking does raise water tables to the desired level, but that this improvement does not necessarily come with the desired recreation of pre-drained hydrological processes.

Only recently peat hydrology experienced increased attention within the scientific community [Daniels et al., 2008]. It appears as if the majority of detailed research started out about 20 years ago, therefore yielding an increasing number of studies. Recently, researchers started to increasingly investigate the impact of peat drainage and other disturbance, in order to provide knowledge for management decisions regarding the restoration of peatlands [Holden, 2005a].

Basically there are two types of peatland. On the one hand bogs that are ombrotrophic (rain-fed) wetlands, therefore nutrient poor and on the other hand fens, which count as minerotrophic wetlands and dependent on groundwater with higher nutrient amounts [Holden, 2005a, Whitfield et al., 2009].

Anaerobic conditions cause an accumulation of organic material due to restricted decomposition [Hebda et al., 2000]. The organic mass causes low pH-values, especially in bogs, due to its ability to adsorb cations [Rydin and Jeglum, 2013]. This extreme environment is favored by Sphagnum vegetation, which spreads widely across peatlands [Whitfield et al., 2009] and counts as one of the most important indicators of a healthy wetland ecosystem.
Typically, peatlands consist of two distinctive layers, namely the upper acrotelm and lower catotelm. Ivanov [1948], who introduced this nomenclature to the scientific world, defined the acrotelm as an active peat layer with high hydraulic conductivity and fluctuating water table, opposed to the permanently saturated catotelm layer, which exhibits low hydraulic conductivities. This definition was complemented by Ingram [1983], who described the acrotelm also as space where peat-forming aerobic bacteria occur, along with other microorganisms and living plant structures. It is broadly agreed that the acrotelm-catotelm-boundary also marks the long-term mean lower water level, as stated for example by [Whitfield et al., 2009]. They also quantify the typical catotelm thickness to vary between 0.3 and 3 to 5 meters; the most commonly observed thickness of the acrotelm layer varies between 40 and 50 cm [Bragg, 2002, Daniels et al., 2008, Whitfield et al., 2006]

Two major features shape each peatland. Most of the research is focused on the center region, where the water table is shallow compared to the margins [Ingram, 1983]. This is caused by the fact that there was only fundamental understanding of the occurring hydrology within peatlands [Holden, 2005a]. For example, research took place in undisturbed bog centers where, in contrast to the lagg, no interfering processes from the surrounding land occur [Howie and van Meerveld, 2013]. The second major feature of all peatlands is the margin of these landscape elements. Predominantly used in connection with ombrotrophic, and therefore raised bogs, are the terms 'lagg' and 'rand'. The term lagg originates from the Swedish language and was first used by Osvald [1933], who used it to define the wet margin of a raised bog. Apart from the lagg there is the second sub feature of raised bog's margins, the rand. The rand is seen as the connecting element between the inner bog and the outer lagg, and therefore shows an outward-sloping shape, most of the time [Wheeler and SC, 1995]. Because of the separating purpose of the lagg, it acts as a transitional zone and thus performs as a critical buffer between differing hydrology and ecology [Whitfield et al., 2009]. Howie and van Meerveld [2011] define the lagg as follows:

> "Lagg: a transition zone at the margin of a (usually raised) bog receiving water from both the bog and surrounding mineral ground, characterized by fen or swamp vegetation, transitional water chemistry, and shallow peat of relatively low hydraulic conductivity; the lagg transition may be sharp or diffuse (depending on the topography), or may not be present as a distinct feature."
>
> [Howie and van Meerveld, 2011, p.614]

As a transitional zone, the lagg also exhibits a thinner acrotelm and catotelm [Levrel et al., 2009]. So far only little attention was given to the lagg zones in the scientific community [Holden, 2005a, Howie and van Meerveld, 2013, Hughes and Barber, 2003].

1.1.2 Lagg

It is not always easy to determine the exact location of lagg and rand, which is because they are influenced from both the bog and the surrounding land [Howie and van Meerveld, 2011] and therefore the transition is rather continuous than distinct [Bourbonniere, 2009]. Due to this variety there are several approaches to finding the boundaries of

mentioned areas [Howie and van Meerveld, 2011]. Due to the contrast in hydrochemistry, the two most common methods use hydrochemical parameters to define the transition zones. One popular parameter is the Ca:Mg ratio. If the the Ca:Mg ratio of the tested water is below the ratio of local precipitation, it is assumed to be bog water [Shotyk, 1996], if the ratio is higher the reason is thought to be the influence of minerotrophic water [Muller et al., 2006]. Others used the pH-value of water to evaluate its origin [Tahvanainen, 2004]. Often combined with the Ca:Mg ratio, Balfour and Banack [2000] used both methods to distinguish 3 types of water in Burns Bog (see Table 1.1).

TABLE 1.1: Three water types in Burns Bog as quantification of minerotrophic water impact from the surrounding lands [Balfour and Banack, 2000].

pH	Ca-Concentration $[mg\,L^{-1}]$	Water type
3.3 - 5.5	0 - 3	Bog water
4.5 - 6.0	3 - 10	Transition water
5.0 - 8.0	>10	Non-bog water

A third and simpler approach is the measurement of electrical conductivity (EC). Blackwell [1992] executed EC-measurements in an Irish bog. He found that EC increased with proximity to boundary ditches and with increasing depth.

As indicated in Figure 1.1 a sharp transition from bog to surrounding land occurs in upland regions, where there is a topographical gradient. The gradient also causes water to flow further into the bog, compared to situations with a gradual lagg. An important feature of both laggs are trees growing along the boundary. Little is known about the impact of trees at the margin. A study by Jutras et al. [2006] showed a significant increase of the water table in the bog's margin, when trees are removed, which also agrees with the findings of Emili and Price [2006]. Additionally, trees are believed to act as buffers for atmospheric deposition like mineral-rich dust, as is reported by Howie and van Meerveld [2012].

1.1.3 Lagg and vegetation

As shown in Figure 1.1 a dense tree population associated with a shrub understory feature the rand of a bog in most cases [Howie and van Meerveld, 2011, Rydin et al., 1999]. Due to this characteristic attribute, Howie et al. [2009a] suggest to use vegetation

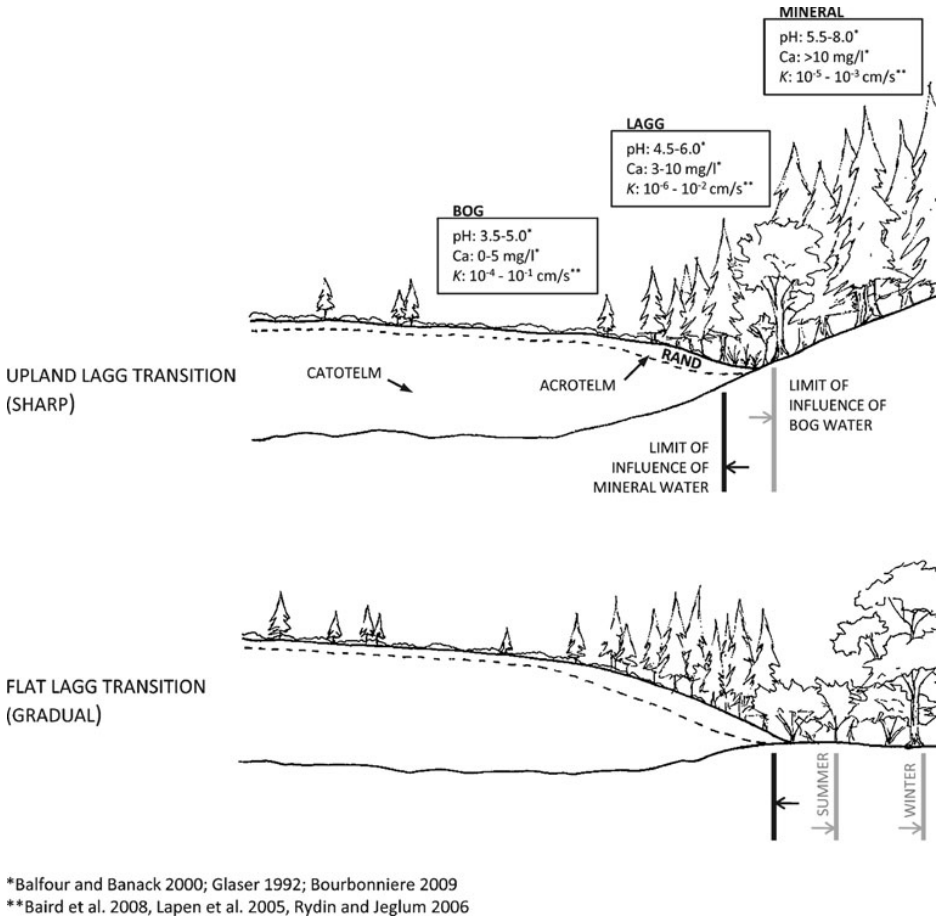

FIGURE 1.1: Schematic cross-sections of a lagg in an upland and flat region. Given parameters were obtained from several studies. [Howie and van Meerveld, 2011]

as lagg indicator, in cases where no detailed hydrochemical analyses are feasible. In contrast to the lagg, larger vegetation in the center of a bog is mostly absent, with only sparse dwarfed coniferous trees (also indicated in Figure 1.1) [Freléchoux et al., 2000, Rydin et al., 1999].

The hydrology of the lagg is governed by higher water table fluctuations which come along with a quick response on precipitation events [Keough and RW, 1984, Malmer, 1986]. Water table fluctuations also affect better aerated peat in the lagg zone [Økland et al., 2001]. The generally lower water table enables the growth of trees, as mentioned above [Howie and van Meerveld, 2011]. Damman [1986] reports not only a lower water table towards the margins of a bog but in some situations also water tables that reach the surface again, which is caused by a lower hydraulic conductivity of the lagg [Lapen et al., 2005].

In conclusion Howie and van Meerveld [2011] state the two key functions of a lagg to be firstly to maintain a high water table in order to conserve the water mount in the bog center and secondly to enable water surplus (e.g.due to rain storms) to exit the bog, if needed. Whitfield et al. [2009] call for additional research to better understand the role of the lagg as boundary and to be able to account for the special hydrological characteristics of it in models.

1.2 Water table

The water table is one of the key variables in a peatland ecosystem, not only because it controls the rate of decomposition as well as the depth at which decomposing bacteria can live in the long term, but also because the types of runoff processes are closely related to the water table height, as was reported by Daniels et al. [2008]. They found, when investigating the hydrology of an ombrotrophic blanket peat bog near Manchester, England, that the antecedent water table is the key control on runoff percentage and the timing when peak runoff occurs.

In most undisturbed peatlands the water table fluctuates within the upper most 40 to 50 cm of the soil throughout the year. For example Holden [2005a], who executed almost all his research in the Northern Pennines, England, a region which provides wide areas of undisturbed blanket peat with a hilly topography, observed the water table 80% of the time at or above 40 cm of the soil surface. During a study of Evans et al. [1999], the water table remained within 5 cm of the soil surface and Daniels et al. [2008] even found the water table ponding up to 5 cm above the soil surface during wet periods.

Emili and Price [2006] did research on hypermaritime forest peatland complexes in western British Columbia, Canada. They focused on the processes causing water redistribution and found a threshold effect when the water table rose during rain events. Significant runoff occurred when the water table reached 5-15 cm below the soil surface, which coincides with numerous other studies, for example Evans et al. [1999], who suggest that the runoff generation is mainly related to high water tables, also because they never observed high discharges correlating with low water tables.
A peatland's water table undergoes a yearly recurring evolution. It is termed 'hydroperiod' and can be, due to its periodicity, predicted [Rydin and Jeglum, 2013]. In Burns

Bog, British Columbia, Canada, for example, the water table is at its highest and most stable during the wet period, which is between October and March. Due to lower precipitation and an increasing evapotranspiration the water table declines from April onwards until September, when it rapidly recharges by reason of increased precipitation [Balfour and Banack, 2000, Golinksi, 2004, Howie et al., 2009b]. Thus if a framework on the behavior of the water table is required, it may be sufficient to measure during the periods of significant change, which is the transition from dry to wet season, as well as the transition in spring [Howie and van Meerveld, 2012].

1.2.1 Water table and lagg

As stated before, the lagg and thus the water table at the lagg of bogs did not receive much attention of the scientific community, yet. Howie and van Meerveld [2012] investigated, among other things, the variation of water tables in three raised bogs along the coast of British Columbia, Canada. As part of their water table investigation, they measured the height of it along transects cutting from the inner bog through the lagg into the surrounding land. One of their findings is the change in water table behavior according to location. During June and December 2011 the observed water table change referenced to the soil surface was as presented in Table 1.2:

Table 1.2: Observed water table depths along lagg cross-sections in three raised bogs in coastal British Columbia, [Howie and van Meerveld, 2012]

Location	Water table depth [cm]
Bog	26 - 42
Transition	33 - 66
Lagg	45 - 72
Surroundings	41 - 79

The values indicate a clear decrease of water table height towards the margins of the bogs as well as a change in water table fluctuation between bog center and margins. Combined with other results Howie and van Meerveld [2012] conclude, that one key factor controlling the water table is the morphology of the lagg.

1.2.2 Water table and vegetation

One feature of a healthy lagg is the growth of more mature vegetation than Sphagnum moss and dwarf tree vegetation, which represents the main vegetation in the center of most raised bogs and peatlands [Hebda et al., 2000]. Kopp et al. [2013] used MODFLOW to model the groundwater flow in the Mer Bleue bog in eastern Ontario, Canada between August and October 2008. During their study of what is thought to be a mainly undisturbed bog site and an adjacent forested site, they observed water tables between 7-15 cm and 24-43 cm at the bog and forested site, respectively. Other studies, for example Fay and Lavoie [2009] agree with these observations by reporting lower water tables as results of afforestation, which increases interception and evapotranspiration losses. Anderson et al. [2000] found a significant decline of 7 cm on average after two years of afforestation of a blanked bog and Jeglum et al. [2003] as well as Roy et al. [2000] report the opposite response after tree removal, which is normally referred to as 'watering-up'.

1.2.3 Water table and drainage

Several studies showed the impact of drainage on the water table. For example Hobbs [1986], Holden et al. [2004], Price et al. [2003], report of drainage in order to facilitate peat harvesting operations and the consequent changes, including compression and oxidation which affected hydraulic conductivity and a reduced water storage capability, as well as irreversible changes in the peat structure, in some cases. Daniels et al. [2008] investigated the hydrology of erosional and therefore accumulated acrotelm at gulley edges and found that during periods of low precipitation the water table can decline up to 80 cm below the soil surface, which was caused by the high connectivity of the accumulated erosional acrotelm. Similar drawdowns are reported by Price [2003], who did research at three sites in Quebec, Canada, to evaluate the differences between an undisturbed and two cutover sites, which were abandoned for two and seven years, respectively. The measured water tables varied between 40 cm at the undisturbed site, 50 cm at the cutover site, which was abandoned for two years and 68 cm depth for the remaining site. In 2011, Wallage and Holden [2011] published a paper on drained peat in which they compare the hydraulic conductivity and near-surface flow of three adjacent hill slopes, to investigate the difference in processes of an undisturbed, drained and restored site.

They found that water tables of the restored and undisturbed sites were significantly higher compared to the drained site, with the restored site exhibiting the highest water levels. Nevertheless, only at the undisturbed site the water table reached the soil surface at 18% of the time, whereas both other sites only experienced full saturation during 2% of the measurement period, therefore showing that the hydrology of restored sites does not simply return to the pre-disturbed behavior.
The range in which drainage occurred and consequently impacted the water table, was reported to vary between 15 m [Roy et al., 2000] and 20 m of a ditch [Price et al., 2003]. Hebda et al. [2000] approximated water table drawdown as far as 100 m distant from the closest ditch, but noted that this estimates referred to well-connected areas with high hydraulic conductivity.

1.3 Runoff processes

It was not until the early 2000s that the interest of the scientific community was raised and research was launched, in order to get a better understanding of the already observed runoff processes in peatlands. The following pages will give a profound overview of the current knowledge regarding these processes. During the last years, especially Professor Joseph Holden from the University of Leeds published a number of papers on runoff production in blanket peats and the associated processes. Since the research sites of his studies lie, as mentioned before, within a hilly blanket peat region, the results are mostly obtained from sites with a considerable topographic gradient.

Holden and Burt [2003a] stated that the acrotelm-catotelm model is a good and simple, approach to investigate runoff behavior and that it is well applicable for raised mires, since they pose as simpler systems compared to blanket mires. Nevertheless, it ignores important features of runoff generation, which is why it has to be established in greater detail.

Already Burt [1992] identified the following 5 potential runoff generating processes for peat catchments, without providing further, more detailed insight on their generation and behavior:

1) Infiltration-excess overland flow,

2) Saturation-excess overland flow,

3) Acrotelm flow as a result of perculation excess at the acrotelm- saturated catotelm boundary,

4) Acrotelm flow as a result of perculation excess at the acrotelm- unsaturated catotelm boundary,

5) Pipeflow

Taking these five potential processes Holden and Burt [2003a] studied their relevance and came to the conclusion that these processes cannot be thought of as separated phenomena. Instead they need to be thought of as well connected, so that surface water may infiltrate at some point and exit the system as macropore or matrix flow, for example.

1.3.1 Saturation-excess overland flow

Evans et al. [1999] used catchment scale runoff data together with water table monitoring information to investigate the importance of infiltration-excess as well as perculation-excess overland flow in relation to saturation-excess overland flow. High stream flows always occurred when water tables were high, thus suggesting that saturation-excess overland flow is the mechanism generating most of the runoff. Detailed knowledge of the infiltration behavior was not received, so that the role of subsurface flow near the surface remained unclear. In 2003, Holden and Burt [2003a,c], published studies in which they investigated the runoff production on the plot, hill slope and catchment scale. The results agree with the previously reported relevance of saturation-excess overland flow. Infiltration experiments helped to identify shallow sub-surface flow within the acrotelm as second dominating runoff process. During their study about 80% of the runoff was produced due to saturation-excess. Since overland flow develops during high flows, it is also the mechanism that generates most of the total runoff in absolute numbers. Topography and preferential flow paths seem to be important controls on the spatial distribution of runoff. Because the catotelm was always saturated when high stream flows appeared, percolation-excess as reason for overland flow was ruled out. In conclusion, saturation-excess overland flow is the most important runoff in undisturbed

peatlands and, as a consequence, water table depth must be an extraordinarily important control on the overall runoff behavior of a peatland catchments.

1.3.2 Subsurface flow

Several studies (e.g. [Evans et al., 1999, Holden, 2005b, Holden and Burt, 2002a, 2003c, Holden et al., 2001]) describe the runoff production of saturation-excess overland flow along with near-surface flow as the two dominant processes, caused by the saturation of the catotelm layer. As for the previously described runoff process, topography and preferential flow control the spatial appearance of subsurface flow [Holden and Burt, 2003a]. Trough measurements executed by Holden and Burt [2003c], show a strong subsurface runoff decrease with depth. During their study the runoff was categorized as presented in Table 1.3:

TABLE 1.3: The runoff fraction is categorized into soil depth classes. The important role of overland flow in comparison to sub-surface flow is evident. Predominant subsurface flow occurs only within the uppermost soil depth., [Holden and Burt, 2003c]

Depth [cm]	Runoff fraction [%]
<0	81.5
0 - 5	17.7
5 - 10	0.7
>10	0.1

During the measurements they observed that these 17.7% provide the greater part of runoff during low flow conditions, opposing to the overland flow, which dominates peak runoff periods.

Using a tension infiltrometer, Holden [2009] measured 80% of the infiltrating water at the soil surface to move through only 0.26% of the peat mass, at 5 cm depth the perculation rate was an order of magnitude lower; 85% moved through 0.01% of the peat volume, therefore strongly emphasizing the role of macropore flow for infiltration and perculation. Only 22% of the flow in the upper 20 cm of the soil occurred in pores with a diameter of less than 0.25 mm, thus suggesting that 78% move through macropores. Similar findings are presented in Baird [1997], who quantified the macropore flow portion to be about 64%. When Baird [1997] and Holden et al. [2001] quantified the macropore flow portion

in relation to the total runoff, both studies found that macropore flow still accounts for over 30% of total runoff.

The difference of water movement within the upper soil at three hill slopes (undisturbed, drained and restored) was later investigated by Wallage and Holden [2011]. The data shows higher flows at the restored site compared to the undisturbed and drained site. They concluded that the restored water table must enable water to move more quickly through micropores, which is interesting, firstly because Holden [2009] found that only 22% of near surface flow occurs in pores with smaller diameters than 0.25 mm and secondly, because it contrasts with laboratory experiments by Holden and Burt [2002b], who found developed macropores due to drought and the resulting shrinkage.

As a summary it is important to recognize the strong decrease in depth, especially since it was shown that there are already drastic differences within the acrotelm and the important role of macropores for runoff generation.

1.3.3 Pipeflow

Pipeflow is a phenomenon which was disregarded for a long time in peatland hydrology [Holden and Burt, 2003a]. Soil pipes are considered to have diameters of at least 1 cm [Holden, 2009]. Some authors distinct pipe behavior between ephemeral and perennial, but Holden and Burt [2002a] state that this distinction could be misleading. According to Holden [2005a] soil pipes greater than 10 cm were surveyed in 160 peatlands in the UK by means of ground penetrating radar. Artificially drained peat showed twice as many soil pipes [Holden, 2005b], caused by desiccation. Ultimately this leads to shrinkage of the peat mass and, due to the altered soil structure, to better connected and larger pipe networks. It was observed by Holden and Burt [2002a] that soil pipes and macropores acted as the only runoff producing features within deep peat, which agrees with Blodau and Moore [2002], who recovered 20-50% of a tracer at depths, which would not be reached by water without preferential flow paths like soil pipes. They seem to be well connected to the acrotelm and contribute substantially to baseflow, which is also caused by the prolonged runoff recession limb. Additionally it was found by Cunliffe et al. [2013], that the hydraulic conductivity around the pipes was significantly higher compared to the surrounding peat matrix, therefore favoring percolation into the pipes. The runoff proportion is estimated to be around 10%, with up to 30% at times. Mean

pipe diameters varied between 3-17 cm in the study by Holden and Burt [2002a] and lengths of up to 150 m were observed.

1.3.4 Seepage

Seepage in general is closely dependent on hydraulic conductivity, which is very low for catotelm peat matrix, as will be shown later in this work. Damman [1986] states that seepage makes up for only 1% of the discharge from an ombrotrophic bog in western Newfoundland. A study by Evans et al. [1999] revealed only sparse baseflow from peat covered catchments, which agrees with Holden and Burt [2003c], who conclude that flow through peat matrix is unimportant. Nevertheless, Bragg [2002] describes seepage as conserving process of year-round baseflow, due to the permanent saturation of the catotelm. An established MODFLOW model for a bog in Ontario, Canada simulated horizontal groundwater flow (therefore excluding shallow subsurface flow) into a drainage ditch and yielded values between 2.2 $L\,m^{-2}\,d^{-1}$ and 4.0 $L\,m^{-2}\,d^{-1}$ [Kopp et al., 2013].

1.4 Saturated hydraulic conductivity

As described by Darcy's Law, hydraulic conductivity has a direct impact on groundwater movement and therefore is one of the key aspects in soil hydrology. As will be presented next, hydraulic conductivity in peatlands poses some specific difficulties, which do not necessarily exist in rigid soils.

As already observed by Ivanov [1948] there are basically 2 layers in peatlands, the upper acrotelm with high hydraulic conductivities and the lower catotelm with low hydraulic conductivities. Over the years, many studies reported conductivity measurements, Table 1.4 gives a selective overview of the most common hydraulic conductivities.

Holden and Burt [2003b] found no significant change of catotelm hydraulic conductivity between 10 to 80 cm soil depth during a study in blanket peat, but emphasized the importance of hillslope- and catchment-scale variability. Such variability was also found by Bromley et al. [2004]. The comparison of compressible versus rigid soil theory applied to hydraulic conductivity measurements suggests that a false application of rigid soil

TABLE 1.4: Typical saturated hydraulic conductivities from other studies. The values show the considerable difference between the acrotelm and catotelm.

Hydraulic Conductivity $[m\ s^{-1}]$	Study
10^{-4}	Acrotelm boreal flat fen Norway Kværner and Kløve [2008]
10^{-3} - 10^{-4}	Undecomposed sphagnum selection of several works Letts et al. [2000]
10^{-9}	Catotelm blanket peat UK Holden and Burt [2003c]
10^{-8} - 10^{-9}	Organic soil forest-peatland Canada Emili and Price [2006]
10^{-6} - 10^{-8}	Catotem ombrothrophic bog Ontario Canada Fraser et al. [2001]
10^{-8} - 10^{-9}	Catotelm ombrothrophic bog Ontario Canada Kopp et al. [2013]

theory leads to an overestimation of hydraulic conductivities in peatlands [Holden and Burt, 2003b]. Contrasting the findings in Holden and Burt [2003b], Holden [2009] found a rapid decrease of hydraulic conductivity, when executing infiltration measurements at various soil depths.

Many studies used piezometers to quantify the hydraulic conductivity in peatlands. Bromley et al. [2004] investigated the scale dependency of hydraulic conductivity measurements in a raised mire in the UK. They found that hydraulic conductivities received from piezometers are only valid locally and that conductivities at larger scales (e.g. hundreds of meters) as used in many models are much higher, which they attribute to matrix inconsistencies like preferential flow paths in soil pipes or macropores.

Large scale variability of hydraulic conductivity as already described is also reported in Baird et al. [2008] and Howie and van Meerveld [2011]. Both studies found evidence of lower hydraulic conductivities in the lagg region, which may help, according to Baird et al. [2008], to conserve high water tables in the bog center.

A study to investigate anisotropy of hydraulic conductivity within peat was launched by Beckwith et al. [2003]. They used a new laboratory method to process 400 samples from Thorne Moor, UK. The larger part of samples exhibited much greater horizontal than vertical hydraulic conductivity at each depth, and therefore displayed anisotropy. As Holden [2009], they found decreasing hydraulic conductivity with depth, but a depth dependency of anisotropy was only found in less than half of the samples. Nevertheless, evident anisotropy 70 cm below the soil surface leads the authors to suggest predominantly horizontal flow in such depths. The calculated mean anisotropy is 0.55. Price [2003] conducted a study on the impact of peat deformation, mainly investigating volume changes at three sites that occur due to water table changes, often referred to as

'mire breathing'. Hydraulic conductivity measurement changes due to deformation were greatest at a depth of 75 cm and lowest at 175 cm. Shrinkage of only 1% reduced the conductivity by more than 2 orders of magnitude, which could be caused by the collapse of macropores as reported by Chow et al. [1992] as well as Price et al. [2003]. Since volume changes can happen within days, he suggests that hydraulic conductivity, as well, is time sensitive. This can be transferred to a seasonal time scale, suggesting hydraulic conductivity measurements throughout the year, or at least during the dry and wet period.

Biogenic gas plays an important role when it comes to hydraulic conductivity in peatland, because of methane producing bacteria that live in the soil. Baird and Gaffney [1995] report an increase of 33% in hydraulic conductivity, when the water table rose 50 cm, which is owned to the compression of occurring gas bubbles. Price [2003] witnessed two orders of magnitude conductivity decrease firstly because of peat compression but also due to probable gas accumulation. Similar observations were made during a laboratory experiment of Beckwith and Baird [2001], who report a 60% decrease of saturated hydraulic conductivity due to methane production in peat. Baird et al. [2008], Fraser et al. [2001] conclude therefore that changes in hydraulic conductivity are, among other mechanisms, a result of gas-filled porosity. During his experiment Price [2003] found that the change in hydraulic conductivity due to water table changes was considerably stronger in disturbed peat and Wallage and Holden [2011] describe a significantly, 1.5 times higher conductivity in restored peatland.

1.5 Groundwater flow

According to Fraser et al. [2001], Kopp et al. [2013], Reeve et al. [2006], groundwater flow patterns are mainly controlled by hydraulic conductivities, water storage capacity and hydraulic gradients. Glaser et al. [1997] observed upward groundwater flow during drought conditions in a bog in Minnesota, whereas infiltration after precipitation events inversed the flow, so that recharge out of the bog took place. Kopp et al. [2013] measured mostly downward flow in a bog in Ontario, Canada, on the adjacent forested peatland, however, water moved upwards during the longer period of the study. Later flow simulations suggested, at least when trees were present, that drainage does impact the water balance and hence should not be excluded from hydrologic model approaches.

MODFLOW simulations by Reeve et al. [2000] show, that the permeability of the underlying soil of peatlands is one main control on vertical water movement. Hence, if low permeability soils separate the peatland from the surrounding land, as it is the case with raised bogs, vertical flow is supposed to be negligible, instead the upper soil becomes more relevant for the occurring hydrology. Important to note is that this finding contradicts the statement of many peatland studies, which base occurring lateral flow on the low permeability of the catotelm. In the case of peatland with high permeability underlay, simulations suggested vertical flow below peat mounds; the vertical hydraulic gradient is influenced more by the permeability difference at the peat base than by the size of the peat dome. Thus, peatlands with a considerable mound tend to dominate the regional hydrology in areas with low topographic gradients.

A two dimensional model using the FLOTRANS software by Lapen et al. [2005], suggested that approximately 90% of the lateral flow happened in the acrotelm layer. The catotelm layer on the other hand discharged downward. The modeled horizontal specific discharge at the margins was high, whereas the vertical specific discharge through the catotelm was very low. The hydrology of the modeled system was sensitive to hydraulic conductivities along the bog margins.

1.6 Modeling

Several studies during the past years used a modeling approach to better understand the hydrology of peatlands, many of which were spatially distributed in order to simulate the hydrology within the peat (e.g. Lapen et al. [2005], Reeve et al. [2000]).

Reeve et al. [2000] used the MODFLOW software with a block-centered finite-difference method, under the assumption of adequate description of flow by commonly used groundwater flow equations like Darcy's Law. Lapen et al. [2005] established a two-dimensional, steady-state finite element flow model with the FLOTRANS software. In order to work, the boundary condition at the base had to be defined as being impermeable.

Jutras et al. [2009] developed a sub-model for the distributed HYDROTEL environment, which works with physically-based algorithms, as well as empirical equations. They evaluated the performance of the PHIM sub-model (organic soils like peat) with the standard sub-model (BV3C) for rigid soils. PHIM, which uses two equations to describe

first water table elevation to discharge and second cumulative water storage to water table elevation, performed well and can therefore, be used as alternative approach, when organic soils are under investigation.

Other studies used stochastic approaches. Letts et al. [2000] employed the Canadian Land Surface Scheme (CLASS) as base for their simulations. After the introduction of several soil layers with differing hydraulic characteristics, the model yielded satisfying results regarding the hydrology of peatlands, thermal simulations were found to be inaccurate. This was a first attempt to introduce organic soils to SVAT models and needs improvements, before it can be applied on a broad set of environments.

Kværner and Kløve [2008] established a model to simulate runoff during summer in a boreal fen. They used, comparable to the PHIM approach, a reservoir routing method which uses the relationships between water level to discharge as well as water level to storage, to describe the hydrologic system. They identified different runoff processes for high and low flows. Therefore the study recommends separate assessments for these situations. They concluded that their model is a good addition to existing models, due to the well performing overland flow simulation, which is not yet well established in some other peatland models.

1.7 Mire breathing

Already Hutchinson [1980] discovered soil surface fluctuations of about 5 cm in a Fen located in eastern England. Several other similar observations were published, for example Howie et al. [2009b] reports soil surface variations due to water table changes in peatlands, which results in an unsteady hydrologic system and therefore complicates the accurate description of water storage or runoff processes. Price [2003] contributed fundamental work in his study. He investigated the swelling and shrinkage behavior of peat at three sites, two of them disturbed but abandoned for several years. He found that the volume change was closely related to the water table and that soil up to a depth of 50 cm reacted most sensitive to the water table fluctuations. Volume changes near the surface were approximately 15% at the site, which was abandoned for only two years. The seven year abandoned site, together with the undisturbed site experienced only changes of about 5%. At 100 cm depth, volume changed less than 1.5% at all sites.

1.8 Study region

Burns Bog is an oval shaped raised bog with a north-south extent of 5.5 km, east-west extent of 9 km [Balfour and Banack, 2000], a total area of approximately 3000 ha [Hebda et al., 2000] and therefore the largest raised bog on the west coast of the Americas [Howie et al., 2009b]. The bog is located about 20 km southeast of Vancouver, British Columbia, within the southern Fraser River delta [Hebda et al., 2000]. Elevation reaches from approximately 5 m.a.s.l. in the center to 1-2 m.a.s.l. at the margins [McElhanney, 1999], resulting in a topographic gradient of about 0.1% [Balfour and Banack, 2000]. Only 29% of the bog remains undisturbed [Howie et al., 2009b]. At locations that have been subject to peat harvesting, it is assumed that the ground level does not exceed 2-3 m [Hebda et al., 2000]. A previously ordered water balance study showed that Burns Bog receives an annual surplus of approximately 200 mm, which does not prevent the summer water table to drop considerably [Hebda et al., 2000]. Because of a negligible topographic gradient, Burns Bog drains in a radial pattern [Whitfield et al., 2006].

1.8.1 Geology and formation

About 10,000 years ago, after glaciers retreated, the Faser River began depositing Pleistocene and Holocene sediments on the much older deposits from the Late Cretaceous Period, resulting in a total sediment layer thickness of 4,000 m [Clague et al., 1998]. The bog, which started to develop during the sea level rise of the Holocene, is hydrologically separated by previously deposited deltaic sands with a thickness of 10-20 m and a layer of silt or clayey silt layer of 1-5 m [Balfour and Banack, 2000, Hebda et al., 2000]. Over time wetlands developed and due to the expansion of the Fraser River Delta, the influence of sea water decreased. The previously sedge and grass dominated area developed shrub vegetation and ultimately sphagnum took over, slowly forming the bog as we know it today [Hebda et al., 2000].

1.8.2 Meteorology

Hebda et al. [2000] report a total annual precipitation of 1000-1200 mm, with less than 10% of it as snow [Howie et al., 2009b]. A precipitation gradient of 20% was found to extend from the south-west to the north-east of the bog, causing lower precipitation in

the south-western part of the bog [Cheng, 2011]. The mean annual temperature was reported to be 9.6 °C with a summer mean of 16.8 °C and a winter mean of 2.5 °C [Hebda et al., 2000]. Table 1.5 provides weather data for the year of this study, 2014 [EnvironmentCanada, 2014].

Table 1.5: Weather data for 2014 from Richmond Nature Park, approximately 11 km north-west of study site, [EnvironmentCanada, 2014].

Month	Mean Temperature °C	Sum Precipitation [mm]
1	4.3	88.8
2	2.9	130.7
3	7.4	184.2
4	10.6	69.6
5	14.8	89.7
6	16	42
7	19.6	29.8
8	19.6	18.2
9	16	15.6
10	13.4	153
11	6.1	184.8
12	4.9	183
Total	**11.3**	**1189.4**

1.8.3 Study site

The study site is located at a section of the south boarder of Burns Bog, across from the Pineland Peat & Soils Ltd property. It ranges 200 m along the boundary ditch and reaches 35 m into the bog. The arbitrary origin of the site's coordinate system in the south-west corner of the site is located at N 5439100 and E 502085, with an elevation of 0.67 m.a.s.l (Figure 1.2). It reaches 200 m east and 35 m north. The mean ground level is 1.54 m.a.s.l. and the underlying silt lies at a mean depth of –1.52 m.a.s.l. As shown in Figure 1.2, vegetation at the site mainly consists of medium dense pine forest with a very dense salal understory. Roots were found up to a depth of 50 cm.

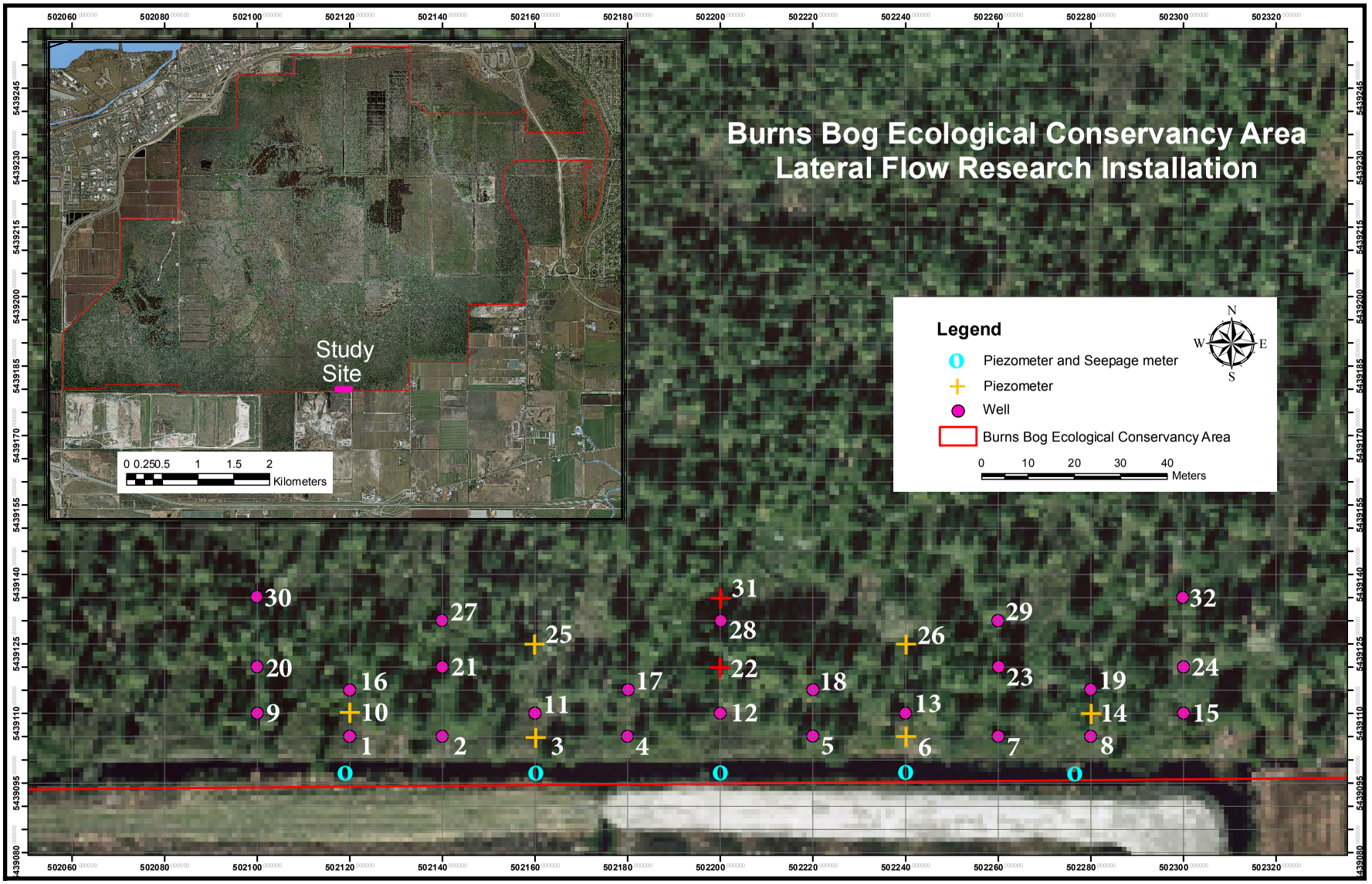

FIGURE 1.2: Areal photo of study site at the southern border of Burns Bog. The numbers indicate field locations, which will be used for reference. Purple dots indicate wells, whereas orange plus-signs represent piezometers. Red plus-signs stand for piezometer nests. Cyan rings represent ditch installations, namely: Piezometer and permanently installed seepage meter (modified from Markus Merkens, MetroVancouver, 2015).

Chapter 2

Material and Methods

2.1 Field campaign

The field campaign was executed between August 22 and December 10, 2014. During this time, water levels and piezometer head measurements were executed automatically; seepage, subsurface lateral flow and pipeflow were quantified manually, usually three times a week on Mondays, Wednesdays and Fridays. Since not all measurements could be conducted during the entire field campaign (e.g. lateral flow did not occur until the beginning of November), Table 2.1 gives an overview when what measurements were done.

Table 2.1: Overview monitoring period for each process

Measurement	Start date	End date
Wells	Aug. 22, 2014	Dec. 8, 2014
Piezometers	Aug. 22, 2014	Dec. 8, 2014
Seepage	Oct. 21, 2014	Nov. 24, 2014
Lateral flow	Nov. 19, 2014	Dec. 8, 2014
Pipeflow	Oct. 29, 2014	Dec. 5, 2014
Electrical Conductivity	Nov. 19, 2014	Dec. 10, 2014

Continuous data was received from all automated measurements in the bog and from the ditch locations 100 and 140, which were also equipped with loggers, during the entire field campaign. Seepage measurements started once the water table in the ditch rose sufficiently for proper seepage meter installations. Lateral flow was quantified when it was established throughout the ditch section and pipeflow was first observed and

measured on October 29, 2014. Electrical conductivity measurements were not executed until November 19 because all measurement devices were unavailable for use at the time.

2.1.1 Scientific approach

A reservoir model approach is a commonly used method to investigate the relationship between the water storage and runoff. Hutchinson and Moore [2000] used it at a forested hillslope in British Columbia, but it was also employed in organic soil settings by Jutras et al. [2009], who successfully implemented it by means of a sub-model to a HYDROTEL environment. This approach was chosen, because current research reports a direct and close relationship between water table and runoff. Observations in a broad range of peatland environments also suggest a water table threshold, above which the system's behavior changes dramatically (e.g. Emili and Price [2006]). Hence, a reservoir model with implemented threshold was deemed appropriate. In the following section, the experimental design as well as data acquisition and processing will be described. As there was no saturation overland flow expected (nor observed for the duration of the study), the focus of the field campaign was on water table and piezometric head changes, seepage, lateral flow close to the soil surface and probable pipeflow.

2.1.2 Experimental design

In order to get a representative elementary volume, a site area of 200 m x 35 m, or 7000 m^2 was selected. This size is, firstly, a realistic cell size of a future spatially-distributed model and, secondly, it is unlikely to receive biased data due to local, unrepresentative features. Next, a grid was established with transects running 20 m apart from each other perpendicular to the ditch and 5 m apart of each other parallel to the ditch (see Figure 1.2) All lateral flow measurements were conducted at the natural ditch face as recommended by Atkinson [1978]. The seepage measurements were executed in the ditch. It is worth noting that the seepage meter installation distance to the bog differed due to irregularities such as small islands or dense vegetation, which made it necessary to move the seepage meters slightly, in order to be able to install them properly.

2.1.3 Measurement schemes and field installation

2.1.3.1 Wells and piezometers

Generally water table draw down towards a ditch is not linear. Instead the change in water table depth increases towards the ditch. In order to include this feature properly into the measurement plan, seven strata were selected. Each gridline parallel to the ditch represented one stratum. Well locations were chosen so that a systematic pattern was established, with a relatively even density along the ditch and a decreasing density with increasing distance from the ditch. Table 2.2 gives an overview of all monitoring installations, including location number, grid coordinates, pipe type, screen center depth below bog/ditch surface, screen length and measurement type. The south-west corner of the study site (left boundary, at the ditch), was chosen as the origin. Thus, when ditch location 100 is mentioned, this refers to the location in the ditch 100 m distant from said origin. In total, data was collected from 27 wells and ten piezometers.

The piezometers were installed at eight locations throughout the site (see Table 2.2 and Figure 1.2). At locations 22 and 31, piezometer nests were installed to provide data to quantify the vertical hydraulic gradient at these locations. The centers of the deep piezometer screens were installed 75 cm above the underlying silt layer, so that the piezometric head of the water right above the silt layer was monitored, without risking interference of irregularities along the peat-silt boundary.

During previous studies, The Corporation of Delta used PVC pipes which were mechanically slotted by cutting thin slots of approximately 0.5 mm along the desired slot length of the pipe. In this way no additional mesh is required to avoid entering of peat mass through the slots. All pipes were capped at the bottom end. To prevent vertical movement due to mire breathing, piezometers were connected to a rebar, which was anchored in the underlying silt.

In this study, PVC pipes with an inner and outer diameter of 4 cm and 5 cm, respectively, were used. This allowed water table sensors to be lowered into the pipe, which was necessary due to low water tables at the beginning of this study. All slot lengths are provided in Table 2.2. Figure 2.1 shows a sketch of such pipe installation. Before the actual insertion of the pipe into the ground, a peat auger was used to prepare the required bore. The diameter of the auger was small enough to guarantee a tight

TABLE 2.2: Pipe installation details. All locations denoted with a "D" are located in the ditch. East and North coordinates are referenced to an arbitrary origin, which is the south-west corner of the study site. Type W = Well, P = Piezometer, SP = Shallow Piezometer, DP = Deep piezometer. Depth describes screen center depth referenced to the soil surface.

Location	East [m]	North [m]	Type	Depth [cm]	Screen Length [cm]	Measurement
1	20	5	W	100	200	Automatic
2	40	5	W	100	200	Automatic
3	60	5	P	204	50	Automatic
4	80	5	W	100	200	Automatic
5	120	5	W	100	200	Automatic
6	140	5	P	145.5	50	Automatic
7	160	5	W	100	200	Automatic
8	180	5	W	100	200	Automatic
9	0	10	W	100	200	Automatic
10	20	10	P	232	50	Automatic
11	60	10	W	100	200	Automatic
12	100	10	W	100	200	Automatic
13	140	10	W	100	200	Automatic
14	180	10	P	202.5	50	Automatic
15	200	10	W	100	200	Automatic
16	20	15	W	100	200	Automatic
17	80	15	W	100	200	Automatic
18	120	15	W	100	200	Automatic
19	180	15	W	100	200	Automatic
20	0	20	W	100	200	Automatic
21	40	20	W	100	200	Automatic
22	100	20	W	100	200	Automatic
22.1	100	20	SP	110.5	50	Automatic
22.2	100	20	DP	242.5	50	Automatic
23	160	20	W	100	200	Automatic
24	200	20	W	100	200	Automatic
25	60	25	W	100	200	Automatic
25.1	60	25	P	247.5	50	Automatic
26	140	25	W	100	200	Automatic
26.1	140	25	P	208.5	50	Automatic
27	40	30	W	100	200	Automatic
28	100	30	W	100	200	Automatic
29	160	30	W	100	200	Automatic
30	0	35	W	100	200	Automatic
31	100	35	SP	104	50	Automatic
31.1	100	35	DP	265.5	50	Automatic
32	200	35	W	100	200	Automatic
D 100	100	-2	P	50.5	50	Automatic
D 140	140	-2	P	47.5	30	Automatic
D 19	19	-2	P	49.0	10	Manual
D 60	60	-2	P	38.0	10	Manual
D 176	176	-2	P	40.0	10	Manual

fit of the pipe, preventing vertical preferential flow along it. Price [1992], too, installed piezometers successfully in peatlands without any filling material around the pipe. After the installation each pipe was developed at least twice [Howie and van Meerveld, 2013, Kopp et al., 2013], to remove debris from the installation. To ensure good practice and to prevent false installation a one day field tutorial by Dr. Sarah Howie, Corporation of Delta was attended.

Data on the hydraulic gradient in the ditch was received from two nests at locations 100 and 140. There, piezometers were installed right above the silt layer and the wells were installed directly next to them. At the remaining permanent seepage locations (19, 60 and 176) manually measured piezometers were installed. The coupling of seepage meters and hydraulic gradient enabled it to calculate the hydraulic conductivity of the ditch bed at these locations using Darcy's law.

2.1.3.2 Seepage

The seepage rate was anticipated to vary along the 200 m ditch section and over time Kennedy et al. [2010]. Hence, a monitoring scheme covering spatial and temporal variation was required. Due to time restrictions and the long duration of seepage measurements, a sampling plan with 15 measurements for each field trip was developed. Figure 2.2 presents a histogram of all seepage measurements. At five locations (19, 60, 100, 140 and 176), seepage meters were installed permanently to obtain time series data. The remaining ten seepage meters were employed to collect spatial data.

An accurate non-biased population mean can be achieved by means of random sampling. Stratified random sampling is useful in situations where a (possibly smaller) subgroup is required to be included in the results or when clustering needs to be avoided. In cases of unequal subgroup sizes it is necessary to apply proportional allocation for each subgroup, thus avoiding an overrepresentation of one group. In the case of seepage measurements, the 200 m section was divided into four strata of 40 m, 60 m, 60 m and 40 m, based on preliminary silt depth observations. Within each stratum the location was chosen randomly by using random numbers from Random.org [2014]. The website creates random values from atmospheric noise, therefore providing true randomness, as opposed to all computer programs, which can only produce pseudo-randomness. With

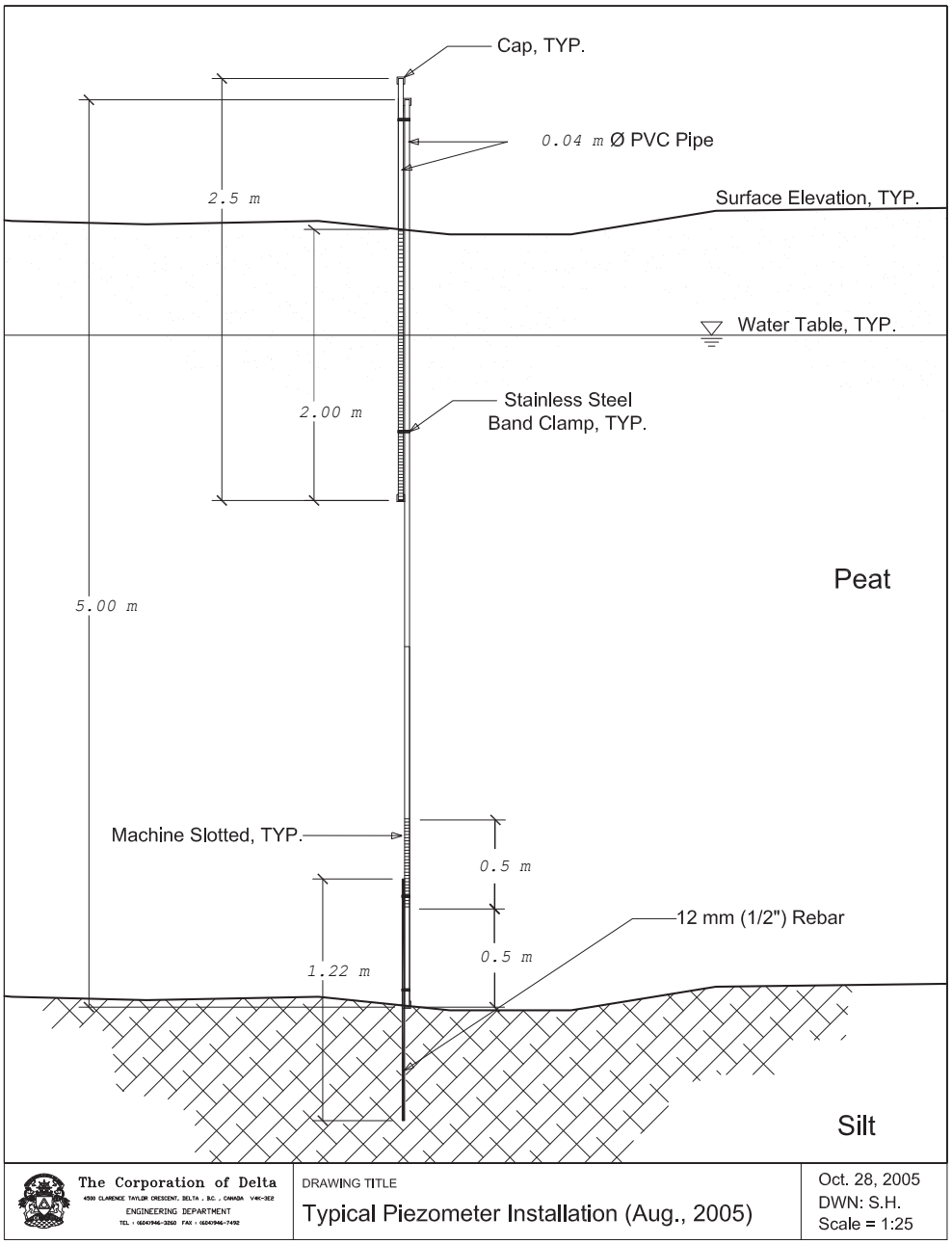

FIGURE 2.1: Piezometer nest installation as recommended by The Corporation of Delta. Note the rebar to anchor the nest, in order to prevent vertical movement. This scetch was modified from the original one, to match the well and piezometer installation of this study. Total height of the nest varies between locations. (modified from Sarah Howie, Corporation of Delta, 2005)

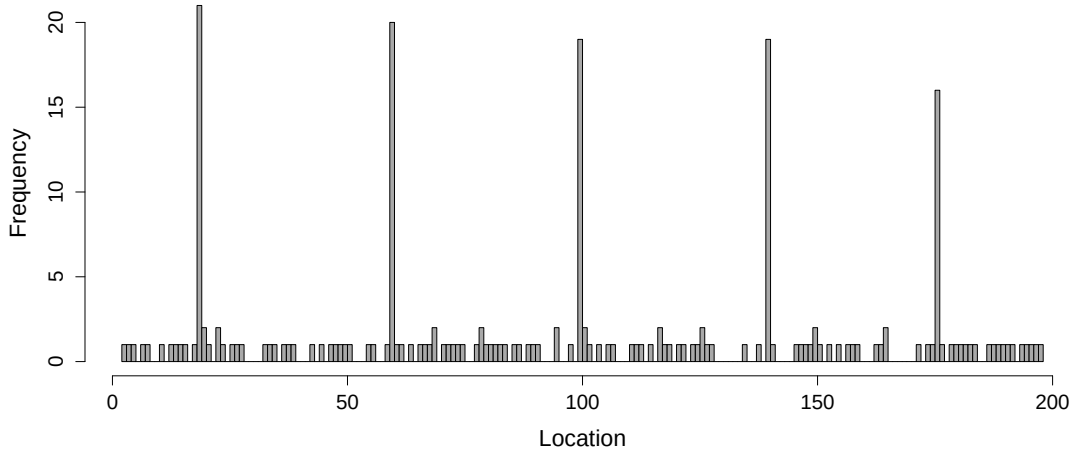

FIGURE 2.2: Histogram of seepage measurements along the ditch. Locations 19, 60, 100, 140 and 176 were used for permanent installations.

this measurement design the possibility of clustering was excluded and data from the entire ditch section was obtained.

To avoid disturbance of the ditch bed, which would yield less reliable measurements, a raft was used from which the piezometers were installed as described by Harvey et al. [2000]. After each installation it was verified that a good soil connection was established. Then the seepage meter was given about 30 minutes before measurements started. Churn sediment could settle down and the system had time to equilibrate, which may be necessary because of soil compaction due to the installation process.

As for the pipe installations, a field course of the Department of Earth and Ocean Science at the University of British Columbia was attended to prevent mistakes when installing the seepage meters.

2.1.3.3 Lateral flow

Trough measurements were executed at 20 locations with troughs of 1 m length, therefore providing a sampling size of 10% of the total population for each field trip. When lateral flow started, it was given several days to develop throughout the study site. On November 12, a survey was done to estimate the variability of lateral flow along the site. This was necessary because a random sampling approach with troughs was not feasible due to time restrictions. In addition to the initial lateral flow survey, another

one was done at the end of the field campaign. The flow was subjectively categorized into four classes: "none", "low", "medium" and "strong" so that the spatial change could be evaluated in this way. After the first survey troughs were installed honoring proportional allocation, Table 2.3 provides a more detailed overview.

TABLE 2.3: Trough installation along the natural ditch face. Location gives the position in meters from the arbitrary site origin. There are troughs assigned to category "none" after the second survey, due to the fact that lateral flow developed throughout the entire site over time.

Location	Category Nov. 12	Category Dec. 8
2	low	medium
4	low	medium
17	strong	strong
26.5	medium	low
32	low	low
55.5	medium	medium
59	strong	strong
66	medium	medium
81	low	low
91	low	none
98	low	medium
104	medium	low
113	low	low
122	strong	strong
147	low	low
167	low	none
171.5	medium	medium
180	low	none
184	strong	strong
190	medium	none

The L-shaped aluminum troughs were installed directly at the natural ditch face, as recommended by Atkinson [1978], with the help of a rubber mallet in such a way that they channeled all runoff water exiting the face above the trough. Due to the strong fluctuation of the water table in the ditch, some troughs had to be moved a few centimeters vertically to avoid drowning.

2.1.3.4 Pipeflow

Pipeflow was planned to be measured separately from case to case. Except for ditch location 177, no pipeflow was observed. Since October 29, the pipeflow was collected with leftovers from the well installation. The outlet of the pipe was situated about 20-25

cm inside a crevice so that a well pipe was cut open to form a gutter which could collect all runoff water.

2.1.3.5 Electrical conductivity

The electrical conductivity (EC) of the opposite soil deposit's groundwater, the ditch water and the bog water was measured at three locations along the ditch to establish a mixing model. To do this, three pipes were installed at the soil deposit. Table 2.4 gives an overview of the locations of these measurements. The locations are in relation to the ditch center.

TABLE 2.4: Electrical conductivity was measured at three locations along the ditch sections. For bog and soil deposit measurements wells were installed at the indicated locations, EC in the ditch was measured approximately in the center.

Transect	East [m]	North [m]	Site
1	40	7	Bog
2	100	7	Bog
3	160	7	Bog
1	40	0	Ditch
2	100	0	Ditch
3	160	0	Ditch
1	40	14	Soil deposit
2	100	12.5	Soil deposit
3	160	14	Soil deposit

2.1.3.6 Ditch face survey

During the survey, the elevation of the face top was measured in together with the ditch bed elevation at the bottom of the face. Bank and bed were surveyed with 180 and 170 measurements respectively, therefore providing the desired density of approximately one measurement per meter.

2.1.3.7 von Post index

During the pipe installation in the bog, the von Post scale was used to describe peat decomposition at locations 11, 13, 27 and 29 vonPost [1924].

2.1.4 Measurement practice

2.1.4.1 Water level

All water levels were measured with Odyssey Capacitive Water Level Loggers, except for the three piezometers at ditch locations 19, 60 and 176. The Odyssey loggers were set to a higher measurement interval (10 minute interval) than in other studies. Jutras et al. [2009] used a 15 minute interval, for example. In this way, possible short time fluctuations were captured, leaving the option to lower the interval for future monitoring. The loggers are able to measure differences at a millimeter level. Before installation, all loggers were calibrated as described in DataflowSystems [2013]. Due to occational considerable water table changes, some of the loggers were reinstalled at a different height. These inconsistencies were later removed when the measurements were processed. During the study, logger data was downloaded several times to avoid long undetected malfunction of the loggers. Nevertheless, most loggers experienced a failure from November 12 onwards; more information will be provided in the processing section.

Water level at the three manual ditch piezometers was measured using a Heron dipper-T water level meter [Heron, 2015]. The approximate accuracy is 1-2 mm, mainly dependent on the person taking the measurement.

2.1.4.2 Seepage

Seepage rates were quantified by means of manual measurements. The initial intent to collect continuous seepage data was dropped, in one instance because of the high cost of the system (USD 15,000) [Rosenberry and Morin, 2004]. Three other systems were custom-made and therefore not available for this study [Krupa et al., 1998, Paulsen et al., 2001, Taniguchi and Fukuo, 1993]. Hence, manual measurements as described by Rosenberry et al. [2008] were executed. The seepage meters covered an area of 0.264 m^2 and an attached plastic bag was used to collect the outflow. The bags were prefilled with 100 ml bog water, so that recharging conditions could be quantified, as well. Additionally, prefilled bags reduce the error of water adhesion in the bag, when emptying it into the measurement cylinder. Due to work-flow purposes it was not feasible to install the barrels long before the measurements, as recommended by Rosenberry et al. [2008]; instead, the barrels were placed in the ditch bed about 30 minutes before measurements

started. After all, Landon et al. [2001], Lewis [1987], Lock and John [1978] reported successful seepage measurements with shorter equilibration time. In most cases, seepage meters were run 1-2 hours before the plastic bags were detached and measured out by using a graded cylinder with 1 milliliter scaling. The changes in water volume together with the duration of the measurements then were used to calculate the actual seepage rate.

2.1.4.3 Trough and Pipeflow

Trough outflow and pipeflow were quantified by simply collecting the runoff in a milliliter scaled graded cylinder over a given amount of time, which was taken by means of a stop watch. In order to minimize the reading error, measurement times were adjusted so that a sufficiently large amount of water was collected.

2.1.4.4 Electrical Conductivity

Electrical conductivity of the water was measured by means of a Tetracon 325 Conductivity Cell, which was attached to a WTW Cond 340i Portable Conductivity Meter. The device works within an accuracy range of 0.5% of the target value [WTW, 2005, 2008].

2.1.4.5 Ditch face survey

The ditch face was surveyed with a Leica TPS800 total station [Leica, 2015]. The total station accuracy lies within 2 mm.

2.1.4.6 Mire breathing

Mire breathing was measured once on November 29, 2014. To quantify it initial soil surface elevation was marked at all piezometer locations, which were anchored in the underlying silt, in order to avoid vertical movement. The change in soil surface elevation was quantified by measuring the difference between inital ground level and ground level on November 29.

2.2 Data processing

All data processing was done using the programming language R version 3.2.0.

2.2.1 Odyssey data logger raw data

As first processing step, all data from the Odyssey loggers was corrected for depth changes due to reinstallation after downloading the data or because of considerable water level changes. Next, the data was flagged during a quality check in order to guarantee good data quality for further analysis. Table 2.5 gives an overview of the applied quality criteria. For each time series, two threshold sets were used since the measurements behaved differently during the dry and wet periods. The split date October 21, 2014 was selected due to visual evaluation of all time series. The ditch data was expected to behave differently than the site data, so different thresholds were applied.

The slug test parameters are used to identify time series, which have not reached equilibrium at the beginning of the measurements. If the water level change is larger than the "slug.diff" threshold over the "slug.lag" time period, the values are excluded from the time series. If the length is longer than "slug.length", they are exported separately to make it possible for use in for further analysis. Due to this step, much of the piezometer data until October 7 was excluded.

The plausibility test parameters check whether all measurements are within realistic boundaries. Different thresholds were used for dry and wet periods. Likewise, wells and piezometers, as well as ditch and site data was differentiated.

The consistency thresholds pose as values of maximum fluctuation between two consecutive measurements. If the threshold is exceeded, the value is flagged.

Finally the stability test searched for identical values over the defined time. If a time series displays less fluctuation than the threshold, it is assumed to be an error. The stable water levels with the high measurement interval made it necessary to pick the smallest possible threshold to avoid false exclusion of data.

As indicated before, many loggers malfunctioned after November 12 due to an unknown reason. Only loggers at locations 7, 12 and 22 worked properly until December 9. To

TABLE 2.5: Quality check parameters, which were used to flag raw data from the Odyssey data loggers. Different parameters were used for the site and ditch measurements, as well as data from the dry and wet periods. Piezometer measurements from within the bog varied considerably, so a different set of plausibility limits was selected.

Quality test parameters	Site	Ditch
Interval [min]	10	10
Transition period [h]	6×24	6×24
Slug test		
Slug lag [h]	36	36
Slug difference [mm]	20	20
Slug length [h]	12	12
Plausibility test		
Plaus.min.dry [mm]	-1500	300
Plaus.min.dry.piezo [mm]	-1500	
Plaus.max.dry [mm]	-300	1500
Plaus.min.wet [mm]	-700	900
Plaus.min.wet.piezo [mm]	-1200	
Plaus.max.wet [mm]	150	2000
Consistency test		
Threshold dry [mm]	40	40
Threshold wet [mm]	80	60
Stability test		
Stability min dry [mm]	1	1
Stability time dry [h]	24	24
Stability min wet [mm]	1	1
Stability time wet [h]	12	24

minimize the data loss, gap filling was conducted. As such, the data sets were split on October 21 and, additionally, a time window of four days prior and after the split date was removed to obtain consistent data with measurements only from the dry and wet periods, respectively. Hence, equal conditions during the calibration and prediction period were provided and, therefore, the assumption of a constant relationship between predictor and estimator was justified. With three estimators and one predictor, there are a total of seven possible model combinations for each time series. After data inspection, it was found that not all relations were simply linear, so that data transformation was performed using Box-Cox-Transformations for the predictor only and a combination of Box-Cox-Transformations and Box-Tidwell-Transformations for both the predictors and the estimators [Box and Cox, 1964, Box and Tidwell, 1962]. In the end there were 21 models for each time series to choose from. To evaluate the models, the following

target functions were used: mean biased error (mbe), root mean square error (rmse), mean absolute error (mae), adjusted R^2 (adj. R^2) and the Nash-Sutcliffe- Efficiency (nse). Only models with a mean absolute error less than 10 mm and a Nash-Sutcliffe-Efficiency equal to or higher than 0.9 were used for gap filling. In some instances, in order to get a continuous time series, it was necessary to apply a lineary varying shift, as presented in Formula 2.1 and 2.2:

$$d(t) = y(t) - x(t) \tag{2.1}$$

$$C(t) = d(t_1) + [d(t_2) - d(t_1)]\frac{(t - t_1)}{(t_2 - t_1)} \tag{2.2}$$

Where *d(t)* = difference of observed and predicted values [mm], *x(t)*, *y(t)* = observed and predicted values [mm], respectively. *C(t)* = linearly varying shift [mm] and t_1, t_2 = time steps before and after gap.

After the raw data processing, bog site data for the entire study period was available from all 10 piezometers and at least 21 wells.

2.2.2 Survey study site

The study site was surveyed to receive data on ground level elevation and silt depth (see appendix: Table A.1 and Figure A.1 for more information). During the pipe installation the silt depth at all locations was measured, so that it was possible to calculate the depth of the silt layer from the ground level data. Additionally, all pipe tops were measured in, primarily to be able to generate a potentiometric map. "Target Land Surveying" executed the survey and provided all data in meters above sea level (m.a.s.l), with one millimeter resolution. Because the initial ditch face survey was in relation to an arbitrary elevation, the mean value of the ditch face height from the professional survey was used to calculate the offset of the unreferenced mean ditch face elevation. Then, a moving average with a window size of 20 was used to reduce noise in the data.

During data processing, the standard version of R was used, including the extension packages "sp", "gstat" and "automap" for the handling of spatial data [Hiemstra, 2013, Pebesma and Graeler, 2015, Pebesma et al., 2015]. Kriging is a popular approach to

spatially interpolate data because of the possibility to better evaluate the results. This is due to the fact that kriging uses models for the calculations (as opposed to other interpolation methods like inverse distance weighting). Preliminary data exploration identified trends in both data sets (silt elevation and soil elevation) so that ordinary kriging was used [Journel and Rossi, 1989]. Nevertheless, the data sets were found to be normally distributed, so that kriging could be employed as interpolation approach. Besides the trend, there were indications of anisotropy, so the models were fitted manually; the employed packages do not possess an automated fitting routine when anisotropy is present. The models were used to calculate ground level and silt depth for a grid with a cell size of $0.5 \times 0.5\ m^2$. For evaluation purposes, leave-one out cross-validation was done to calculate the mbe, rmse, mae and nse (see Table A.2 for target functions). Each data set was interpolated automatically using a spherical, exponential, Gaussian and linear model for performance reference of the manually fitted models. One criterion during manual fitting was that the range of the model had to be larger than the minimum distance of measurements. All models were not only evaluated statistically by calculating target functions, but also visually to make sure that no unrealistic inconsistencies occurred. Manual model are marked by a *, whereas the finally used ones are labelled ".

2.2.3 Saturated hydraulic conductivity

Because a suitable hydraulic pump was unavailable during the study, it was not possible to execute proper slug tests with the installed piezometers at the site. However, four piezometers at locations 22 (shallow and deep piezometer), 26 and 31 (deep piezometer), experienced slow equilibration after they were installed and the water table loggers were able to capture most of the equilibration process. Even though the conditions are not well defined, the data was used for hydraulic conductivity calculations because even with boundary assumptions and the resulting uncertainties, the data is thought to give an idea of the real values until proper measurements can be executed.

In order to calculate the saturated hydraulic conductivity, the head recovery method by Hvorslev [1951], which was also employed in peatlands by Reeve et al. [2000], was used (see. Formula 2.3):

$$K = \frac{r^2 \ln(\frac{L}{R})}{2LT_0} \tag{2.3}$$

Where K = saturated hydraulic conductivity [$m\,s^{-1}$], r = inner radius of casing [m], L = length of screen [m], R = outer radius [m] and T_0 = required time to recharge 37% of initial water level [s].

Inner and outer radius of the piezometer pipes were known, together with the screen length. The initial water table height in the pipe was unknown, thus it was assumed to be the water table after equilibration, which seemed appropriate due to the stable character of the water table during dry conditions. Equilibration was assumed to be reached when water table changes were less than 1 mm for at least 20 minutes. This assumption was motivated by the fact, that the surrounding conditions were not stationary, so that perfectly equilibrated water tables at a later point in time would be subject to a different error. Saturated hydraulic conductivities of the ditch bed were calculated using the seepage meter rates and hydraulic gradients. Darcy's law (Formula 2.4) then provided the hydraulic conductivities [Maidment et al., 1992].

$$Q = KA\frac{\delta h}{\delta l} \tag{2.4}$$

Where Q = volumetric discharge [$m^3\,s^{-1}$], A = cross-sectional area [m^2], δh = hydraulic head difference [m], δl = distance between head measurements [m] and K = saturated hydraulic conductivity [$m\,s^{-1}$].

2.2.4 Flow analysis and hydraulic gradients

At bog locations 22 and 31 as well as ditch locations 100 and 140, the vertical hydraulic gradients were calculated continuously, whereas discrete values were received for the remaining piezometers in the ditch. Formula 2.5 was used for the calculations:

$$g = \frac{\delta h}{\delta l} \tag{2.5}$$

Where g = hydraulic gradient [-], δh = hydraulic head difference [cm] and δl = distance between head measurements [cm].

For piezometric map computations, measurements from the deep piezometers were used. The spatially low measurement density made it necessary to use inverse distance weighting as the interpolation approach instead of ordinary kriging because there were not enough data points to fit a model properly. As for ground level and silt layer interpolations, a grid with a cell size of $0.5 \times 0.5\ m^2$ was used.

2.2.5 Water table analysis

Because of the malfunction of a number of loggers after November 9, only data from before was used for the calculation of basic water table statistics. In this way the introduction of uncertainties due to gap filling was prevented. The time windows were from August 30 to October 12 and October 25 to November 11 for dry and wet periods, respectively. 10 minute interval measurements were aggregated to hourly values by means of the "xts" and "zoo" packages [Ryan and JM, 2013, Zeileis A., 2015].

As described by Hutchinson and Moore [2000], only steady-state measurements were used for basic statistics. Here steady-state was defined as water table fluctuations 12 hours prior to and following the measurement in question, of less than 20 mm during the dry period and 40 mm during the wet period, for at least 22 of all available measurements. Furthermore, data was used only if there was data available from at least 20 wells. As explained before, well measurements were split up in strata running parallel to the ditch at distances of 5 m, 10 m, 15 m, 20 m, 25 m, 30 m and 35 m. Hence, basic statistics were calculated for each stratum and the mean value of all strata was used for the whole study area.

As for the ground level and silt layer interpolation, ordinary kriging was used to compute two water table maps for the dry and wet periods, to get a visual representation of how the water tables looked during these periods. For the calculations mean, values of both periods at each location were used with the sea level as reference. The target functions are provided in the appendix (Table A.4).

In order to test whether soil surface or silt layer act as topographic control, the shape of the groundwater table was compared to the soil surface and silt layer shapes. As described by Hutchinson and Moore [2000], the standard deviation of the separation

distance between water table and soil/silt is a measure for shape similarity. Formula 2.6 and 2.7 were used, as in Hutchinson and Moore [2000]:

$$\alpha_{it} = h_{it} - z_{gi} \tag{2.6}$$

$$\beta_{it} = h_{it} - z_{si} \tag{2.7}$$

Where i = location of well, t = point in time, h = water level height [cm], z_{gi} and z_{si} = elevation of ground and silt [cm] and α_{it} and β_{it} = vertical separation between water table and ground surface and silt layer [cm], respectively.

2.2.6 Seepage

The first two seepage measurement dates (October 15 and October 17) were excluded due to unrealistically high values. This was justified by too low water levels in the ditch, at which the seepage meters do not work reliably. Seepage rates were calculated from seepage yield and the duration of measurements. The rates then were divided by the seepage meter area to receive the absolute value in $L\,m^{-2}\,d^{-1}$. There were no correction coefficients applied for inefficiencies in flow within the meter [Rosenberry et al., 2008], because no such coefficient was determined for these seepage meters.

The seepage mean for the entire site was then calculated by using an approach as described by Gilbert [1987]. In order to get an unbiased estimator of the real mean value of the population under investigation when stratified random sampling is employed, the following equations are necessary. The mean value of the population is a weighted mean of the strata means as given in Formulae 2.8 and 2.8.

$$\bar{x}_h = \frac{1}{n_h} \sum_{i=1}^{n_h} x_{hi} \tag{2.8}$$

Where $\bar{x}_h$ = estimator of true stratum mean, n_h = number of randomly selected units from stratum h and x_{hi} = estimator of true value of ith unit in hth stratum.

$$\bar{x}_{st} = \sum_{h=1}^{L} W_h \bar{x}_h \tag{2.9}$$

Where $\bar{x}_{st}$ = unbiased estimator of true mean, h = stratum, L = all strata, W_h = weight (relative size) of stratum h and $\bar{x}_h$ = estimator of mean of stratum h.

When proportional allocation is used, Formula 2.8 and 2.9 combined reduce to the simple arithmetic mean as in Formula 2.10

$$\bar{x}_{st} = \frac{1}{n} \sum_{h=1}^{L} \sum_{i=1}^{n_h} x_{hi} \tag{2.10}$$

With this formula and the estimated seepage area of 800 m^2 the total seepage was calculated.

2.2.7 Lateral flow

As will be shown next, there was no proportional allocation for the trough installations so the mean site runoff was calculated according to Formula 2.9.

Two surveys were executed to estimate the distribution of each of the four predefined strata (”none”, ”low”, ”medium” and ”strong”). The results showed a change in strata size, indicating that the fraction each stratum contributed to the total population change. The shift was assumed to be linear. Hence, the fraction of each stratum was linearly interpolated, so that continuous strata fractions were determined.

Despite the change in stratum size, there was also a change in spatial distribution of the strata over time. This posed a problem because of the fixed trough positions during the entire field campaign. As a consequence, the assigned stratum to a trough from the beginning when it was installed may not correspond with the real stratum at a different point in time. Hence, three approaches were chosen to process the problem differently, in order to provide the possibility to compare the results.

It is important to note that after November 26, it was observed that all “none” locations exhibited very low lateral flow. The strata were not modified to preserve consistency

among each other. Over the time all strata showed a relatively consistent change in outflow.

Approach 1: "Assigned"

The troughs are assigned to one stratum after both surveys. It is worth mentioning that no trough was assigned to "none" after the first survey since there was no lateral flow. The trough assignment after the first survey was done according to proportional allocation. After the second survey, trough assignments were evaluated and it was found that at this time four troughs were installed to stratum "none". Table 2.3 gives an overview of the assignments. For the runoff calculations November 26 was used as split date, meaning that before, the troughs were assigned to the initial strata, whereas after November 26, it was assumed that the troughs were installed in the strata as was evaluated after the second survey. Hence after November 26, when there was runoff observed from the "none" stratum, there were four troughs to quantify the lateral flow in this stratum.

Approach 2: "Ranked"

The second approach is based on proportional allocation. For both surveys it was calculated how many troughs needed to be installed in which stratum (see Table 2.6). November 26 was, again, used as split date. For the calculations, the troughs were assigned to the strata by runoff amount. In the case of measurements after November 26, this means, for example, that the lowest 11 measurements were assigned to stratum "none".

TABLE 2.6: Trough number assigned to lateral flow category, according to proportional allocation.

Category	Survey Nov. 12	Survey Dec. 8
None	0	11
Low	10	4
Medium	6	4
Strong	4	1

Approach 3: "Threshold"

This approach is similar to approach 2, but instead of proportional allocation, the troughs were categorized as presented in Table 2.7. This approach is sensitive to the subjectively chosen thresholds of strata separation.

TABLE 2.7: Runoff fraction, which is assigned to a lateral flow category according to subjectively selected thresholds.

Category	Before Nov. 26	After Nov. 26
None		0-20%
Low	0-30%	21-50%
Medium	31-60%	51-80%
Strong	61-100%	81-100%

2.2.8 Pipeflow

Because there was no spatial dimension to the pipeflow measurements, it was quantified by simply calculating the mean of all five measurements at one point in time.

2.2.9 Reservoir model

The reservoir model uses daily input data, which is received from data aggregation in case of water table measurements and already described mean value calculations in the case of all runoff processes. Input data inspection suggested a lag of one day between water table and runoff data. Models as described by Formula 2.11 were fitted for seepage, the three lateral flow approaches and pipeflow.

$$S = aQ^b + c \tag{2.11}$$

Where S = storage (here water table) [cm], Q = runoff [$L\,d^{-1}$] and a, b and c = fitted model parameters. c acts as threshold, which defines above what water table the process occurs.

Model parameters were fitted using a modified quasi-Newton method in which the upper and lower boundaries of the parameters can be defined [Byrd et al., 1995]. For the final model, water table data from the entire period (August 25 to December 8) were used.

2.2.10 Mixing model

Electrical conductivity measurements of bog water, ditch water and opposite soil deposit were applied to a mixing model in order to estimate the bog water fraction of total water

volume in the ditch. Formula 2.12 was used to calculate the percentage of bog water. To receive estimates for each day, an interpolation spline was used.

$$frac_b = \frac{cond_d - cond_s}{cond_s - cond_b} \tag{2.12}$$

Where $frac_b$ = fraction of bog water in ditch, $cond_x$ = electrical conductivity [μS cm^{-1}], b = bog, s = soil deposit and d = ditch.

2.2.11 Precipitation

Precipitation data was downloaded from EnvironmentCanada [2014] for the weather station "Richmond Nature Park" which is located 11.5 km north-west of the study site. No topographical barriers separate the station from the site. The data is not used for any calculations, but only to provide background information, so the downloaded data are assumed to be sufficiently accurate. EnvironmentCanada [2014] only offers data, which are already quality verified, so no further processing was necessary.

Chapter 3

Results

3.1 Precipitation

An overview of the precipitation during the study is provided in Figure 3.1. Daily precipitation events are presented as gray bars; the black line represents the accumulated precipitation since August 1, 2014. Until the beginning of October there is little precipitation, totaling 34 mm. The first heavy rains occur during the transition from October 12 to October 25 and yield a total of 100 mm. It is also during this transition that the longest rain event of six consecutive days takes place. Afterwards, daily total precipitation increases further with a maximum of 35.6 $mm\,day^{-1}$ on November 3. It rained a total of 548.6 mm in the time between August 1 and December 31, 2014.

3.2 Topography

During the pipe installation soil samples were taken at locations 11, 13, 27 and 29. They were characterized using the von Post scale; the results are presented in Table 3.1. At a depth of 80 cm von Post indices were estimated to be H4/H5. They increased with depth at all locations, reaching up to levels of H7 and H8 at depths below 200 cm at all locations, except for location 13. Roots were found to reach down to a depth of 50 cm.

Mire breathing results suggest a mean increase in ground elevation of 3.9 cm. When taking a closer look at the distribution it appears that soil surface elevation changes in

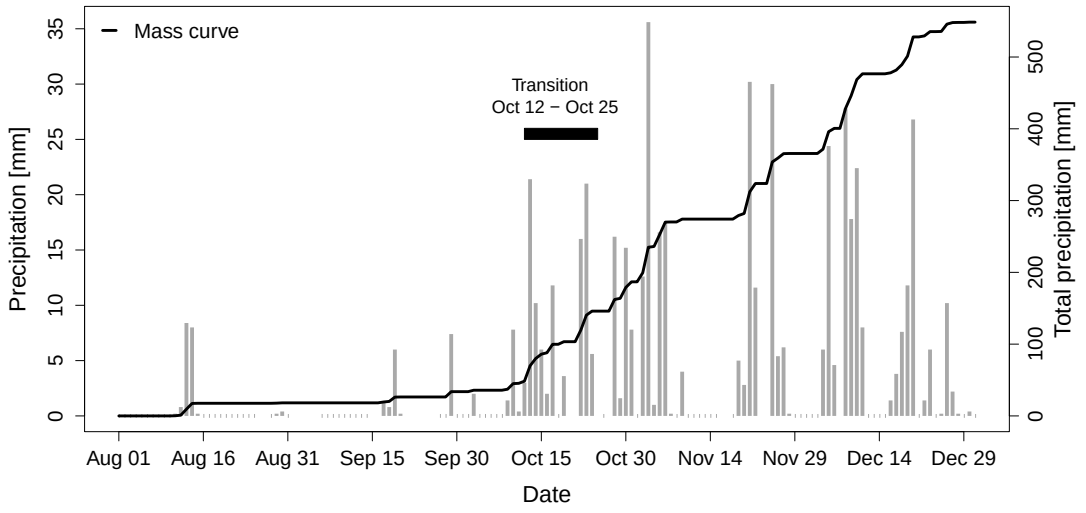

FIGURE 3.1: Precipitaion data from the "Richmond Nature Park" weather station 11.5 km north-west of the study site for the period between August 1 and December 31, 2014. [EnvironmentCanada, 2014]

the left half of the study site, where the peat is thicker, are stronger developed, thus suggesting a positive effect of peat thickness on mire breathing (see Table 3.2).

TABLE 3.1: Von Post indices at four locations at the site. Decomposition increases with ditch proximity and peat depth.

Location	Depth [cm]	von Post index
11	80 - 90	H4
11	100 - 130	H5 - H6
11	220 - 270	H8 (silty)
13	80 - 105	H4
13	105 - 130	H5
13	227 - 252	H5 - H6
27	80 - 130	H4 - H5
27	225 - 275	H8 (silty)
27	264 - 314	H8
27	422 - 472	H7 - H8
29	80 - 90	H5
29	90 - 120	H4
29	220 - 270	H7

Figure 3.2 shows the interpolated maps of the ground level and silt layer underlying the peat. The contour lines are spaced in 10 cm intervals and the colors indicate elevations in centimeters above sea level. Diagnostic plots of the input data (Figures A.2 and A.3), as well as variance maps and variograms (Figures A.4 and A.5), in addition to the target functions (Table A.2) are provided in the appendix. The values were interpolated to a

TABLE 3.2: Results from mire breathing measurements on November 29, 2014. The ground level changes in the left half of the study site, where the peat is thicker, are higher.

Location	North [m]	East [m]	Elevation change [cm]
3	5	60	6
6	5	140	2.5
10	10	20	6
14	10	80	2.5
22	20	100	4
25	25	60	5
26	25	140	3
31	35	100	2.5
Mean			**3.9**

$0.5 \times 0.5\ m^2$ grid, using a spline function and an exponential function for ground level and silt layer respectively. The mean ground level and mean silt depth lie at 1.542 m.a.s.l. and -1.529 m.a.s.l., respectively, yielding a mean peat thickness of 3.071 m (Table 3.3). The ground level map indicates a clear gradient towards the ditch. Table 3.4 provides the calculated gradients along transects running perpendicular to the ditch every 20 m. All measurements in ditch proximity were taken at a distance of 5 m, except for location 100, where the measurement was made 10 m away from the ditch. The strongest gradients occur in the eastern half of the site at a distance of 160 m along the ditch, which agrees with the interpolated map. Gradients calculated further to the west indicate still considerable slopes (e.g. at 80 m), which are not necessarily found on the map. This is due to the fact that not all gradients were calculated using the same distance. In this instance, the gradient was calculated between 5 and 15 m distance of the ditch, which covers only the steep zone at this location.

The underlying silt does not show as distinct of a gradient as the soil surface, being split into a shallower eastern part and a deeper western part, with mean silt depths of -1.288 m.a.s.l. and -1.723 m.a.s.l., respectively. The lowest point at location 27 with a depth of -2.798 m.a.s.l clearly sticks out of the otherwise fairly consistent zone in the west.

Figure 3.3 illustrates the surveyed ditch face where all trough and pipeflow measurements were executed. The mean elevation at the top is 0.756 m.a.s.l , while the ditch bed lies at -0.385 m.a.s.l, therefore yielding a mean height of 1.14 m. The face shows a mostly parallel shape of top and bottom, except for the section between 10-50 m. Here, a vegetated island caused the increased elevation at the face bottom and also narrowed

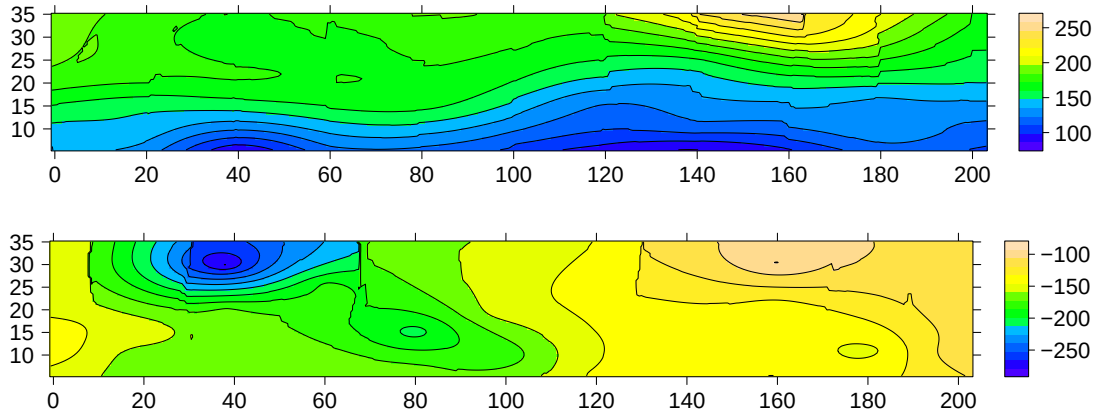

FIGURE 3.2: Soil surface (top) and silt layer (bottom) maps of the study site. Kriging was used to interpolate measurements to a 0.5×0.5 m^2 grid; the contour lines are spaced in 10 cm intervals. The boundary ditch forms the southern limit at the bottom of the maps.

TABLE 3.3: Main parameters soil surface and silt layer. The data is aggregated to strata running parallel to the ditch. All measurements are provided in cm above sea level.

Stratum	Ground			Silt			Difference		
	Min [cm]	Max [cm]	Mean [cm]	Min [cm]	Max [cm]	Mean [cm]	Min [cm]	Max [cm]	Mean [cm]
5	87.6	128.8	106.8	-170.3	-132.1	-151.1	222	296.5	257.9
10	118.6	147.3	132.3	-181.7	-110.6	-149.4	231	310	281.7
15	124.1	163.4	142.9	-204.6	-135.8	-158.9	269	368	301.8
20	148.4	178.3	162.2	-169	-109.6	-143.4	258	340	305.6
25	160.6	169.8	165.2	-182.2	-125.4	-153.8	286	352	319
30	167.2	222.1	188.4	-279.8	-91.9	-174.6	314	447	363
35	170.8	191	181.3	-156.3	-112.2	-139.2	283	340	320.5
Mean	**87.6**	**222.1**	**154.2**	**-279.8**	**-91.9**	**-152.9**	**222**	**447**	**307.1**

the ditch by approximately 1 m. A general difference between east and west as evident in the silt layer was not noted.

3.3 Water table analysis

Two water table maps in Figure 3.4 present the mean water tables in cm above sea level during the dry and wet periods of the study. An exponential function was used to interpolate the measurements to a 0.5×0.5 m^2 grid, with contour lines of 10 cm spacing. Diagnostic plots (Figures A.6 and A.7), variance maps (Figure A.8), variograms

TABLE 3.4: Soil surface gradients perpendicular along the ditch every 20 m. The gradients were calculated from the two furthest appart locations at each stratum. North refers to the location further away (therefore north) of the ditch, whereas south is the measurement next to the ditch.

Location [m]	Easting	North [cm]	South [cm]	Distance [m]	Gradient [%]
0	502084	191	147.3	25	1.75
20	502105	150.8	128.8	10	2.20
40	502125	167.2	89.7	25	3.10
60	502145	169.8	119.8	20	2.50
80	502165	163.4	118.3	10	4.51
100	502185	182.2	124.8	25	2.3
120	502204	124.1	94.8	10	2.93
140	502224	160.6	87.6	20	3.65
160	502244	222.1	95.9	25	5.05
180	502265	133.2	119.6	10	1.36
200	502285	170.8	147.3	25	0.94
Mean					**2.753**

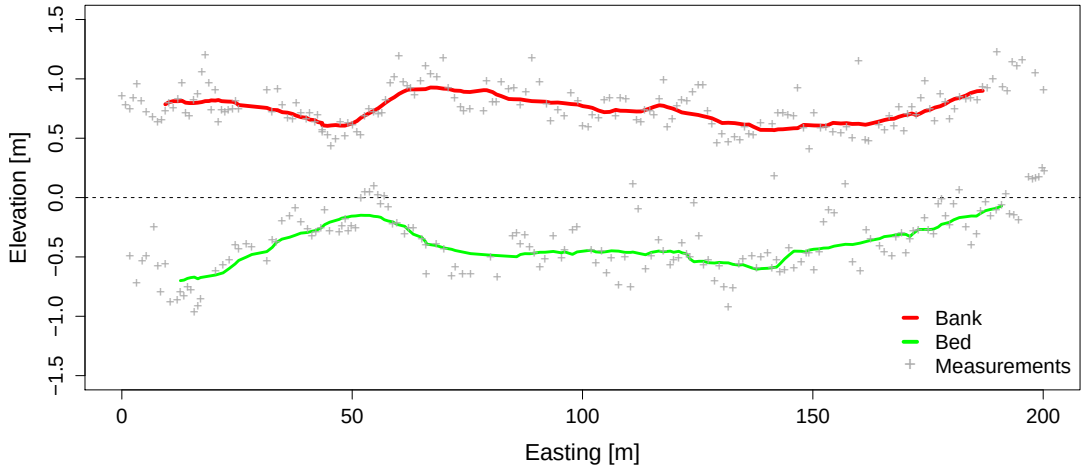

FIGURE 3.3: Surveyed bog face along the ditch section, where all trough and pipeflow measurements were executed. The mean height is 114 cm. A total of 350 measurements was used to create the profile. To compute this figure a moving average with a window size of 20 was run.

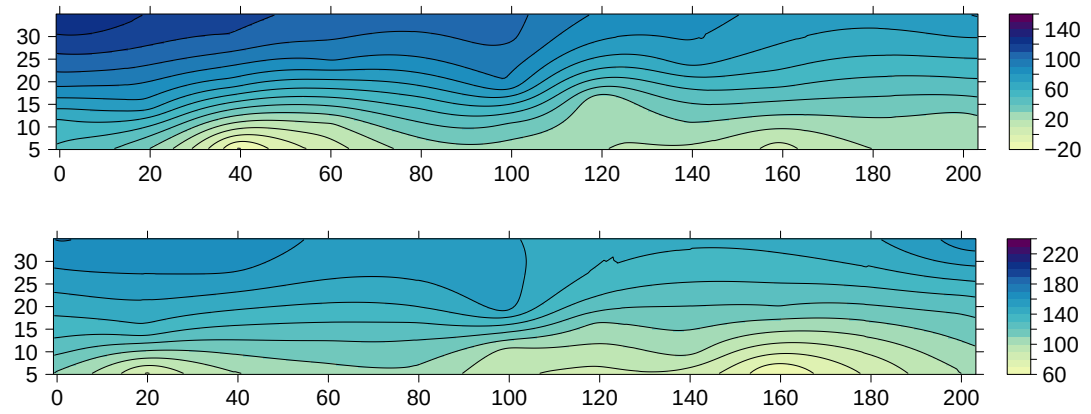

FIGURE 3.4: Water table during the dry (top) and wet period (bottom) at the study site. Kriging was used to interpolate measurements to a 0.5×0.5 m^2 grid; the contour lines are spaced in 10 cm intervals. The boundary ditch forms the southern limit at the bottom of the maps.

(Figure A.9) and target functions (Table A.4) can be found in the appendix. Both water tables show a clearly formed gradient towards the ditch.

During the dry period a stronger gradient became established in the left half of the site, which coincided with the deeper silt layer in this part. A zone with a particularly deep water table developed at a distance of 50 m along the ditch, at the same location where the ground level was lowest. It is worth noting that the ground level gradients, up to a distance of 15 m from the ditch in Figure 3.2, seem to be adapted to the water table. Further back in the bog, where the ground level in the right part of the site experiences a steep slope, the water table is not affected.

High water tables after the transition from dry to wet period show a similar spatial pattern as prior low water tables. The strong gradient within the first 90 m along the ditch disappeared. Instead the zone of lowest water table shifted towards the 150 m mark. At the same location the bog face exhibits a depression, as observable in Figure 3.3. When comparing face shape and water table further, one can find more conformity at a distance of 75 m, where the water table is more elevated than the water table in its proximity.

The different water table gradients towards the ditch during dry and wet periods as observed on the maps are also evident when comparing water table depths of the strata in Table 3.5. Water level changes with distance to the ditch are more consistent during

Table 3.5: Main parameters of water tables during dry and wet period. All measurements are given in cm below soil surface.

Stratum	Dry			Wet			Difference
	Min [cm]	Max [cm]	Mean [cm]	Min [cm]	Max [cm]	Mean [cm]	Mean [cm]
5	-111.9	-72.9	-94.1	-49.9	-6.8	-30.6	63.5
10	-127.2	-81.4	-98.4	-29.8	-9.9	-19.3	79.1
15	-114.7	-65.8	-96.3	-37.5	-13.2	-22	74.3
20	-103.8	-67.1	-91.5	-34.2	-4.3	-24.3	67.2
25	-92.7	-76.2	-83.5	-30.2	-20	-25	58.5
30	-148.2	-56.5	-90.2	-24.2	-1.6	-12.4	77.8
35	-102.3	-58.4	-79.6	-19.7	-0.8	-10.4	69.2
Mean	**-114.4**	**-68.3**	**-90.5**	**-32.2**	**-8.1**	**-20.6**	**69.9**

the end of summer than after the transition. These inconsistencies are, however, not necessarily noticeable on the maps.

Prior observations indicate a relationship between water table and ground level. Table 3.6 lists the results from the shape comparison between dry and wet water tables with the soil surface and silt layer respectively, under steady-state conditions. The output from the wet period was negligibly influenced by the sample size, so the 15 values from the wet period provide a reliable estimation. A standard deviation of zero would proove perfectly identical shapes, but there is no lower limit for it. It is obvious that the water table shape is always closer related to the shape of the soil surface than the silt layer. This supports prior observations, when water table maps and topographic maps were compared. To further investigate this relationship a correlation was executed between ground level and water table height. As expected the positive relation is considerably close with an R^2 of 0.86 and 0.83 for the dry and wet period, respectively (Figure 3.5).

During the dry period the water table had a mean depth of -90.5 cm below the ground considerably lower than the wet water table at -20.6 cm (Table 3.5). Once precipitation started at the beginning of the transition, it took only 13 days for the water level to rise from 66.2 cm.a.s.l to 123.0 cm.a.s.l, which equals a rate of 4.4 $cm\ day^{-1}$ (Figure 3.6). A lack of precipitation between November 10 and November 18 caused a nicely formed recession curve of the mean water table; a second considerable water table decrease occurred between November 29 and December 3, due to the absence of rain as well.

TABLE 3.6: Calculated standard deviation of separation distance between dry/wet water table and soil surface/silt layer to evaluate similarity of shapes. A value of 0 suggests perfect unity of shapes; there is no lower boundary. The small sample size during the wet period did not affect the result.

	StandDev	No. Measurements
Dry		
Ground	178.63	814
Silt	477.09	814
Wet		
Ground	122.55	15
Silt	490.85	15

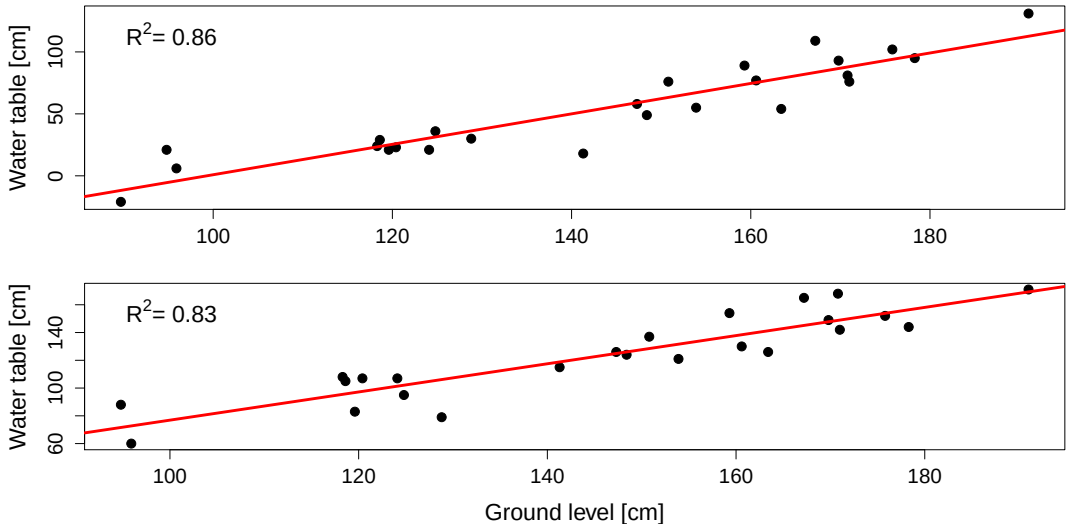

FIGURE 3.5: Correlation plots of dry water table (top), and wet water table (bottom), with ground level. The R^2 values suggest a rather close relationship between the variables.

3.4 Groundwater flow analysis — Bog

3.4.1 Horizontal flow

Potentiometric maps were computed in a weekly interval. Due to the consistent behavior of the system, three maps were selected to provide an overview. The maps were calculated for October 9, October 30 and December 4, 2014 (see Figure 3.7). The remaining maps are provided in the appendix (Figure A.10). A 0.5×0.5 m^2 grid was used to compute the maps with contour lines equally spaced at a 10 cm interval. The hydraulic heads are measured 75 cm above the silt layer. The general water flow directions are

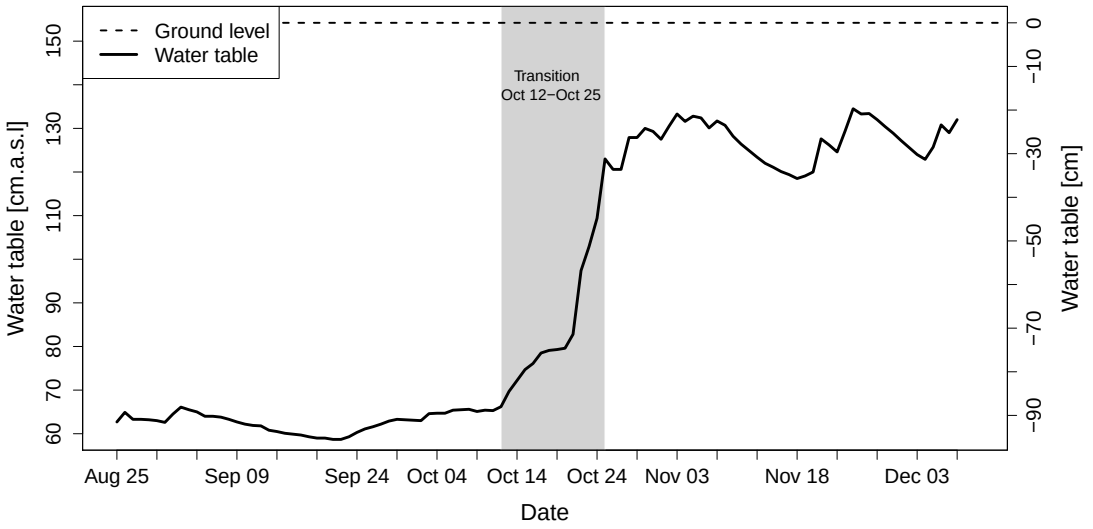

FIGURE 3.6: Mean water table during the study period. During the transition from dry to wet conditions, which took 13 days, the mean water table change was 4.4 $cm\,day^{-1}$.

towards the ditch during the entire field campaign. The hydraulic heads change rather consistently over the whole site, except for location 6.

From October 9 until October 23 the ground water flow pattern is quite similar. 160 m along the ditch at location 6, the hydraulic head was much lower than at the rest of the site. The strong hydraulic gradient reaches up to 15 m into the bog and spreads approximately up to 45 m parallel to the ditch. The same behavior but with a less strong extent can be observed at location 3, where the second piezometer at this distance is installed. The hydraulic heads further inside the bog are higher and with more similar values so that a zone of more or less equal hydraulic potential develops over several tens of meters parallel to the ditch.

After October 23 the hydraulic head at location 6 changes dramatically. As indicated on the map from October 30, the hydraulic head adapted to the surrounding conditions, therefore changing the flow on the right of the study site. The smaller gradient shows a smaller impact on its proximity, thus enabling groundwater flow to become more similar to the flow in the western part of the site.

From October 30 onwards, there are only minor changes over time. The rate of hydraulic head change is similar throughout the site, hence preserving similar flow directions. It is interesting to note that the piezometer in the center at location 22 is always in good accordance with the surrounding hydraulic heads. There is no map on which it develops

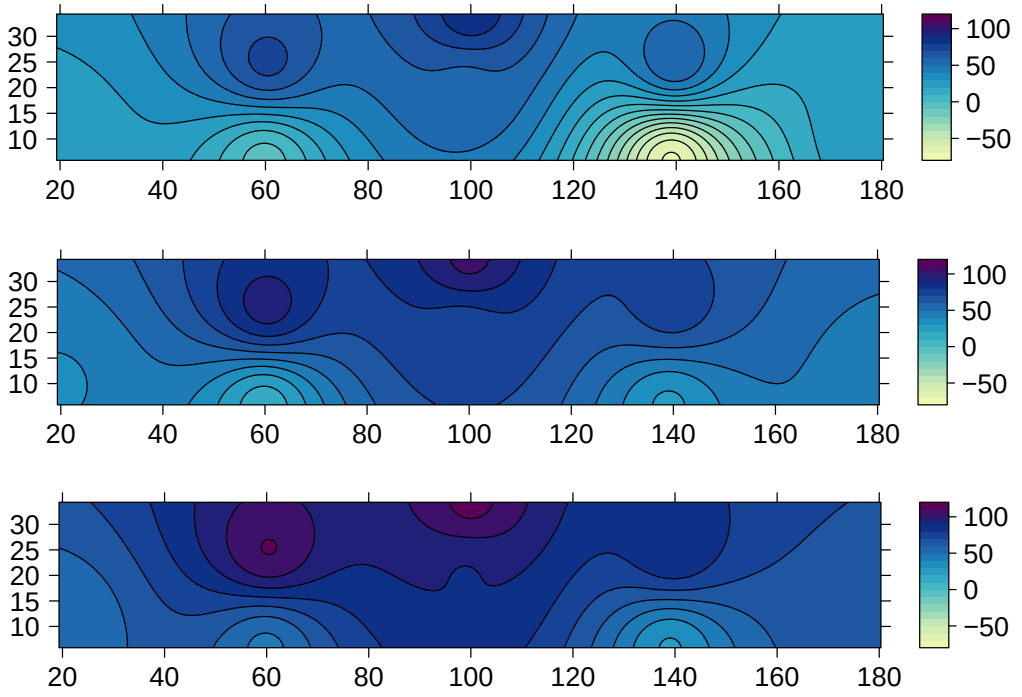

FIGURE 3.7: Potentiometric maps of the groundwater at the site on: October 9, 2014 (top), October 30, 2014 (middle) and December 4, 2014 (bottom). All values are presented in cm above sea level. Inverse distance weighting was used to interpolate measurements to a 0.5×0.5 m^2 grid; the contour lines are spaced in 10 cm intervals. The boundary ditch forms the southern limit at the bottom of the maps.

a circular gradient as most others do. The same can be said about the piezometers at locations 10 and 14 for most of the time.

The similar increase in hydraulic head throughout the site is clearly evident in Figure 3.8, which shows measurements between October 7 and December 6. On October 25 hydraulic head at piezometer 6 increases dramatically from -52 cm up to 24 cm above sea level. Piezometer 3 experiences a change in recharge rate as well, together with the shallow piezometers 22.1 and 31, which already experienced a significant change in hydraulic head on October 21. 25.1 and 26.1 are the only deep piezometers that show a small but noticeable reaction.

3.4.2 Vertical flow

Figure 3.9 displays the computed vertical hydraulic gradients at locations 22 and 31 between October 7 and December 6. Due to logger maintenance there is a data gap

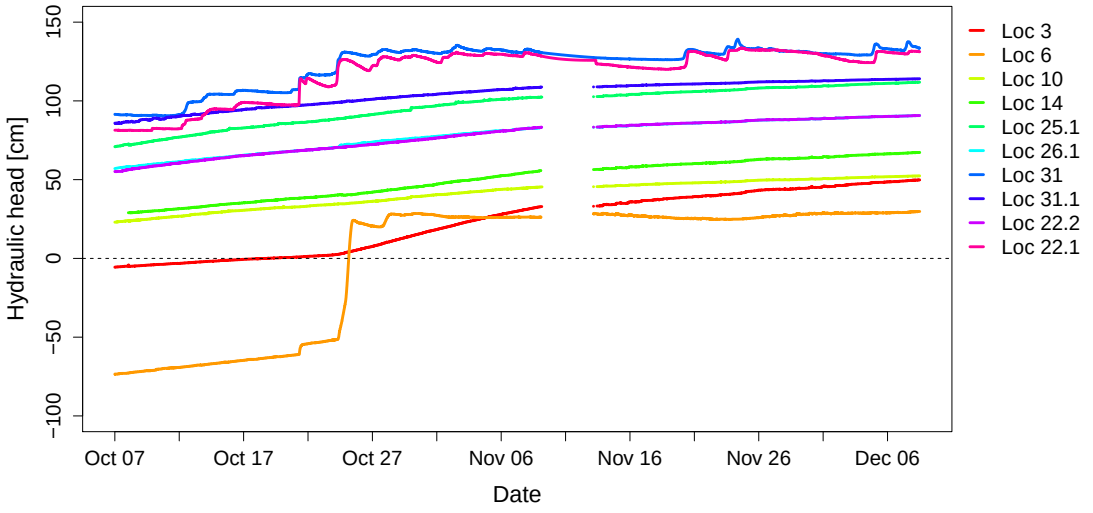

FIGURE 3.8: Time series of all piezometer measurements. Data prior to October 7 was removed during quality tests, because it was suggested to not having equilibrated at that point. The data gap is a result from logger maintenance. Hydraulic heads are given in cm above sea level.

between November 10 and November 12, 2014. The gradients at both sites are always negative, therefore indicating downward percolation through the peat. They vary between -0.13 and -0.33 as well as 0 and -0.16 at piezometer 22 and piezometer 31, respectively. Location 31, which is 15 m further inside the bog, shows a less negative hydraulic gradient throughout the measurement period. Generally, both gradients display considerable fluctuations, which result from the rather steady behavior of the deep piezometers and the contrasting, therefore inconsistent, behavior of the upper piezometers (see Figure 3.8). Fluctuations at both locations follow the water table changes, whereas the stronger changes occur at piezometer 22.

3.5 Water table and hydraulic gradients — Ditch

Water table and hydraulic head measurements in the ditch are illustrated in Figure 3.10 and 3.11. All measurements were referenced to an arbitrary datum so that the absolute values cannot be compared among each other. The shapes, on the contrary, are comparable.

It is striking that the automated water table measurements at locations 100 and 140 are almost identical, whereas all manually measured values seem to show no relationship to the continuous measurements. Between October 21 and November 5, the water table

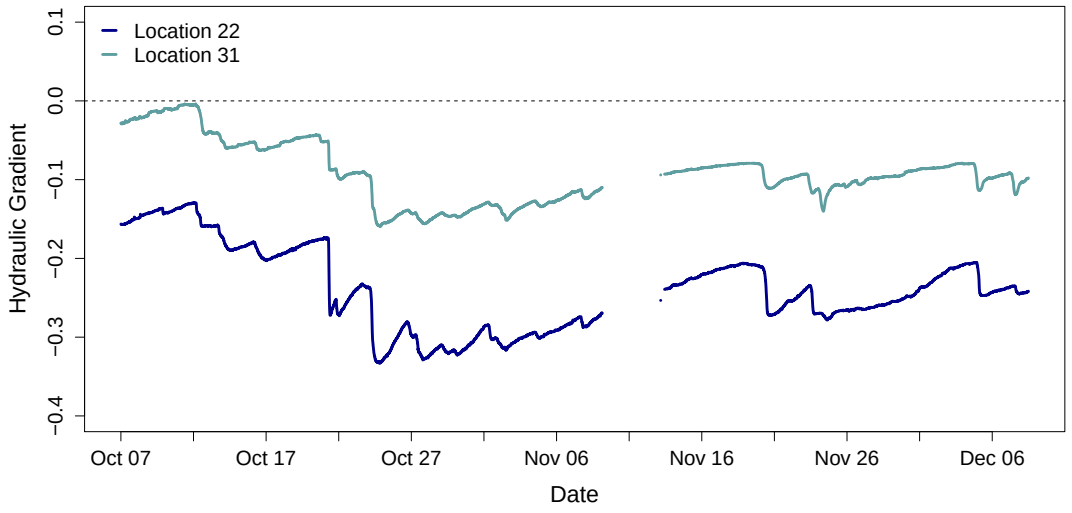

FIGURE 3.9: Vertical hydraulic gradient at locations 22 and 31. All hydraulic heads are given in cm above sea level. The fluctuations originate from the inconsistent upper piezometer measurements, which fluctuated due to water table changes.

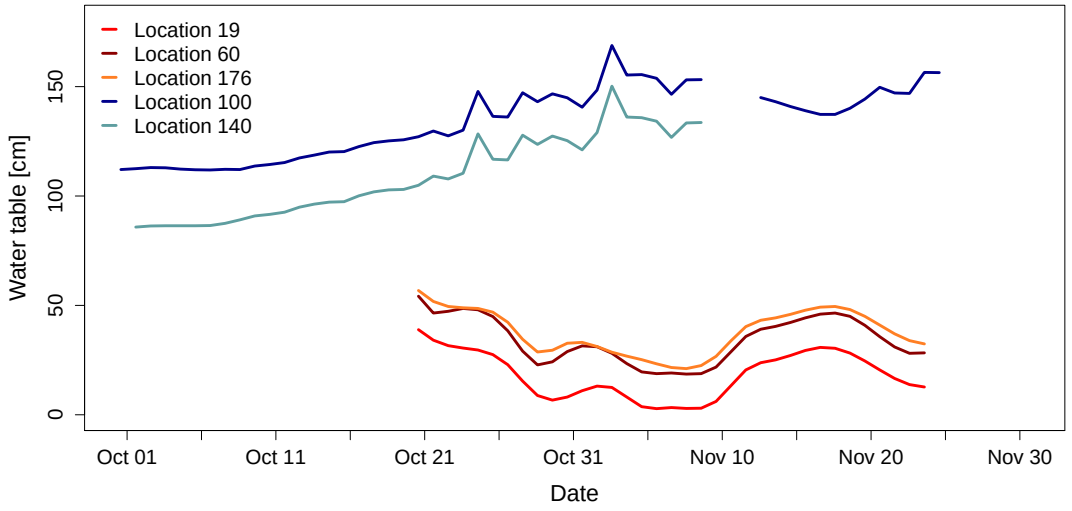

FIGURE 3.10: Ditch water levels at locations 19, 60, 100, 140 and 176. All water levels are presented in cm above the silt layer, therefore an arbitrary datum, which is why the absolute heights cannot be compared. Nevertheless, the shapes of the water tables are very well comparable.

increased at locations 100 and 140, whereas the other measurements suggest a decreasing water level.

Results from the piezometers are illustrated in Figure 3.11. The measurements are similar to the water tables heights. Except for location 100, all piezometers experience considerable hydraulic head fluctuations, which resemble the water table changes at these locations. Again automated and manual measurements behave contrarily. Because of

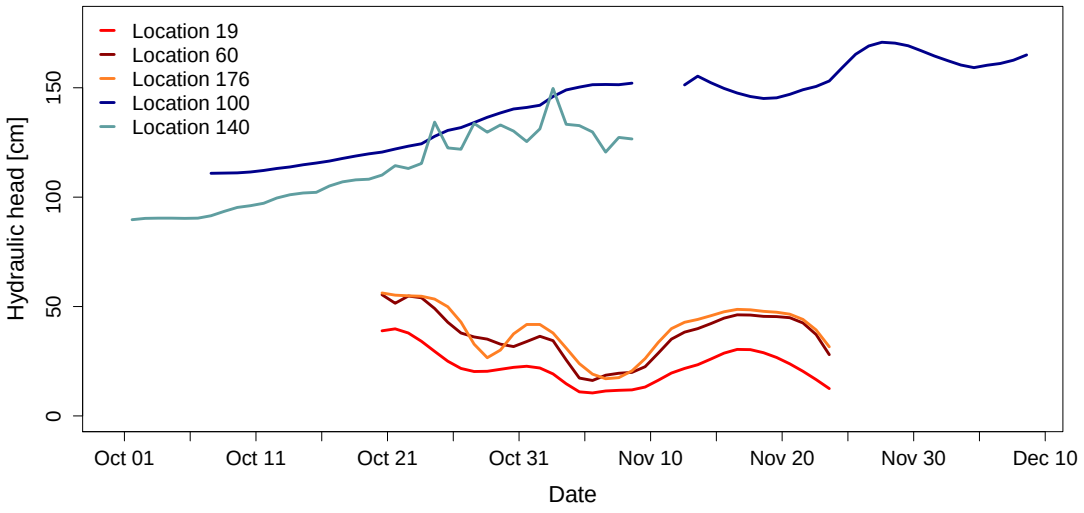

FIGURE 3.11: Hydraulic heads in the ditch at locations 19, 60, 100, 140 and 176. All water levels are presented in cm above an arbitrary datum.

the lower measurement interval of water table heights as well as hydraulic heads, the manual values show a steadier development over time.

The computed hydraulic gradients are given in Figure 3.12. All gradients vary between 0.3 and -0.45. Before the transition the two automated locations show very constant gradients; -0.03 and 0.08 for locations 100 and 140, respectively. Afterwards, location 140 stays rather steady until November 3, when it turns negative. Location 100 on the other hand experiences more negative gradients, once the transition starts. After October 24, piezometer 100 displays strong fluctuations in hydraulic gradient. It stays mainly negative, hence discharging into the ground, until November 9 when the gradient changes direction.

The manually quantified gradients at locations 19, 60 and 176 roughly act alike. It seems as if locations 19 and 176 lag behind location 60, even though the lag time varies. For example, piezometer 60 shows a peak on October 29; piezometer 19 displays the same peak on October 30, whereas piezometer 176 does not experience the same peak until November 2. At the end of the measurement period all three locations show a simultaneous reaction again, as in the beginning.

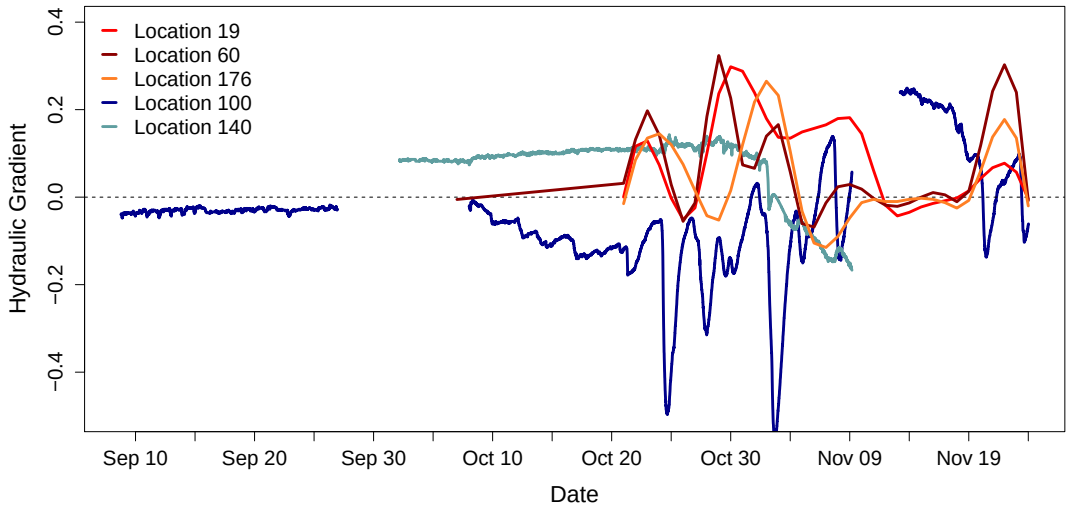

FIGURE 3.12: Hydraulic gradients in the ditch at locations 19, 60, 100, 140 and 176.

3.6 Saturated hydraulic conductivity

Saturated hydraulic conductivities are listed in Table 3.7. The bog conductivities were calculated by means of slug tests, whereas the ditch conductivities were quantified using Darcy's law. Bog measurements vary within one order of magnitude, except for location 26, whose hydraulic conductivity is one order of magnitude higher. The conductivities increase a little with distance from the ditch. A depth related trend is also observable; conductivities decrease with increasing depth.

In contrast to the relatively consistent bog measurements, ditch saturated hydraulic conductivities vary considerably over three orders of magnitude. At location 100 the piezometer is installed the deepest. It showed a less flashy hydraulic head regime and experiences the lowest hydraulic conductivities. The other piezometers show no depth related pattern in conductivities.

3.7 Lateral flow survey

Figure 3.13 illustrates the results of the two lateral flow surveys on November 12 and December 5, 2014. Black bars indicate installed troughs. Note that the "none" category of the second survey experienced small outflow after November 26. During both surveys more than half of the ditch section is classified as "none" (see Table 3.8). "Low" and

TABLE 3.7: Calculated hydraulic conductivities for bog and ditch in $[m s^{-1}]$. Hydraulic conductivities in the bog were received from slug test with the approach introduces by Hvorslev [1951], whereas the ditch hydraulic conductivities were obtained by employing Darcy's law with seepage measurements and hydraulic gradients.

Location	Type	Depth [m]	Screen length [m]	Hydraulic Conductivity $[m\ s^{-1}]$
Bog				
31	DP	2.655	0.5	1.18×10^{-8}
26	P	2.085	0.5	1.22×10^{-7}
22	SP	1.105	0.5	6.18×10^{-8}
22	DP	2.425	0.5	1.25×10^{-8}
Mean				$\mathbf{5.21 \times 10^{-8}}$
Ditch				
19	P	0.49	0.1	1.54×10^{-3}
60	P	0.38	0.1	6.32×10^{-4}
100	P	0.505	0.5	7.91×10^{-5}
140	P	0.475	0.3	1.41×10^{-4}
176	P	0.4	0.1	1.19×10^{-3}
Mean				$\mathbf{7.15 \times 10^{-4}}$

"medium" contribute about the same fraction and "strong" is by far the smallest class. Category size change over time is most relevant for classes "strong", which is reduced to about half its initial size and "medium", which gains approximately one fifth. The other two categories stay roughly the same.

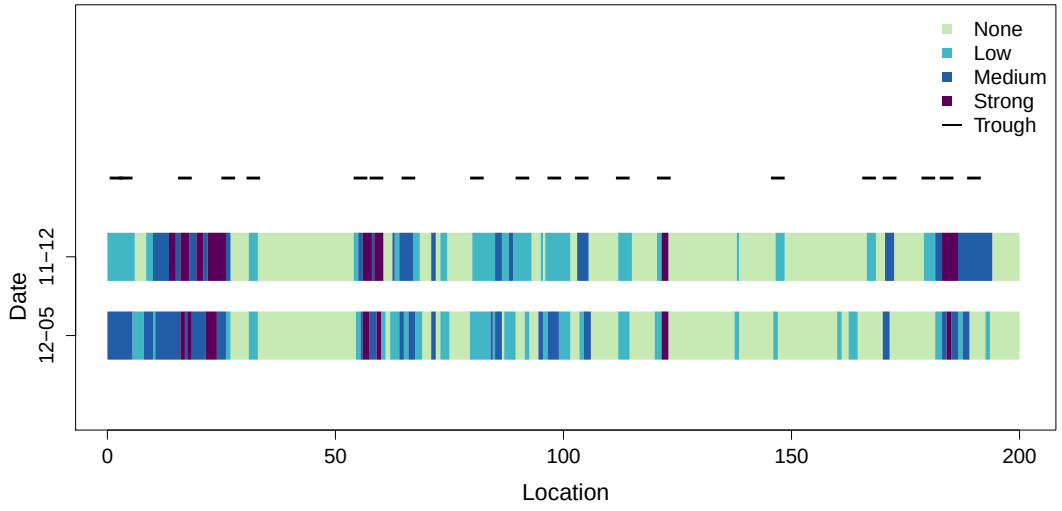

FIGURE 3.13: Lateral flow survey on November 12 and December 5, 2014. The occurring lateral flow at the bog face was categorized in four classes, which were used as strata for the runoff estimation by means of trough measurements.

The spatial distribution of runoff stays about the same in most cases. "Strong" sections

TABLE 3.8: Fractions of lateral flow categories at the bog face. Each category acts as stratum for later outflow quantification. Values are provided as accumulated bog face lengths of the category.

	Category				
	None [m]	Low [m]	Medium [m]	Strong [m]	Sum [m]
November 12, 2014	110	42	30	18	200
December 5, 2014	114	40	36.5	9.5	200

within the first 50 m and at location 185 shift towards "medium" classification. When comparing the runoff classes with the surveyed ditch face, it is remarkable that strong flow was almost exclusively found at elevated face top locations, which is contrary to what one might assume at first.

3.8 Outflow

All lateral flow measurements show a data gap between November 24 and December 1, which was caused by a complete flooding of the entire ditch section, thus making it impossible to run any outflow measurements.

By means of cross-correlation it was found that all runoff processes show the closest relation to the water table when a time lag of one day was applied. To facilitate the evaluation of the relationships between water table and total seepage, as well as total lateral outflow and pipeflow, the water table in the following figures was shifted by one day. Lines in the plots do not represent interpolated data. They were added to facilitate distinction between time series.

3.8.1 Seepage

The mean value of all seepage measurements is 5.43 $m^3\,day^{-1}$. Figure 3.14 shows all seepage measurements along the ditch section. Early measurements are held in a light blue color, whereas later measurements are colored dark blue and purple. The greatest part of the measurements is within a range of up to 30 $L\,m^{-2}\,day^{-1}$. Higher values are restricted to location 19, as well as the section between 70-105 m and one more at 190 m. It is notable that there are no measurements below 10 $L\,m^{-2}\,day^{-1}$ in the section

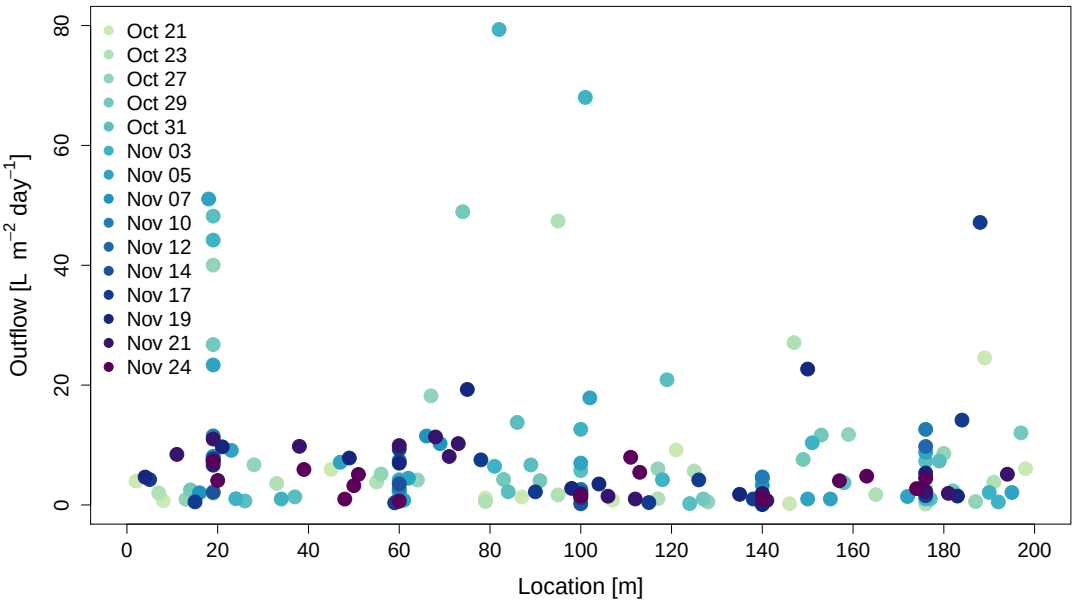

FIGURE 3.14: Spatially resolved seepage rates along the ditch section in $L\,m^{-2}\,day^{-1}$. Light colors indicate early measurements during the campaign, whereas dark blue and purple represent measurements from during the end of the study period.

60-80 m and except for location 19 there are no values above 17.5 $L\,m^{-2}\,day^{-1}$ along the ditch between 0-60 m.

It is striking that with exception of the measurement on the far right side, all high seepage rates were measured early during the campaign. Aside from that, there is no obvious pattern recognizable in this figure.

When taking a closer look at the permanently installed seepage meters, location 60 stands out by not showing predominantly low values later in the campaign, as all others do. Location 19 shows by far the largest range in values over the measurement period, followed by locations 60, 100 and 176 with a rather stable behavior and finally location 140 with only small fluctuations over time.

The total seepage varies between 1 $m^3\,day^{-1}$ and 8 $m^3\,day^{-1}$ (Figure 3.15). During the transition the total seepage increases as does the water table, until it reaches a level above 5.8 $m^3\,day^{-1}$ where it remains until November 5. Afterwards the total amount decreases to values around 5 $m^3\,day^{-1}$ where it remains until November 19, after which it reduces further. November 14 marks a day of extraordinarily low seepage with only 1.1 $m^3 day^{-1}$. The relationship between water table and total seepage seems to be rather loose. The seepage amount roughly follows the regime of the water table in the sense

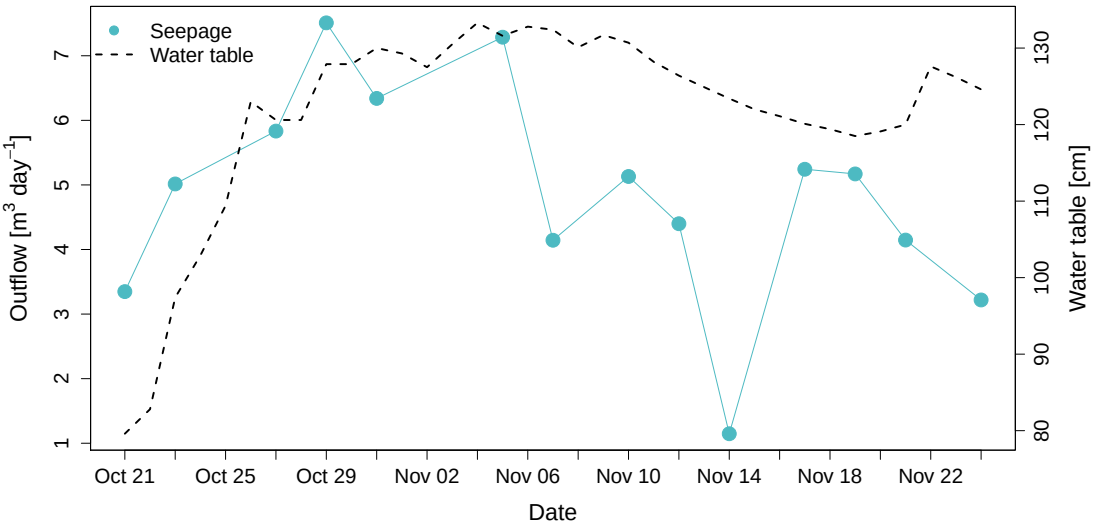

FIGURE 3.15: Time series of total seepage for the entire site in $m^3 day^{-1}$ The connection between seepage yield and water table seems to be only loose.

that it increases during the transition and decreases from November 5 onwards, but smaller fluctuations of the water table do not seem to affect the seepage curve, which is also reasoned by the low measurement interval.

Figures with time series of all permanent installed seepage meters are provided in the appendix (Figure A.11).

3.8.2 Lateral flow

The mean values of all measurements for the "assigned", "ranked" and "threshold" approach are 90.44 $m^3\ day^{-1}$, 174.79 $m^3\ day^{-1}$ and 249.46 $m^3\ day^{-1}$, respectively. In Figure 3.16, all trough measurements are illustrated along the ditch section. As displayed previously, early measurements are colored lighter than later ones. All troughs indicate low runoff measurements in the beginning, so that higher lateral flows only developed over time. "Strong" categorized troughs (17, 59, 122 and 184) show, with exception of location 59, a large range of runoff values. Locations 98, 104, 147 and 190 show particularly little change in runoff during the entire field campaign.

The three different approaches to quantify lateral flow are presented in Figure 3.17. They range between almost 0 $m^3 day^{-1}$ and up to 600 $m^3 day^{-1}$, depending on the calculation method. All three approaches respond according to water table fluctuations and therefore suggest a close relation between water table and lateral flow. Until November 24 all

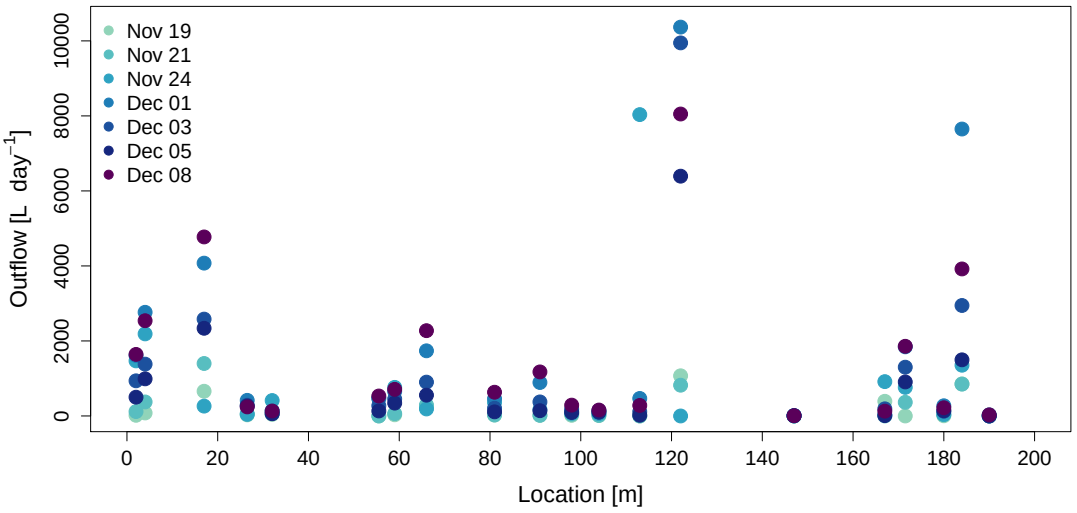

FIGURE 3.16: Spatially resolved lateral outflow rates along the ditch section in $Lday^{-1}$. Light colors indicate early measurements during the campaign, whereas dark blue and purple represent measurements from during the end of the study period.

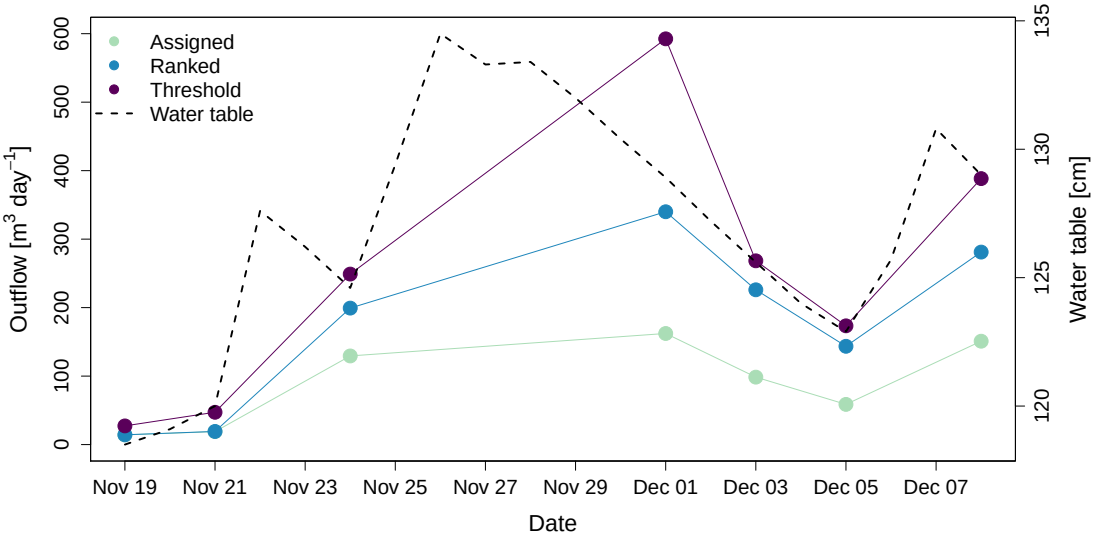

FIGURE 3.17: Time series of total lateral flow for the entire site in $m^3\ day^{-1}$. Apparently the relationship between water table and lateral flow is very close.

three curves behave quite similar, especially the runoff amounts are fairly the same. It is striking, that with increasing water table the difference in lateral flow yield amplifies until December 3. When the water table falls afterwards, so do the runoffs in all three time series. The disagreement of runoff and water table height between November 24 and December 5 is caused by the data gap due to the flooded ditch section.

Time series of each trough are grouped by runoff volume and added to the appendix (Figure A.12 and A.13).

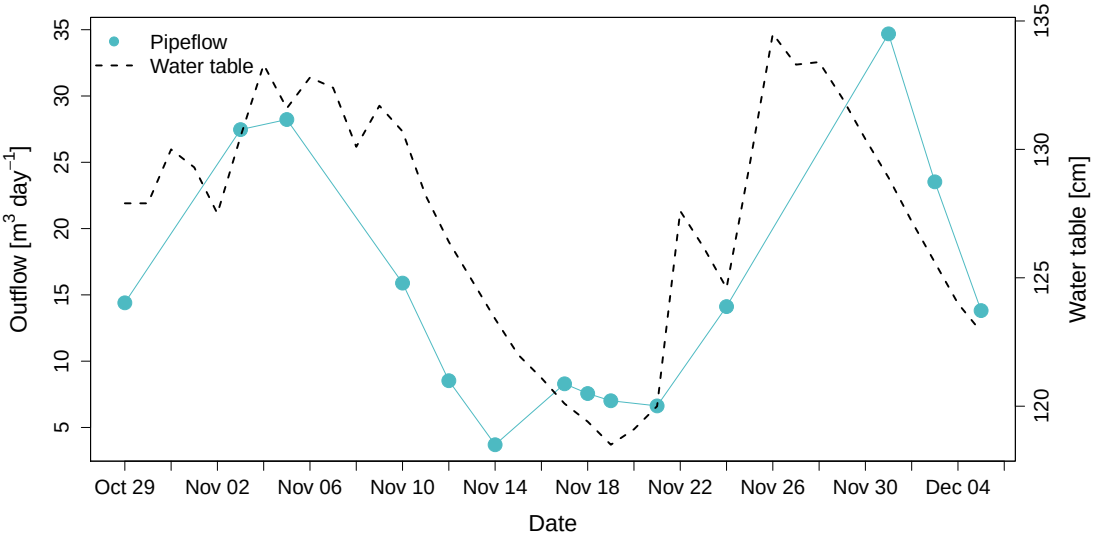

FIGURE 3.18: Time series of total pipeflow for the entire site in $m^3\ day^{-1}$.The relationship between pipeflow and water table seems to be fairly good.

3.8.3 Pipeflow

Mean value of all pipeflow measurements is 15.28 $m^3 day^{-1}$. Figure Figure 3.18 illustrates the measured pipeflow at location 177. During the measurements pipeflow occurred with rates of up to 35 $m^3\ day^{-1}$. The response on water table changes is fairly consistent. Only the increase in pipeflow from November 14 to November 17 does not agree with the falling water table.

3.9 Reservoir Model

The reservoir model used water table heights in relation to the sea level, in order to avoid uncertainties due to mire breathing. The mean ground elevation is 1.542 m.a.s.l, so that measurements can be easily converted. For the reservoir model each process (seepage, lateral flow and pipeflow), was fitted separately. The target functions are given in Table 3.9; all errors were calculated in $m^3\ day^{-1}$.

3.9.1 Seepage

Figure 3.19 presents the fitted model for measured seepage rates. The measurements generally show a loose relationship, as three values stick out notably. The two values

TABLE 3.9: Target functions and fitted parameters for each process of the reservoir model. "a.fit" determines the slope of the model and dictates together with "b.fit", which defines the curvature of the model, how sensitive the model reacts to water table fluctuations. "c.fit" controls at which water table the process initializes and thus acts as threshold.

	Seepage	Assigned	Ranked	Threshold	Pipeflow
mbe	0.24	0.39	1.92	2.87	0.98
rmse	1.84	17.34	23.07	62.31	7.57
mae	1.5	12.93	19.24	41.26	6.63
nse	-0.2094	0.9193	0.9656	0.9002	0.3775
a.fit	36.14	0.27	0.07	1.47	2.99
b.fit	0.5	0.73	0.88	0.38	0.49
c.fit	40	117.14	118	113.44	114.19

at water tables of 83 cm and 103 cm were surveyed on October 21 and October 23, respectively. Even though they do not fit in nicely with the rest of the data points, they are important, because they are the only measurements providing data at lower water levels in the ditch. The third dot which does not agree with most of the other values was measured at a water table height of 122 cm, on November 14. Most seepage rates were quantified at water tables between 120-135 cm. The measurements suggest a broad range of seepage volume, which is minimally influenced by water table fluctuations. This observation agrees with the previously presented seepage rates and the target functions of the model. The Nash-Sutcliffe-Efficiency is -0.21, thus indicating that the simple mean of all measurements would perform better than the model. The models y-intercept at 40 cm.a.s.l or -114.2 cm below the soil surface indicates at which water level the process initializes according to the model.

3.9.2 Lateral flow

All three lateral flow models are plotted in Figure 3.20. Even though the absolute flow rate differs considerably, all measurements line up nicely without outliners, so that good model fits were achieved. The Nash-Sutcliffe-Efficiencies for the "assigned", "ranked" and "threshold" approach are respectively, 0.92, 0.97 and 0.9. Generally, all three models agree well at low lateral flows up to 50 $m^3\ day^{-1}$; the first two measurements of approach "assigned" and "ranked" are even identical. Because of differently fitted slope and curvature parameters, the models start to spread considerably with increasing water tables. The modeled runoffs at a water table of 125 cm yielded values of 101 $m^3\ day^{-1}$,

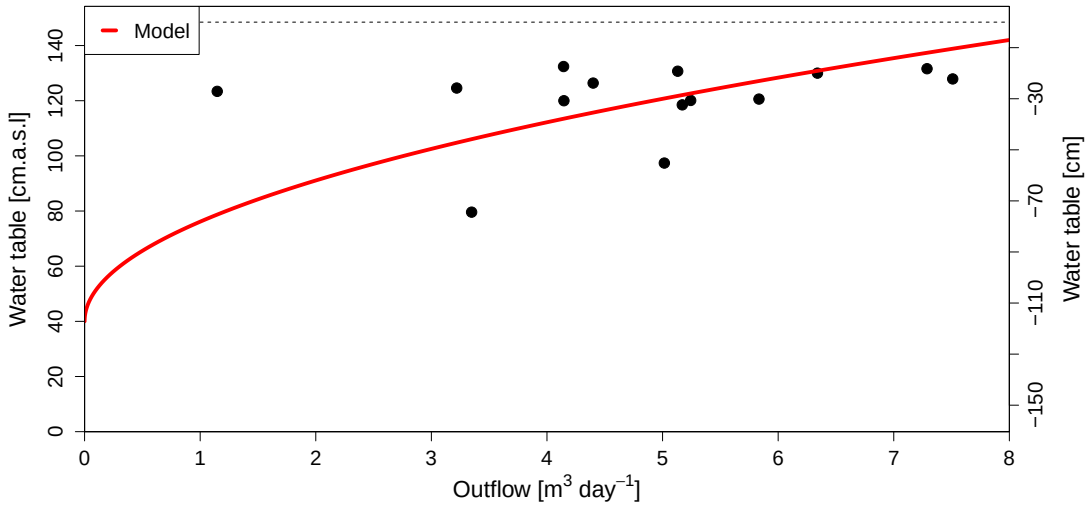

FIGURE 3.19: Seepage model, which was fitted at 15 seepage measurements. The performance is poor, so that the simple mean value acts as better estimator in theory.

198 $m^3\ day^{-1}$ and 241 $m^3\ day^{-1}$for the "assigned", "ranked" and "threshold" model, respectively. The reason lies again with the fitted parameters. Small slope parameters as for example in the "threshold" model make it very sensitive to water table changes. Consequently, model "assigned" is more robust in this sense, which is evident in the smaller range of runoff measurements. It is noteworthy that the y-intercepts ("c" parameter) of all models are quite similar (see Table 3.9). The parameter marks the water table at which the processes initialize. This is for the "assigned", "ranked" and "threshold" model, resepctively: 117.1 cm.a.s.l, 118 cm.a.s.l and 113.4 cm.a.s.l or with the soil surface as reference, -37.1 cm, -36.2 cm and -40.8 cm.

3.9.3 Pipeflow

All pipeflow measurements are presented in Figure 3.21. The behavior is comparable to the observed lateral flow. Even though the measurements do not line up as nicely as the lateral flow, they still display a clear pattern without any outliners. The Nash-Sutcliffe-Efficiency of 0.38 is not great but decent enough to get a good idea of the behavior of the observed outflow. It is striking that the y-intersect is very similar to the ones obtained from all lateral flow models (114.2 cm.a.s.l or in relation to the soil surface -40 cm). This suggests that the processes generating the outflow must be the same or at least closely related. The relatively flat slope makes the pipeflow sensitive to only small changes in water table.

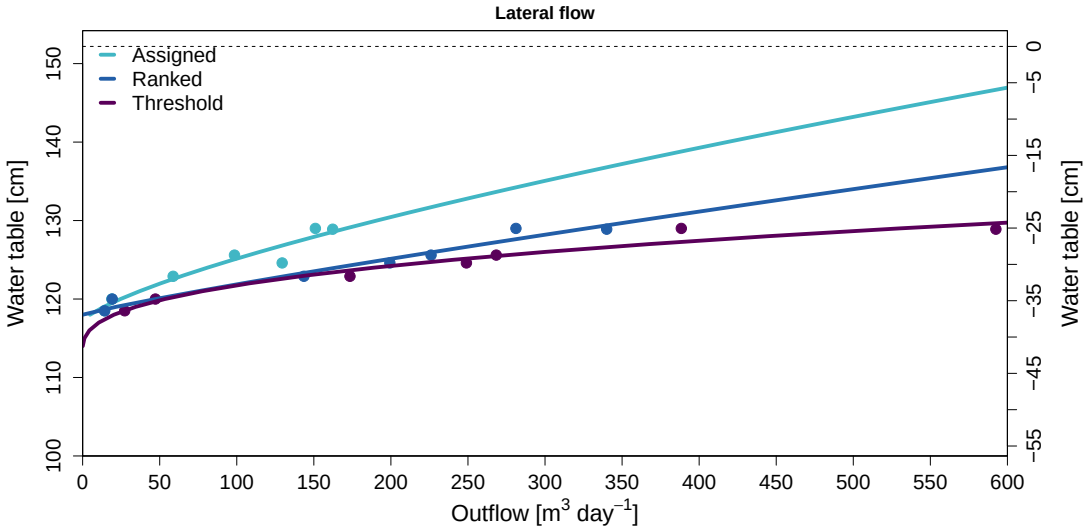

FIGURE 3.20: Three different lateral flow models were fitted with data from seven lateral flow measurements. Due to spatial and temporal variations three approaches were employed to provide a range of possible scenarios. The performance of all three models is very good.

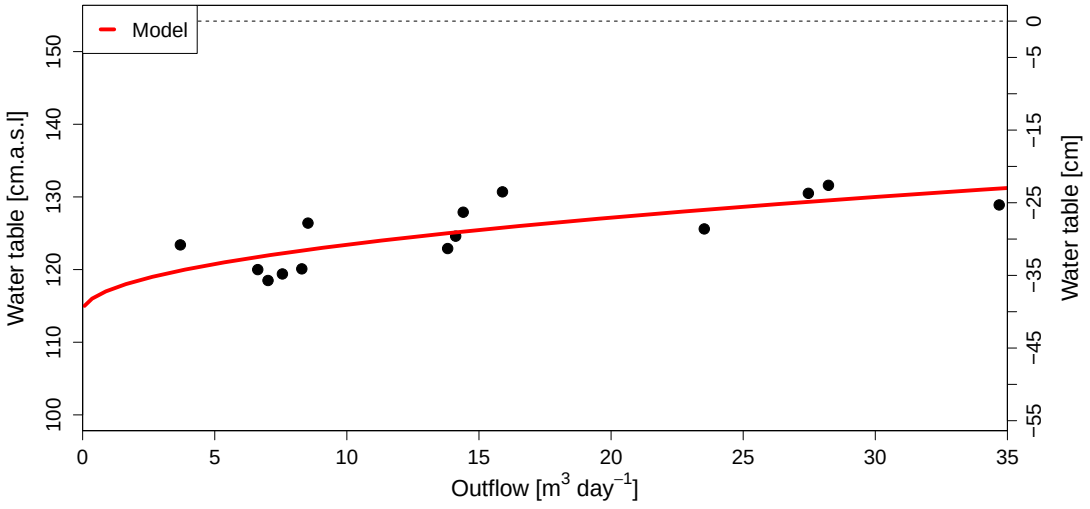

FIGURE 3.21: Pipeflow model, which was fitted at 14 pipeflow measurements. The performance fairly good.

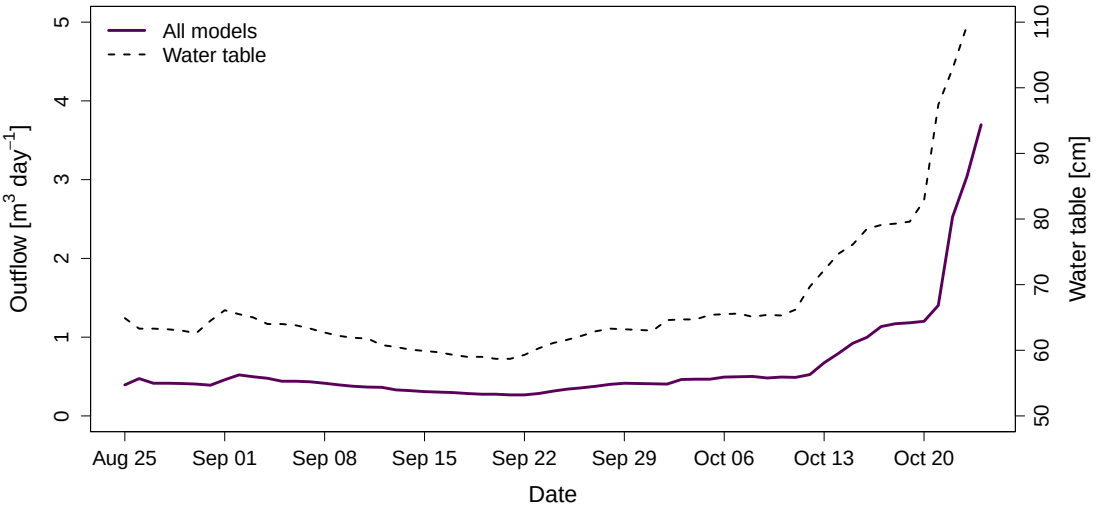

FIGURE 3.22: Modeled total outflow during dry conditions between August 25 and October 24, 2014 in $m^3\ day^{-1}$. Due to low water tables seepage is the only occuring process.

3.10 Reservoir Model Output

Figures 3.22 and 3.23 show the modeled total outflow for the entire study site, between August 25 and December 8. The output figures are split into low and high runoff periods to be able to evaluate the results more easily. During the dry period outflow is very low, never exceeding 4 $m^3\ day^{-1}$. It follows the regime of the water table with a strong and quick increase after October 21, when the transition took place. At such low water table heights only seepage takes place, which is why all three models agree exactly with each other.

During and after the transition the runoff behavior of the site changes dramatically. The difference between the three approaches is now clearly present. On October 27, November 17 and December 5, all models show about the same runoff volumes due to lower water tables and therefore better model agreement as mentioned before. Especially between November 2 and November 10, as well as November 24 and December 1, the differences between the models are considerably big. The lag of one day between water table change and runoff response is also nicely illustrated.

Table 3.10 lists the total outflows at the end of the dry and wet period, as well as the total outflow throughout the entire measurement campaign for all three model approaches. Outflow during the dry period, when there is neither lateral flow nor pipeflow is obviously

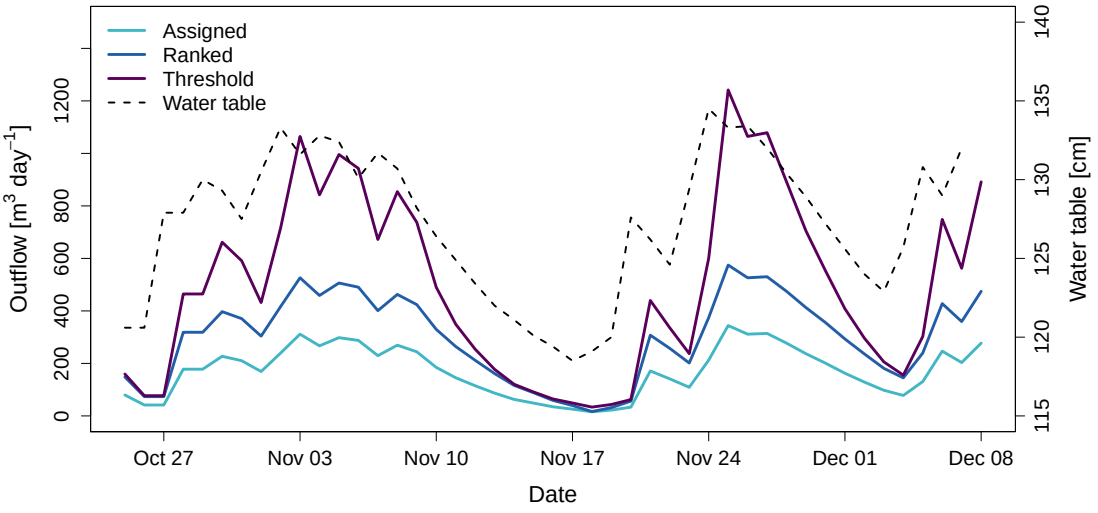

FIGURE 3.23: Modeled total outflow during wet conditions between October 25 and December 8, 2014 in $m^3\ day^{-1}$. High water tables enable not only seepage but also lateral flow and pipeflow to drain the bog.

negligible. Almost the complete outflow occurs during the wet period. The sums are fairly equally spaced ranging from approximately 7,730 m^3 up to almost 22,245 m^3.}

TABLE 3.10: Accumulated total outflows of all models over the entire study period in m^3. Apparently runoff during the dry period is negligible, the total sums vary considerably.

	Assigned $[m^3]$	Ranked $[m^3]$	Threshold $[m^3]$
Dry	38.3	38.3	38.3
Wet	7691.8	13435.6	22204.2
Total	**7730.2**	**13473.9**	**22242.5**

Figure 3.24 shows the wet period with separated processes. As indicated before lateral flow, independent of which model is used, contributes the greatest outflow during the entire time. Furthermore, lateral flow as well as pipeflow behave similar in dependency to the water table. This is why both processes decrease on November 17, when the water table drops below 35 cm of the soil surface. As will be explained next, this leads to an increase of relative contribution of seepage, since the seepage rates are less influenced by the water level, therefore generating a constant amount of outflow.

For visualization of the relative process importance, Figure 3.25 illustrates the fraction of each process of the total outflow in percent. It is clear that 100% runoff was generated by seepage, when water tables were low and no other process occurred. After the transition,

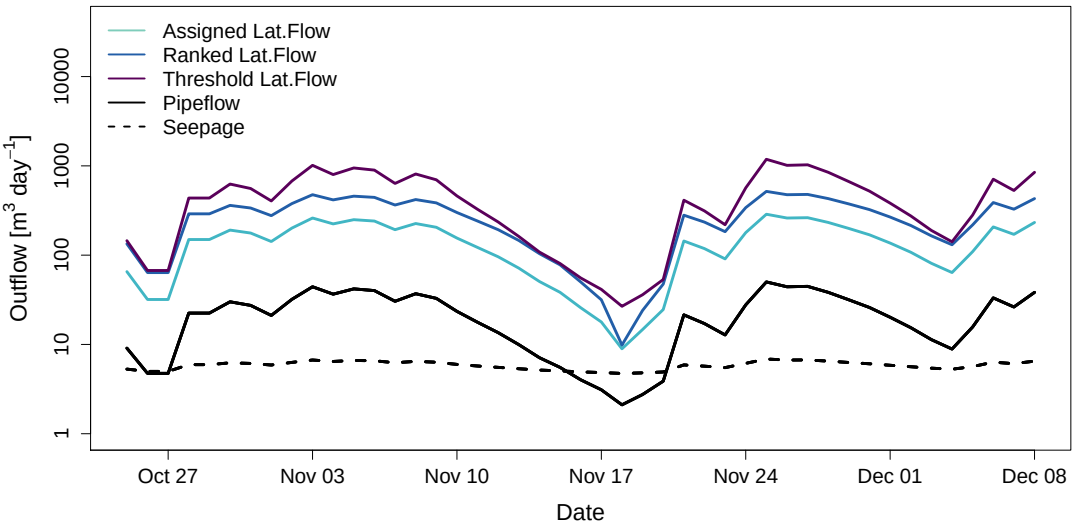

FIGURE 3.24: Daily runoff of separated processes during the wet period in $m^3\ day^{-1}$. Seepage contributes a continuous baseflow, whereas pipeflow and lateral flows vary considerably according to water level height.

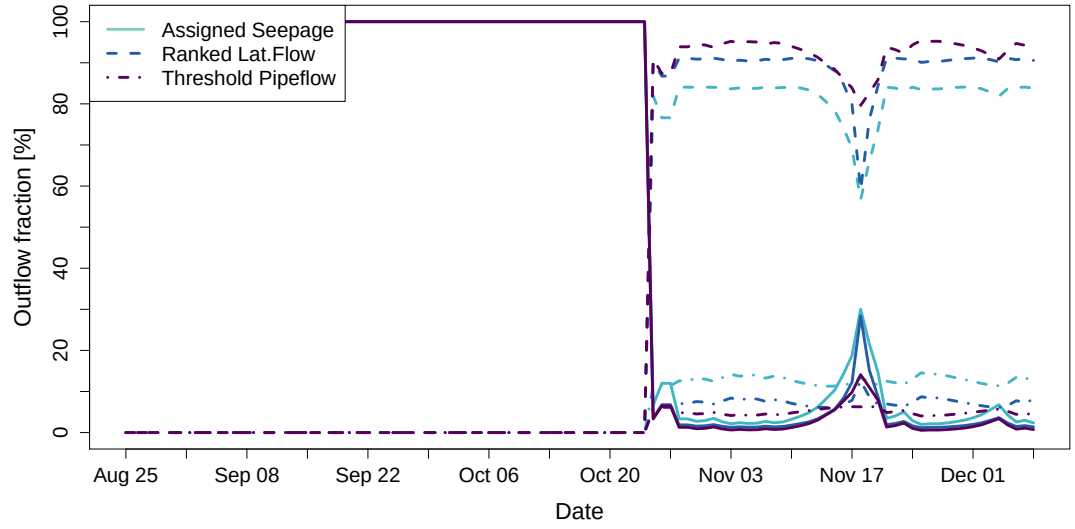

FIGURE 3.25: Relative contributions of each process over the entire study period in %.

lateral flow takes over the role as dominant process, contributing between 80-95% most of the time, depending on the model. The seepage fraction mostly ranges between 2.5-6% and pipeflow continuously provides 5-13%, independent from water table fluctuations (see Table 3.11). This is interesting, because it suggests that the pipeflow decrease is proportional to the total runoff decrease.

Lateral flow and seepage experience considerable change around November 17 when the water table height decreases below -35 cm to the surface.

TABLE 3.11: Main parameters of outflow process fractions

	Seepage [%]	Lateral Flow [%]	Pipeflow [%]
Assigned			
Min	2	56.6	11.3
Max	30	84.1	14.6
Mean	5.9	81.4	12.7
Ranked			
Min	1.2	59	6.1
Max	28.4	91.1	12.6
Mean	3.7	89	7.4
Threshold			
Min	0.6	79.6	4
Max	14.1	95.4	6.3
Mean	2.7	92.3	5

3.11 Mixing model

Figure 3.26 presents the bog water portion in the ditch, which was calculated by means of a simple mixing model. The portion of bog water fluctuates gradually, with two peaks, one on November 20 and the other on December 2. The measurements suggest that water originating from the bog always contributed more than half of the ditch water at times even up to 85%.

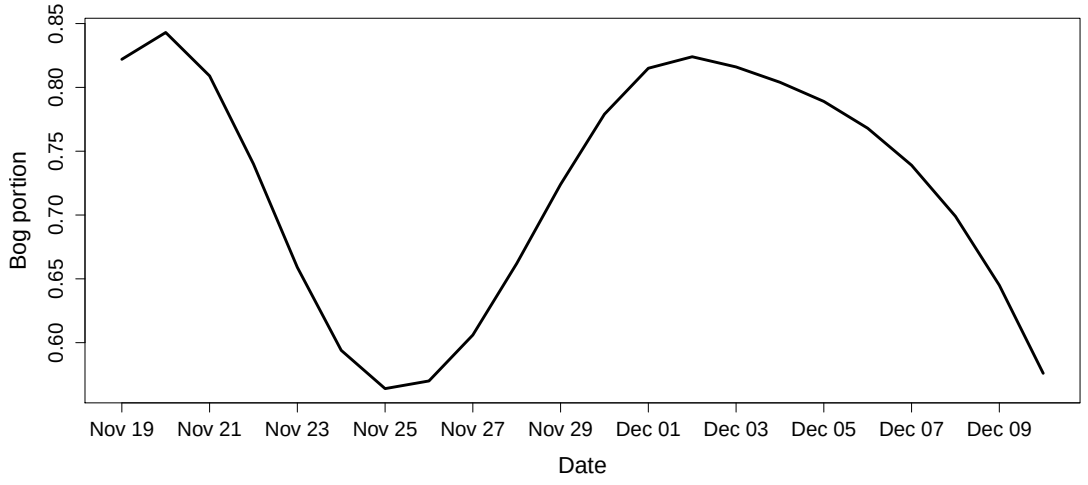

FIGURE 3.26: Electrical conductivity measurements of bog water, opposite soil depoits' water and ditch water were used to calculate a mixing model, which provides the bog water portion in the ditch.

Chapter 4

Discussion

4.1 Precipitation

Precipitation data was downloaded from a station 11.5 km north-west of the study site. There are no topographic barriers between study site and weather station, so the data give a good estimation of the precipitation at the site. The values were only used to introduce the surrounding conditions, so they did not impact the study findings. Cheng [2011] used data from a more distant weather station in 2010 and quantified the total precipitation between August 1 and December 31 to be 561.9 mm. During this study, precipitation for the same time period added up to 548.6 mm, thus implying comparable precipitation conditions.

4.2 Topography

Von Post indices are determined by subjectively describing the characteristics of a peat sample in the field. In this study the classification was done by two students without prior experience in using the von Post scale, except for a tutorial obtained from an expert in this field. Nevertheless, classification results were achieved independently with very similar results for each sample. In the bog center the same students gathered more samples for von Post classification and found a lower degree of decomposition [Chestnutt, 2015], which agrees with findings by Howie and van Meerveld [2011], Lapen et al. [2005], who report higher decomposition stages of peat in the rand and lagg region.

The results are thought to be reliable, since the error due to inexperience in von Post classification is assumed to be less than the uncertainty introduced by subjectivity of different researchers assigning von Post indices to soil samples. Thus comparability of the results in this case is higher than between independently conducted studies.

Mire breathing was quantified only on November 29, 2014, in order to provide background information on the significance of the process. It was found that peat thickness positively impacts the swelling process, which coincides with Whitfield et al. [2006], who reports larger values from inside Burns Bog, where the peat thickness is considerably higher. The impact of the unaccounted for ground level change is estimated to be only minor.

Variograms from the soil surface interpolation data do not show any nugget effects, therefore suggesting high quality survey data, obtained by "Target Land Surveying". The indicated gradient towards the boundary ditch was also reported by other studies like Howie and van Meerveld [2011], Ingram [1983]. Nevertheless, as the variance maps suggest, interpolated data show a considerable uncertainty because of the low measurement density. However, since the data was used to obtain a general idea of the soil surface shape and elevation only, and never for further calculations, these interpolation uncertainties do not interfere with the outcome of this study. These circumstances apply for the silt depth interpolations, too. In case of the silt depth measurements, additional uncertainties may be introduced due to the peat auger method to detect the silt layer, but are assumed to be within a very few centimeters, so that the total errors are thought to be minimal.

4.3 Water table analysis

Water table measurements were obtained with the same density as soil surface and silt depth measurements, thus leading to the same issue. The measurement density for detailed spatial mapping of the water table was too low, but it was sufficient to identify general trends at the study site. In regards to provide input data for a reservoir model the experimental design is robust and well suited.

Water table shape investigations by means of standard deviation calculations at the monitoring locations indicate a closer relation of water table shape and soil surface,

which agrees with the interpolated maps and computed correlation between water table height and soil surface. The calculated mean water table change between dry and wet period of 69.9 cm lies within values of other studies, e.g. Howie et al. [2009b], who reported changes up to 99 cm in the same bog. Price [2003] reported ditch related water table depression impacts up to a distance of 20 m and Hebda et al. [2000] describes observations of drainage impacts of up to 100 m into the bog. These studies make the findings of this study of a ditch impact on the water table up to 35 m into the bog, seem realistic. Additionally, the water table depth of -90.5 cm at the end of the summer integrates well into the whole picture, since Howie et al. [2009b] found similar values. The transition from such dry conditions took only 13 days with a mean recovery rate of 4.4 $cm\ day^{-1}$, thus agreeing with the hypothesized quick rise between dry and wet period.

The results from the standard deviation calculations, as well as the positive correlation between ground elevation and water table identify the soil surface as rather important topographic control on the water table. Interpolation maps match these conclusions and complement a spatial dimension to the findings. This dependence applies during both dry and wet conditions.

4.4 Groundwater flow analysis — Bog

4.4.1 Horizontal flow

Because inverse distance weighting was used, no target functions are available to evaluate the interpolation quality of the potentiometric maps. Piezometer data was only used after October 7, because they were thought to have not reached equilibrium before the date. Cheng [2011] too reported similarly long recharge times after slug tests in deep peat layers. A possible time lag of the deep piezometers was not quantified. If not simply caused by the low saturated hydraulic conductivity of the peat, a possible reason for the slow hydraulic head response could be too short slotted sections along the piezometers. Howie and van Meerveld [2013] used pipes with a 40 cm slotted section in shallow peat, but there was no data on the present hydraulic conductivities in these depths. During this study pipes with a slotted section of 50 cm were employed. It is reasonable to think of the head measurements as dampened, such that short term fluctuations are covered

up, thus providing long term trends, instead. Because the recharge rate of most pipes is fairly similar, the relative error between the piezometers due to a potential lag might be small. Hence the potentiometric maps may be used as indicators of basic flow directions, but not for detailed interpretations. This conclusion is supported by the fact that the flow directions are mostly consistent in space and time and agree with the common theory of drainage towards the ditch, which in turn is evident from other measurements of this study, as well.

4.4.2 Vertical flow

The vertical hydraulic gradients are about one order of magnitude higher, compared to other reported gradients in peatlands (e.g. Kopp et al. [2013] 0.03 – 0.06 and Fraser et al. [2001] 0.02-0.03). Early values at location 31 are well within reported boundaries, therefore suggesting that equilibrium was reached, which was overthrown when transition took place. Thus accurate statements on the real hydraulic gradients are difficult. Nevertheless it is safe to assume that the gradient direction can still be obtained with high certainty. So, as negative gradients were measured, this suggests downward percolation, which makes sense due to high precipitation. This agrees well with Reeve et al. [2000], who reported that not low hydraulic conductivity of the peat, but of the underlying mineral soil control downward water movement. Since, for Burns Bog, very low saturated hydraulic conductivities of the underlying silt were reported [Hebda et al., 2000], this suggests, that the downward percolating water would flow vertically towards the ditch, which was observed during horizontal flow analysis.

4.5 Water table and hydraulic gradient — Ditch

The ditch was always hydraulically well connected, so that no backwater occurred. Automatic measurements at locations 100 and 140 therefore provide accurate and reliable data, as anticipated. It is interesting that all manually measured water levels behave almost contrary to the automated measurements, especially because all manual wells exhibit a similar behavior. A systematic bias introduced due to the manual measurement process could be a logical reason, but the simplicity of measurement practice does

not really allow for any misreadings. The flashy character of the manually measured piezometers might be, as at location 100, be caused by a lag of the piezometers.

Except for early measurements at location 100, when there was no flashy gradient present, calculated gradients at this location are unusually high, due to the lag of the piezometer. The fact that location 100 is the only piezometer nest recording opposite flow directions is not necessarily a sign of poor data quality. For example, Kennedy et al. [2010], Kopp et al. [2013] reported the occurrence of the same phenomenon; small scale changes in seepage and hydraulic gradient direction. One reason for this behavior might be the location at the transition from shallow to deeper silt layer.

The mostly positive gradients as recorded at locations 19, 60, 140 and 176 agree with the seepage measurements executed along the entire ditch section. The high values may to some extent be results of inaccuracy, but they do agree with the unusually high seepage measurements in the ditch.

4.6 Saturated hydraulic conductivity

The saturated hydraulic conductivity obtained from the improvised slug tests coincides with measurements from many other studies presented by Letts et al. [2000] and therefore appears to be good and reliable. The evident decrease with depth was also reported by Beckwith et al. [2003]. Even though Holden and Burt [2003b] recommend not using common rigid soil approaches for saturated hydraulic conductivity quantifications, many studies still use such methods, also receiving reasonable results [Kopp et al., 2013].

4.7 Outflow

4.7.1 Seepage

The experimental design employed for the seepage rate quantification is solid and reliable because of its coverage of spatial and temporal fluctuations of the target process. However due to work flow restrictions some compromise had to be made in order to be able to execute said experimental plan. Rosenberry et al. [2008] list the most commonly occurring errors connected to seepage meter measurements. In opposition to what is

recommended, the seepage meters were installed only about 30 minutes before measurements started. However Landon et al. [2001], Lewis [1987], Lock and John [1978], Rosenberry and Morin [2004] report of much shorter equilibration times (5-10 minutes and 10-15 minutes), but mostly in sandy environments. The potential uncertainty was accepted nevertheless, in order to be able to catch spatial variance of seepage rates. Other common errors occur from inadequate running times and consequently too low or high seepage amounts for the employed bag volume. In this study seepage meters yielded a mean of 100 ml, thus well within an accurately measureable range and also far from being affected by the maximum bag volume of 800 ml. Seepage meters were installed for 89 minutes on average. The measurement time might be a little short, but longer running times would again decrease the number of total measurements and also increase the chance of gas accumulation in the seepage meters (which is a frequently reported issue in wetlands [Harvey et al., 2000]), therefore a compromise was found. The mean value of all measurements for the entire site lies with 6.79 $L\,m^{-2}\,d^{-1}$, indeed above reported values of 2.2- 4.0 $L\,m^{-2}\,d^{-1}$ [Kopp et al., 2013], but reported hydraulic gradients in Kopp et al. [2013] were considerably lower, as well. Furthermore, as mentioned the impact is reasonably small, due to other more dominant outflow processes.

Since the measurements can be seen, after all, as considerably accurate and reliable, the poor relationship between water table and seepage rate might originate from a deeper flow system. Equally important is the valid assumption that the opposite soil deposit's seepage regime behaves distinctively different and therefore covers up the clear signal from the bog due to measurement interference. Electrical conductivity measurements of the samples could have helped to identify the origin of the seepage, but as stated before, the required equipment was not available at the time. After all, the impact of these uncertainties on the final model are thought to be low (see target function errors), because of the small over all contribution of this process. For more accurate measurements, especially during low ditch water levels when seepage meter measurements are not feasible, tracers should be considered as valid alternative.

4.7.2 Lateral flow

As with the pipeflow, trough measurements are simple and easy. The error introduced due to measurement inaccuracies is assumed to be negligible. Measurements were obtained over the complete range of water table heights during the wet season, therefore providing good input data for the model, so that there were no water table elevations without measurements to fit the model to.

The main problem with the lateral flow quantification was the lateral heterogeneity. The resulting error from having four or six measurements to calculate a mean value, thus due to non-existing proportional allocation, is not assumed to be the biggest source of uncertainty. Much more important is the possibility of a discrepancy between real and assigned stratum. For example the error of a wrongly assigned value, therefore an outliner, to a stratum, if the sample size is low or moderate, is higher than just using four instead of six values, which are already similar in the first place, to calculate the mean of a stratum.

To tackle this issue, three approaches were executed. Whether a completely random approach would have been more accurate, when sampling only 10% of the population, or not, is difficult to say.

Another possible source of error is the subjective stratum survey in the field. This is because all subjective estimates are in some way biased. Since the fractions of all strata did not change very much, this source of error is thought to be a minor one.

Generally the observed initiation of lateral flow and pipeflow at a water level height between 110-120 cm (34-44 cm below mean ground elevation), therefore at a distinct threshold, agrees well with a broad variety of literature (e.g. [Emili and Price, 2006, Holden and Burt, 2003c]). The difference between these studies and this one lies in the value of the threshold. Mostly it was found to be 5 cm below the surface, therefore considerably higher than the one found in this study. This is due to the fact, that most studies were executed in an undisturbed peatland, often within the wetland and not at the lagg. Therefore different surrounding conditions existed, favoring lateral flow closer to the surface (e.g. due to soil saturation). It is interesting to note that it took until November 26 for the entire site to develop a final stage of lateral flow. This refers to

the fact that on November 26 the initially as "none" classified stratum was found to produce "low" lateral flow.

4.7.3 Pipeflow

The pipeflow measurements were simple and accurate. There was no spatial pattern that caused uncertainties and the straight forward measurement method minimizes possible quantification errors. The target function of the model is moderate. The relationship between water table and outflow is close enough to get a reasonable estimate without too much negative impacts on the final model, due to the only moderate contribution to total runoffs. One reason for the less tight relation between water table and outflow, compared to the lateral flow measurements, might be the runoff generating area for this pipe. Holden and Burt [2002a] found pipes with a length of up to 150 m, which would in this case place the contributing area to this pipe far outside the monitored area. As a consequence, water tables changes in the source area of the pipe would therefore go unrecognized and would not be included in the model.

4.8 Reservoir model

A direct model evaluation due to comparisons of modelled runoff with measured ditch runoffs is not possible, because no weir and therefore no ditch runoff data are available. However target functions of the contributing processes are available. Nash-Sutcliffe-Efficiencies of the two less important processes (pipeflow and seepage) are moderate and considerably poor, respectively. But due to the fact that they are only minor contributing processes the absolute errors of both processes are relatively small, after all. The dominant lateral flow presents very good Nash-Sutcliffe-Efficiencies, which means reliable and high quality estimations of the real process. Despite the good overall performance the introduced errors due to lateral flow are by far the highest. It is also important to see, that the modeled absolute lateral outflow is not evaluated in the target functions. Each approach by itself performs well, but this does not change the fact that there is a considerable difference in absolute outflow, depending on what approach is chosen. Thus it is in the hands of the user to decide, which approach is the best one.

The fitted model parameters give a good indication on how the model acts in dependence on storage changes. Here, “a” describes the slope of the model and “b” the curvature. Both impact the water table sensitivity crucially. A low “a” parameter, therefore flat slope, creates a water table sensitive model. Both “a” and “b” influence each other’s importance. If the “b” parameter is 1, it would describe a straight line, therefore “a” would control the whole water table sensitivity, whereas a “b” parameter of 0 would describe a horizontal line, therefore completely cancelling the dependency on the water table and thus the impact of “a”. A good example of the impact of the “a” and “b” parameters is the threshold model, which agrees nicely with the other two models during low water tables, but once water tables rise, it quickly generates high outflows, therefore setting it apart from the other two approaches.

When taking a look at the model parameters, the threshold approach displays a clearly smaller “b” parameter, therefore a smaller curvature (see Table 3.9). As just explained this high sensitivity causes increased instability in the model during high water tables. At the same time visual evaluation would suggest that the threshold model is most accurate at low flows, because it fits the two measurement points at low water tables best. The ranked model with the highest “b” parameter is already close to a linear model (with b = 1), therefore handing “a” much of the sensitivity influence. It yields a moderate outflow with constant behavior throughout the range of water tables (again caused by the high “b” parameter value). Finally the assigned model approach displays the steepest slope and therefore computes the smallest runoffs during high water levels, which is caused by a relatively high “a” parameter, in combination with only little curvature (high “b” parameter).

The fitted “c” parameters, which represent the threshold above which water level the process occurs, agree very good with each other. They range from 113-118 cm above sea level, therefore 36-41 cm below the soil surface. These values lie closely together and agree well with common acrotelm depths. Additionally, the pipeflow threshold was calculated to be 114 cm, therefore 40 cm below the soil surface, which also joins in nicely with the thresholds of the lateral flow models.

Especially the seepage model is restricted by its boundaries. This is due to the data point allocation. The Nash-Sutcliffe-Efficiency indicates that the simple mean value is a better estimator than this model. Thus the boundaries were selected, in order to force the

model into a more or less natural behavior. The upper boundary for the threshold was set because without this boundary the model would suggest initial seepage at water table heights, where lateral flow started to develop. This is obviously unrealistic. Like this the model is forced to model seepage already at lower water table heights, as was observed in the field. The slope then was restricted so that the model fitted the measurements best by visual evaluation and according to calculated Nash-Sutcliffe-Efficiencies. The process was iterated until the manually set parameters yielded the desired model quality. The fitting algorithm was not able to perform properly, in this case.

The overall model performs well. The mean relative contribution of pipeflow ranges between 5-13%, depending on the model, which coincides with reported values of 10% by Holden and Burt [2002a]. Seepage was reported to contribute only 1% [Damman, 1986] or insignificantly [Holden and Burt, 2003c] to the total runoff, which is not the case here. The mean contribution varies between 2.5-6%, but as mentioned before seepage rates may be overestimated. Lateral outflow which is reported by Evans et al. [1999], Holden [2005b], Holden et al. [2001], to be the dominant runoff process after saturated overland flow, was identified as most important runoff process in this study, due to the non-existence of overland flow. Thus, the relative contribution of 81.5-92.5% in this study fits in with the reported findings.

As intended the key processes were identified and with the help of the model it was possible to quantify relative contributions of each process. Reliable and accurate thresholds, which trigger a drastic change in runoff behavior, were found. The relative contributions of lateral flow and pipeflow identify both as significant outflow generating processes, so that these mechanisms need to be included in a spatially distributed model of this environment. Nash-Sutcliffe-Efficiencies proove to be a very close relation of subsurface flow to water table heights; pipeflow still displays considerable dependency on the water table, as well.

4.9 Mixing model

The mixing model gives a reliable estimate of the integrated relative bog contribution to the total ditch runoff. The drop around November 25 marks a flooding of the whole site, which made outflow measurements impossible. The flooding was caused by the overflow

of a separating dam at the adjacent soil deposit by a storage reservoir. The uncontrolled flooding with minerotrophic water caused a strong increase of electrical conductivity in the ditch, which was correctly converted to a lower bog water portion by the mixing model. The results can be assumed to be reliable, thus suggesting a bog water portion in the ditch between 70-80% during normal conditions. The possibility to quantify bog water portions in the bog is interesting for future research at this site, when there is data available on the total ditch runoff. In that case, a mixing model could provide crucial data for performance evaluations of the entire model.

Chapter 5

Conclusions

This study was launched to create a better understanding of the occurring runoff processes in the lagg of Burns Bog, British Columbia, Canada. The aims included the identification of runoff processes, the assessment of their significance, as well as the development of a threshold integrating non-linear reservoir model to be able to describe runoff behavior from water table data. Measurements in the field were conducted between August 22 and December 10, 2014.

Topographical features as the ground level and silt depth were surveyed, decomposition was described with the help of von Post indices and mire breathing measurements were conducted, as well. The water table was monitored over an area of 7000 m^2 by means of 27 wells and the hydraulic head was measured at eight locations throughout the site, including two piezometer nests. The saturated hydraulic conductivity was quantified, too. Further processes under investigation were seepage rates into the boundary ditch, as well as lateral flow close to the soil surface and pipeflow. Additional monitoring in the ditch included water level and hydraulic head measurements at five locations. A mixing model fed with electrical conductivity data estimated the bog water portion in the boundary ditch.

The ground level was found to decrease towards the ditch, therefore yielding a mean gradient of 2.8%. Mean ground elevation is at 1.542 m.a.s.l, whereas the silt layer lies at a depth of -1.529 m.a.s.l, thus yielding a mean peat thickness of 3.701 m. Von Post indices ranged from H4-H5 at 80 cm depth to up to H7-H8 below 2 m. Mire breathing

was quantified to be 3.9 cm on average. The bog face at the ditch lies at a mean elevation of 0.756 m.a.s.l and exhibits a mean height of 1.14 m.

The water table changed dramatically during the transition between October 12 and October 25, 2014. During this time the water level rose from 0.662 m.a.s.l to 1.23 m.a.s.l, which equals a rate of 4.4 $cm\ day^{-1}$. During the dry period the mean water table had a depth of -90.5 cm below the ground and -20.6 cm during the wet period. The fluctuation range is therefore 69.9 cm. As the soil surface, the water table showed a gradient towards the ditch. Moreover ground level was found to be an important control on the water table shape.

Saturated hydraulic conductivity measurements in the bog and the ditch yielded mean values of $5.21 \times 10^{-8}\ m\ s^{-1}$ and $7.15 \times 10^{-4}\ m\ s^{-1}$, respectively. In addition, hydraulic conductivities in the bog decreased with depth and increased with distance from the ditch. No clear pattern was identified for saturated hydraulic conductivities in the ditch.

Throughout the measurement campaign, the groundwater flow in the bog was oriented downwards. Horizontal flow was directed toward the ditch, where mainly positive hydraulic gradients suggest discharging groundwater into the ditch.

The three identified runoff processes were seepage, lateral flow and pipeflow. Seepage measurements yielded a mean value of 5.34 $m^3 d^{-1}$. The relationship between water table and seepage rate was low with a Nash-Sutcliffe-Efficiency of -0.21. It contributed between 2.5-6% of the total runoff during the wet period and 100% before the transition. The spatial distribution of lateral flow over time was found to be fairly consistent. Mean values of three quantification approaches for lateral flow were 90.44 $m^3 d^{-1}$, 174.79 $m^3 d^{-1}$ and 249.46 $m^3\ d^{-1}$. All three approaches showed very close connections to the water table with Nash-Sutcliffe-Efficiencies of 0.92, 0.97 and 0.9. The relative contributions varied between 81-92.5% of total outflow. Pipeflow was quantified to be 15.28 $m^3\ d^{-1}$ on average, thus contributing between 5-13% of the total runoff. The dependency on the water table is with a Nash-Sutcliffe-Efficiency of 0.38 moderate. Thresholds for all processes except seepage were found to be between -40.5 cm and -36 cm below the soil surface.

Modeled total outflow amount for the entire monitoring period varied between 7730 m^3 and 22245 m^3. Additionally to the relative contributions of each process, the model also revealed that almost all runoff occurs during the wet period.

According to the mixing model the bog water portion in the boundary ditch varies between 70-80%, during normal conditions.

All findings combined give a clear picture of the occurring hydrological system. Groundwater flows downwards and towards the ditch, where it seeps out of the ditch bed into the channel when water tables are below -40.5 cm to the soil surface. Once the water table reached this threshold lateral flow starts to develop together with pipeflow, so that all three processes drain into the ditch, where they contribute up to 80% of the total ditch runoff. Both runoff processes, lateral flow and pipeflow, outweigh seepage by far under these conditions, hence a completely different hydrological system establishes during the wet period of the year. In this case, lateral flow plays by far the most important role, when it comes to runoff generation. Pipeflow is less important, however still contributes considerably to the total runoff. During this time, when the water table is within the upper most -45 cm of the soil, seepage is negligible.

As a consequence, when a spatially distributed model is being developed, it is crucial to include lateral flow and pipeflow to the model. A threshold is necessary to be able to time the initialization of these processes.

Future research should, when lateral flow is under investigation, develop a denser and more accurate experimental design for lateral flow quantification, since this is where the most uncertainty is introduced to the model. Furthermore, seepage needs to be measured during dry conditions, in order to collect more data for times of low water levels. Then, a better seepage model performance will be obtained, which is crucial for summertime runoff modeling. Tracer could proove as helpful and practical approach in this matter. In order to be able to not only evaluate single components of the model but all processes combined, total ditch runoff data is needed. Generally, lateral flow needs to be understood in greater detail, including lag times and initiation times, referring to the required time between the reach of the threshold and first occurrence of lateral flow.

Appendix A

Appendix

A.1 Topography

Table A.1 provides the used topographic data for this study. The soil surface data was obtained from a contractor firm. The survey plan is provided in Figure A.1.

Diagnostic plots of the input data for soil and silt interpolation are provided in Figures A.2 and A.3. The north directed trend of the ground level is well illustrated. The silt input data shows the observed difference in silt depth between the eastern and western part of the study site. Variance maps of the soil surface and silt layer interpolation are provided in Figures A.4. The distortion in the soil surface variance map originates from the applied anisotropy during modeling. The variograms (Figures A.5) are split into four diagrams with different directions in order to provide visual support, when fitting the models manually. Especially towards north the soil surface model provides a good fit. All target functions are summarized in Table A.2.

A.2 Water table

Table A.3 lists some basic statistics obtained from steady-state conditions at each well location.

As for ground level and silt depth, the input data for groundwater table interpolations were evaluated before use. The diagnostic plots are provided in Figures A.6 and A.7.

TABLE A.1: Ground elevation was obtained from a professional survey company. The silt depth was quantified with the help of a peat auger. All heights are in relation to the sea level.

Location	Northing	Easting	Ground [cm]	Silt [cm]	Difference [cm]
1	5439105.18	502104.86	128.8	-167.7	296.5
2	5439105.18	502124.56	89.7	-170.3	260
3	5439105.61	502144.86	119.8	-160.7	280.5
4	5439105.07	502164.65	118.3	-160.7	279
5	5439105.69	502204.17	94.8	-143.7	238.5
6	5439105.74	502224.03	87.6	-134.4	222
7	5439105.28	502244.03	95.9	-132.1	228
8	5439105.93	502265.16	119.6	-139.4	259
9	5439111.17	502084.21	147.3	-136.2	283.5
10	5439110.02	502104.22	143.2	-166.8	310
11	5439110.32	502145.16	141.3	-167.7	309
12	5439109.86	502184.64	124.8	-181.7	306.5
13	5439110.49	502224.41	118.6	-133.4	252
14	5439111.01	502265.45	130.7	-149.3	280
15	5439110.4	502284.82	120.4	-110.6	231
16	5439114.82	502104.15	150.8	-149.7	300.5
17	5439115.14	502164.95	163.4	-204.6	368
18	5439115.71	502204.58	124.1	-145.4	269.5
19	5439115.97	502265.71	133.2	-135.8	269
20	5439120.26	502084.47	178.3	-147.7	326
21	5439119.9	502123.24	171	-169	340
22	5439119.71	502183.92	159.3	-150.7	310
23	5439120.45	502244.61	153.9	-140.1	294
24	5439120.35	502285.7	148.4	-109.6	258
25	5439125.49	502145.44	169.8	-182.2	352
26	5439125.39	502224.7	160.6	-125.4	286
27	5439130.02	502122.83	167.2	-279.8	447
28	5439129.75	502184.06	175.8	-152.2	328
29	5439130.32	502244.73	222.1	-91.9	314
30	5439135.19	502085.49	191	-149	340
31	5439134.8	502185.05	182.2	-156.3	338.5
32	5439134.92	502288.31	170.8	-112.2	283

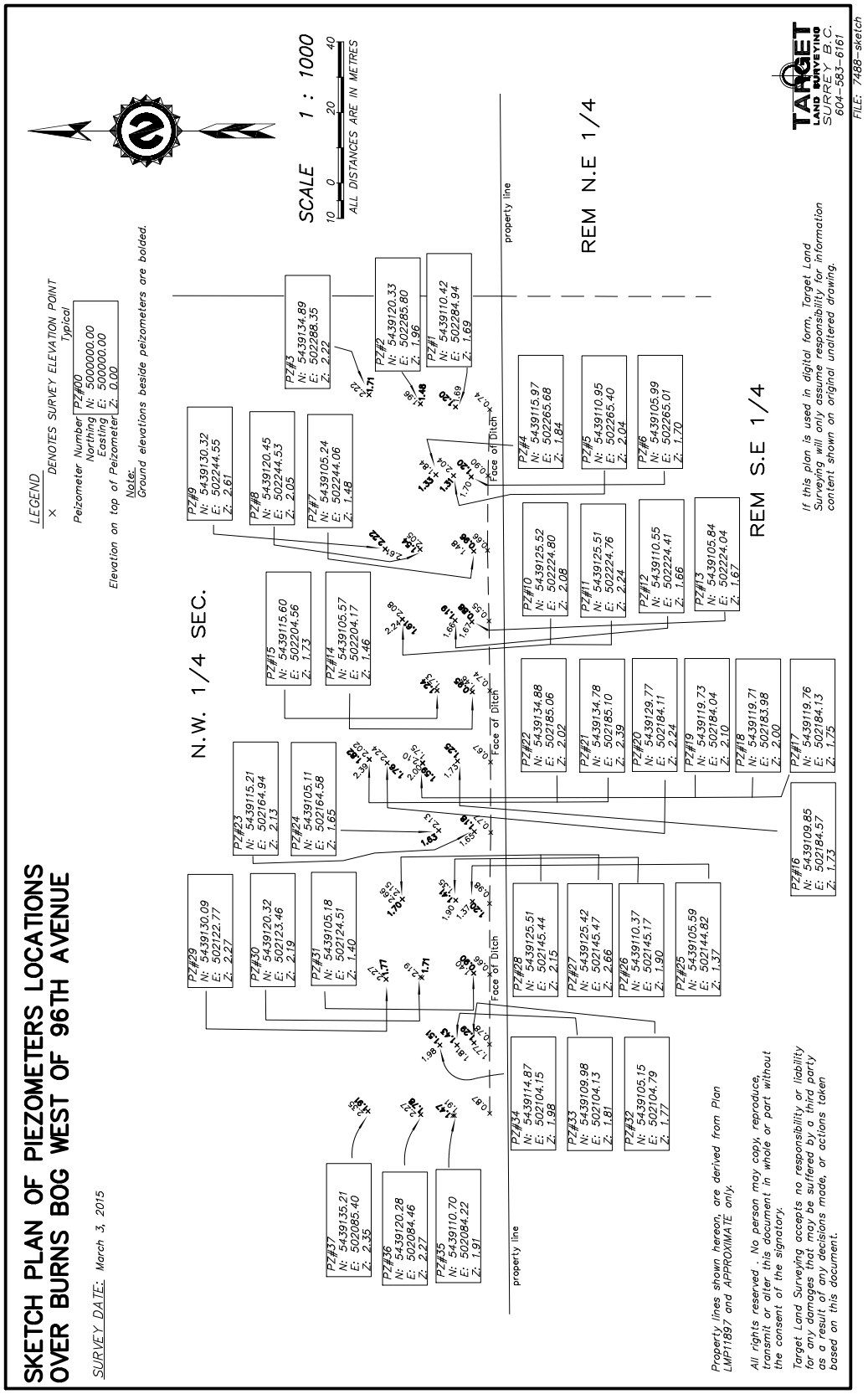

FIGURE A.1: Survey plan from March 3, 2015. The original data are provided in a file on the attached DVD.

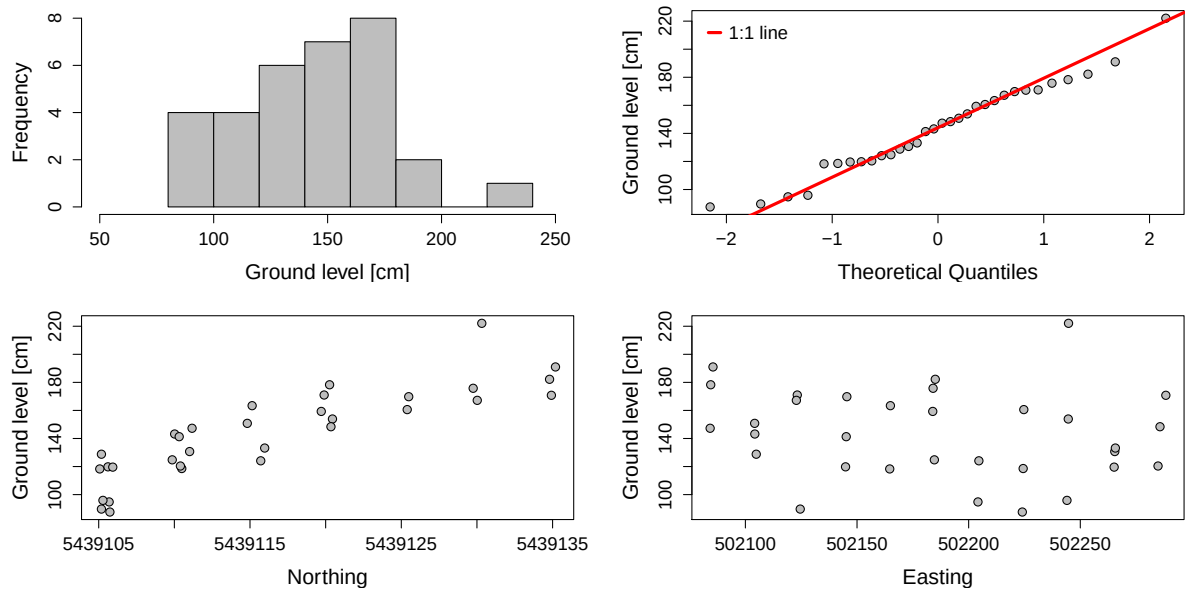

FIGURE A.2: Diagnostic plots of the ground level input data. The gradient in the northern direction is clearly visible.

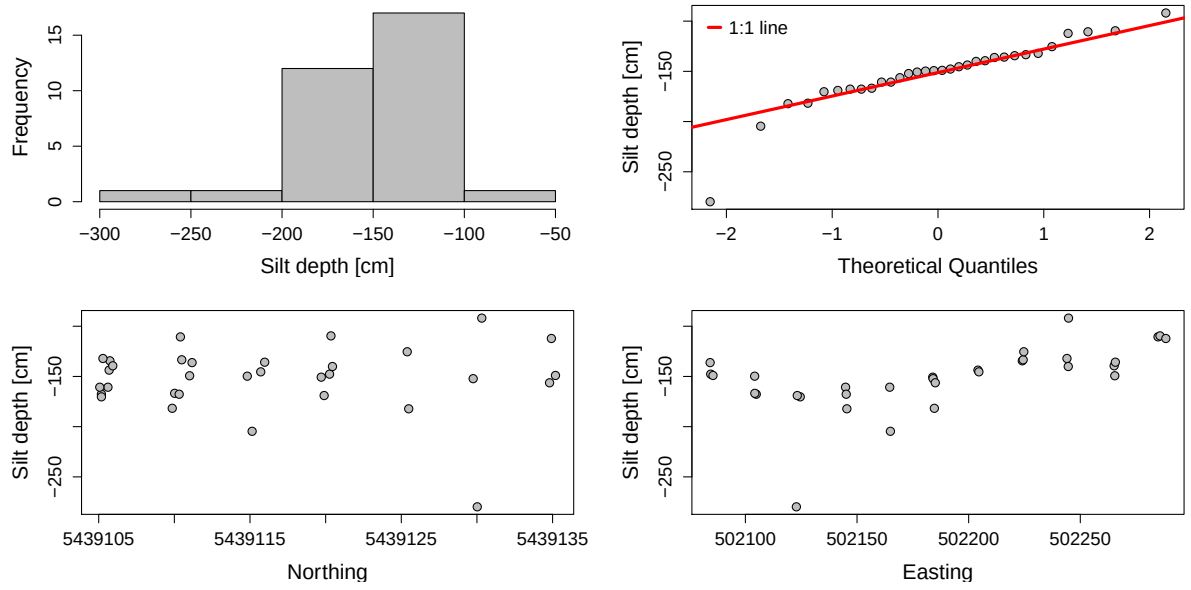

FIGURE A.3: Diagnostic plots of the silt depth input data. The difference between eastern and western half is well observable.

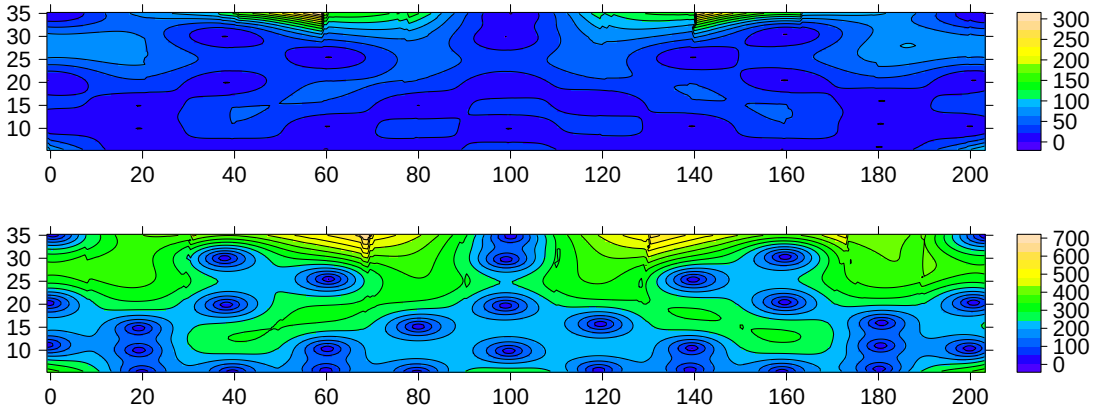

FIGURE A.4: Variance maps of the ground level (top) and silt depth (bottom) interpolation.

TABLE A.2: Target functions of the ground level and silt depth interpolation. Models marked with an * were manually fitted, the ones denoted with an ", were used to compute the maps.

Model	Mbe [cm]	Rmse [cm]	Mae [cm]	Nse
Ground				
Spherical	-0.22	23.35	17.71	0.43
Exponential	-0.1	21.4	16.04	0.53
Gaussian	0	24.74	19.66	0.37
Linear	-0.02	26.07	20.53	0.3
Linear*	-0.22	14.82	10.02	0.77
Spline* "	-1.2	15.43	11.9	0.75
Silt				
Spherical	0.4	30.39	19.16	0.13
Exponential	0.3	27.58	16.55	0.28
Gaussian	0.25	30.85	19.7	0.1
Linear	0.38	31.03	20.13	0.09
Exponential* "	0.23	24.92	14.83	0.41

The same trend as in the soil surface data is identifiable, when water table height is plotted versus northing. As indicated in Figure A.8 the variance is considerably high. It is higher than for both soil surface and silt depth interpolations. When taking a closer look at the variograms (Figure A.9), one can see the poorly fit data, which yields after all, moderately target functions (Table A.4).

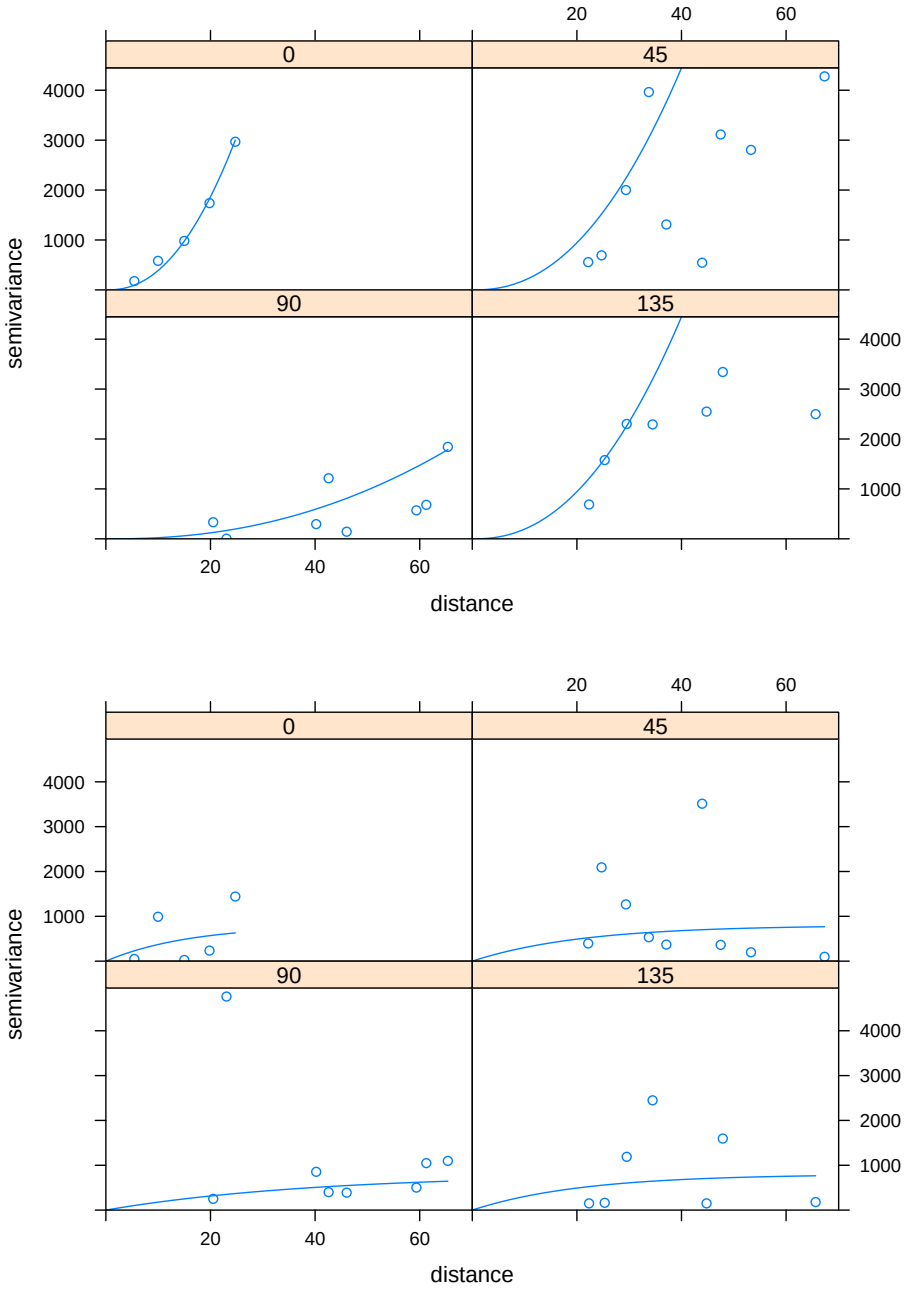

FIGURE A.5: Variograms of the ground level (top) and silt depth (bottom) kriging models. The non-existent nugget effect is a sign for good data quality.

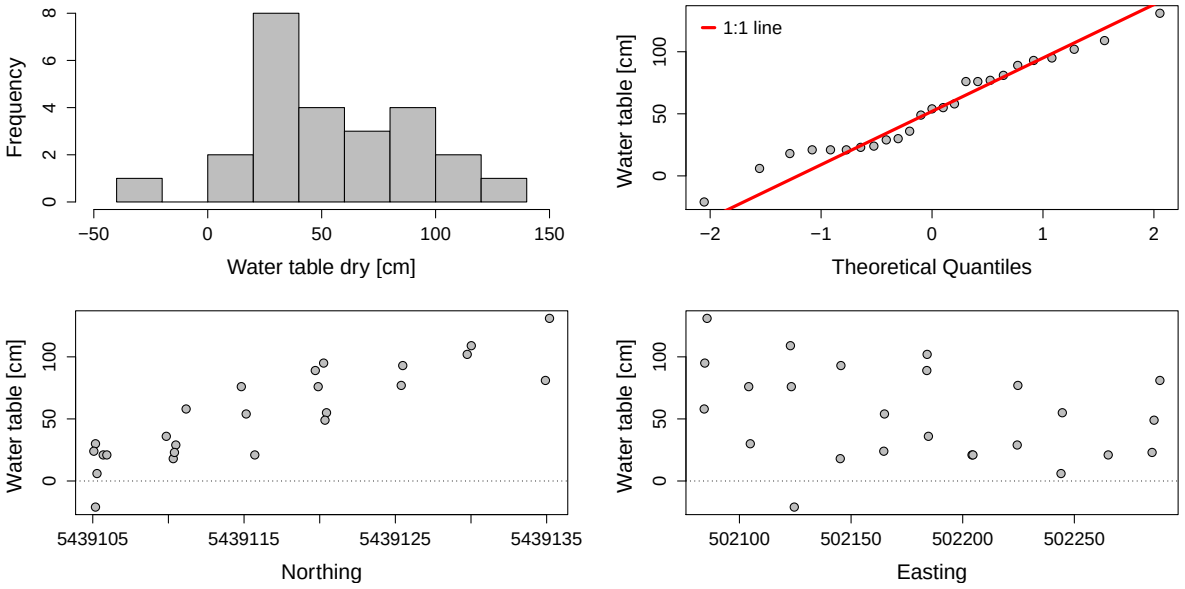

FIGURE A.6: Diagnostic plots of the water table input data, during the dry period. A gradient as in the soil surface plot is visible, when looking at the water level versus northing.

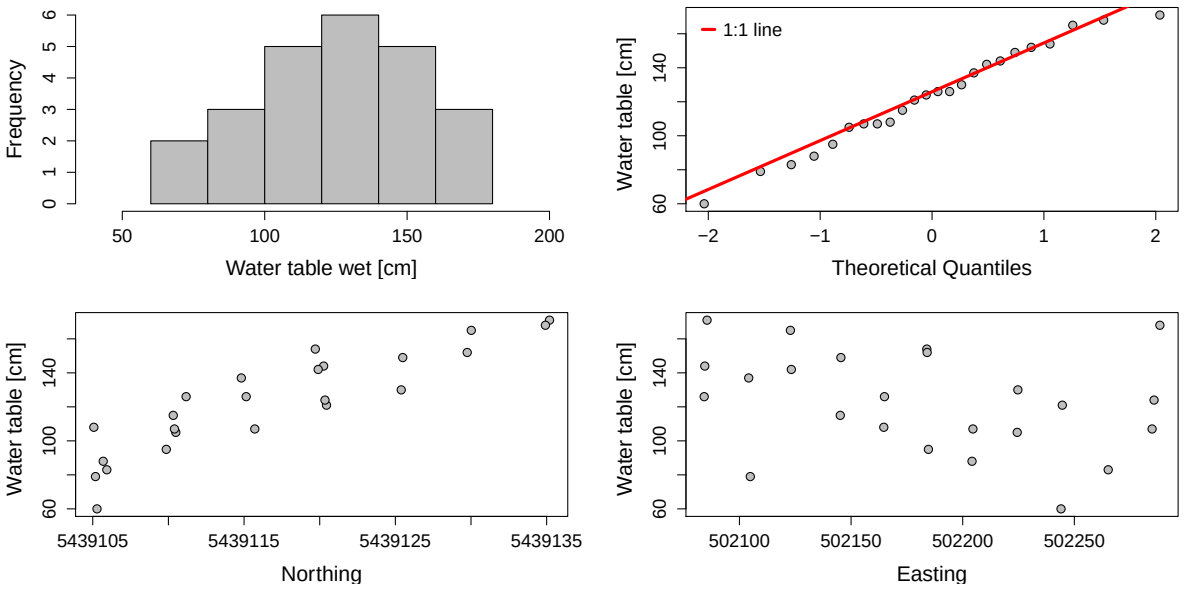

FIGURE A.7: Diagnostic plots of the water table input data, during the wet period. A gradient as in the soil surface plot is visible, when looking at the water level versus northing.

TABLE A.3: Basic statistics of the water table during dry and wet period at each location.

Location	Dry				Wet			
	Range [cm]	Mean [cm]	Variance [cm]	Sample no.	Range [cm]	Mean [cm]	Variance [cm]	Sample no.
1	5	-99.9	18.6	814	0.5	-49.5	0.2	15
2	3.7	-110.8	6.9	371				0
4	7.6	-95.1	13.2	82	2.3	-8.8	5.8	15
5	11	-78.4	143.7	814	0.8	-7.2	1.6	3
7	5.9	-92.3	38.4	576	4.1	-33.4	20	15
8	2.5	-97.9	4.8	733	2	-35.1	4.3	15
9	12.9	-88.8	87.6	785	0.6	-20.6	0.5	15
11	7.7	-124.7	33.7	814	2	-25.2	4.2	15
12	5.4	-87.7	20.5	814	3.7	-27.3	15.6	15
13	11.6	-95.8	113.4	814	3.9	-11.2	18.7	15
15	5.6	-94.7	23.8	814	2.7	-12.1	8.5	15
16	1.6	-75.6	3.6	121	1.3	-13.6	1.2	15
17	5.7	-111.4	31.6	814	1.1	-36.7	1.5	15
18	7.9	-106.1	65	814	3.1	-15.6	10.7	15
19	11.1	-71.8	140.3	728				0
20	13	-87.2	228.2	814	0.7	-33.7	0.7	15
21	4.5	-96.4	25.6	814	0.4	-28.3	0.3	15
22	12.2	-74.3	93.2	814	1.4	-4.6	2.9	15
23	5.9	-99.9	23.4	814	2.4	-31.6	6	15
24	1.8	-100.1	2	778	1.7	-23.2	3.3	15
25	7.1	-78.9	52.4	814	1.3	-20.5	1.8	15
26	9.9	-88.2	102.8	814	1.2	-29.5	1.3	15
27	11.4	-61.5	152.6	814	1	-1.9	1.3	15
28	18.2	-78.1	443.5	814	1.8	-22.9	4.4	15
29	5.2	-145.6	23.3	599				0
30	10.7	-63.5	143.7	814	0.4	-19.4	0.2	15
32	13.1	-95.8	224	814	2.2	-1.4	6.6	15

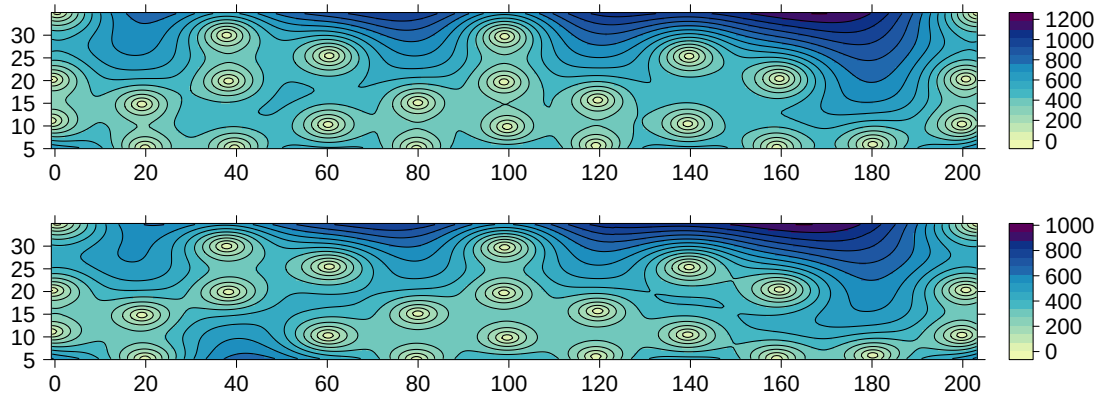

FIGURE A.8: Interpolation variance maps of the water table during dry conditions (top) and the water table during wet conditions (bottom) interpolation.

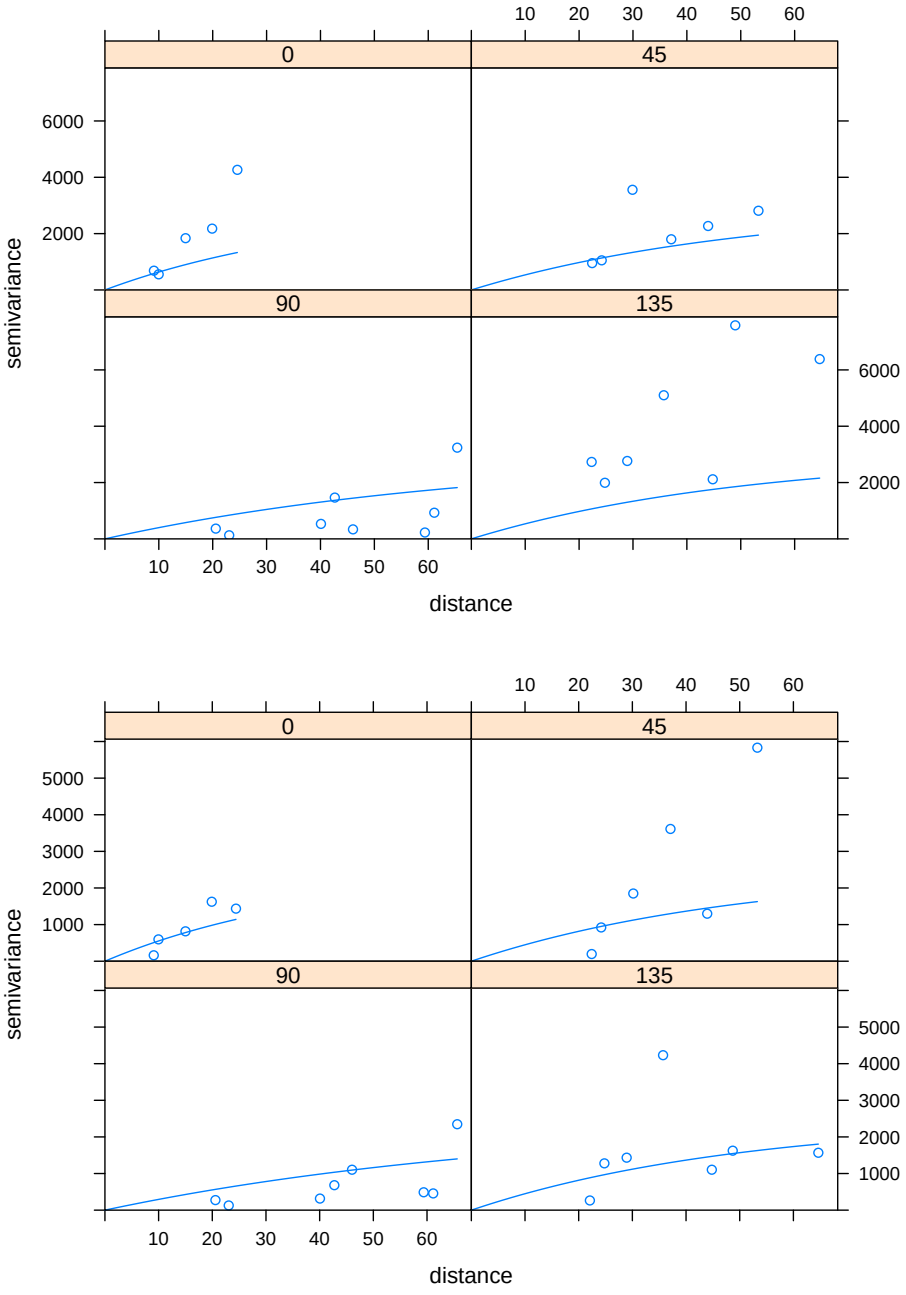

FIGURE A.9: Kriging variograms of the water table during dry conditions (top) and water table during wet conditions (bottom). The non-existent nugget effect is a sign for good data quality.

TABLE A.4: Target functions of the water table interpolation during dry and wet periods, respectively. Models marked with an * were manually fitted, the ones denoted with an ", were used to compute the maps.

Model	Mbe [cm]	Rmse [cm]	Mae [cm]	Nse
Dry				
Spherical	-0.01	38.19	32.6	-0.08
Exponential	0.01	37.86	32.24	-0.06
Gaussian	-0.01	38.1	32.55	-0.07
Linear	0.01	37.74	32.16	-0.05
Spherical Ground	0.21	21.34	16.47	0.66
Exponential Ground	0.23	21.33	16.45	0.66
Gaussian Ground	0.22	21.34	16.46	0.66
Linear Ground	0.22	21.33	16.48	0.66
Exponential* "	0.96	18.19	13.49	0.76
Linear ground*	-0.1	16.25	13.41	0.8
Wet				
Spherical	-0.01	30.22	24.8	-0.08
Exponential	0.02	29.5	24.06	-0.03
Gaussian	-0.02	30.09	24.63	-0.07
Linear	0.01	29.39	23.98	-0.02
Spherical Ground	-0.09	13.23	11.06	0.79
Exponential Ground	-0.08	13.21	11.04	0.79
Gaussian Ground	-0.08	13.23	11.06	0.79
Linear Ground	-0.09	13.25	11.08	0.79
Exponential* "	0.94	17.9	12.08	0.62
Linear ground*	-0.1	13.4	11.22	0.79

A.3 Groundwater flow analysis - horizontal flow

As mentioned before horizontal groundwater flow was found to be consistent in space and time. Because potentiometric maps were only presented from October 9, October 30 and December 4, Figure A.10 fills the time series gaps with weekly computed maps. As already described, horizontal flow always occurred towards the ditch.

A.4 Seepage

Figure A.11 presents time series seepage rates at the locations of permanent installation (19, 60, 100, 140 and 176). All time series measurements fluctuate below 15 $Lm^{-2}day^{-1}$, except for location 19, where rates of almost up to 50 $Lm^{-2}day^{-1}$ were reached between

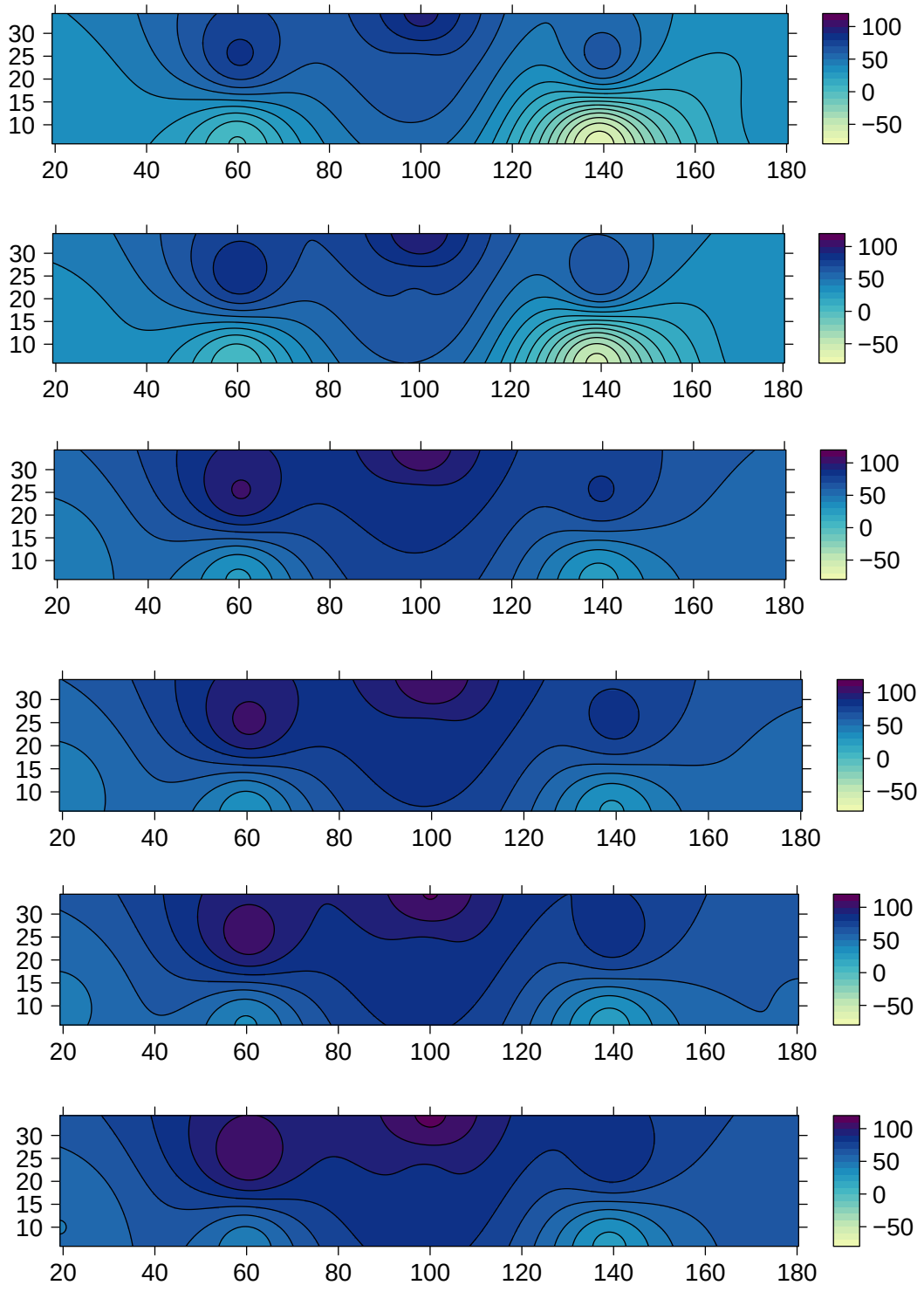

FIGURE A.10: The potentiometric maps fill in the gaps between the presented maps in the results secion of this work. They were computed for the following dates, from top to bottom: October 16, October 23, November 6, November 13, November 20, November 27.

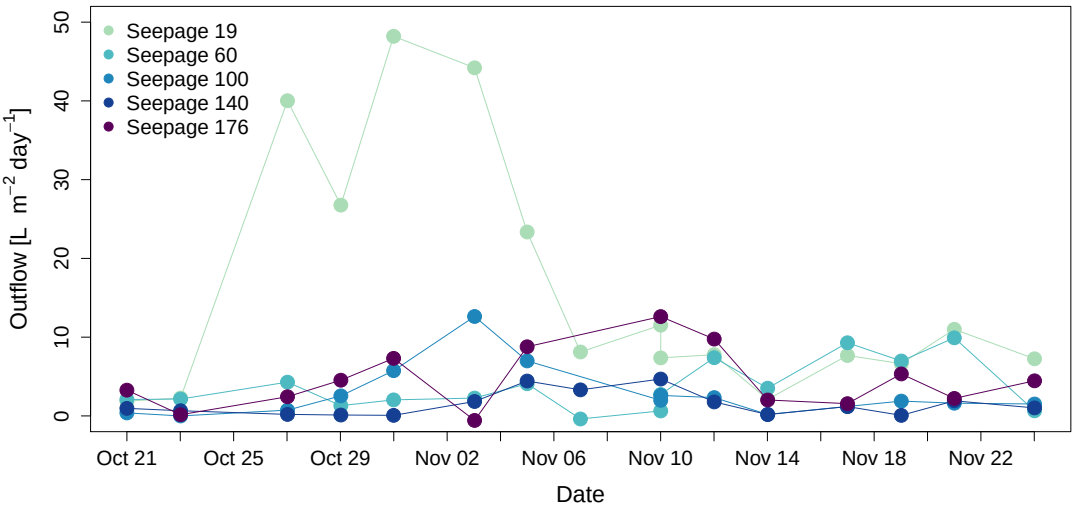

FIGURE A.11: Time series from the locations of permanent seepage meter installation (19, 60, 100, 140 and 176).

October 27 and November 5. It appears as if seepage varies throughout the site with no particular spatial pattern.

When comparing the time series with the total seepage rate for the entire site (Figure 3.15), several conformities can be found. On November 14 for example, total seepage, which includes data from the spatial measurements shows a low point, as do all permanently installed seepage meters. Two peaks in the time series at location 19 on October 27 and October 31 are also observable in Figure 3.15, but with a time lag of 2 and 5 days, respectively. The peak on November 10 in Figure 3.15, can be found in time series 176; the behavior after November 14 partly agrees with locations 19 and 60.

A.5 Lateral flow

Figure A.12 and A.13 display the temporal regime of all trough locations. The troughs were split into several plots, to preserve clarity and to be able to easily compare lateral flow of the same magnitude. Figure A.12 (top) shows troughs with a rather small runoff. Except for trough 180, all flows show a similar temporal regime. Especially locations 98 and 104, as well as 190 and 147 behave similar and therefore yield comparable runoff amounts. Figure A.12 (bottom) presents troughs with lateral flow between 0 and 900 $L\ day^{-1}$. At locations 55.5, 59 and 81 the temporal regimes are alike. Almost all troughs experience lower runoff on December 5 and most of the outflows increase from

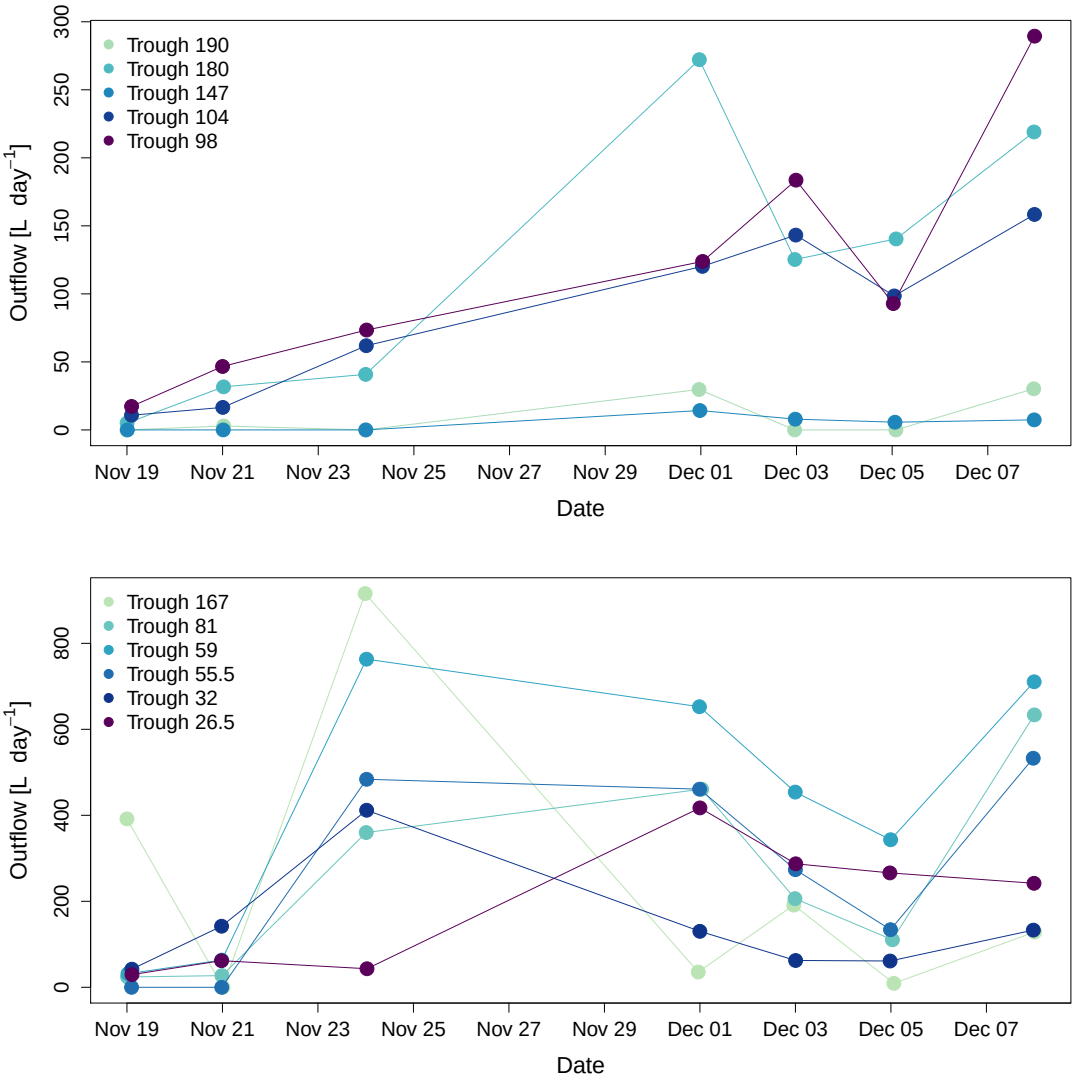

FIGURE A.12: Trough measurement time series of all measurements up to 900 $L day^{-1}$. The runoffs amounts were grouped, in order to provide clear view.

November 21 to November 24. Troughs with lateral flows of up to 4000 $L\,day^{-1}$ behave surprisingly consistent (Figure A.13 (top)). They agree with troughs in Figure A.12 (bottom) in that the runoff response from November 19 to November 24 is quite similar, but afterwards lateral flows increase further, contrasting to the troughs with less runoff volume. Finally Figure A.13 (bottom) presents trough locations 113, 122 and 184, which exhibit the strongest lateral outflow. Trough 113 sticks out in that it does not follow the temporal regime of the other two troughs, rather than showing a comparable response to trough 167 with much less lateral flow volume.

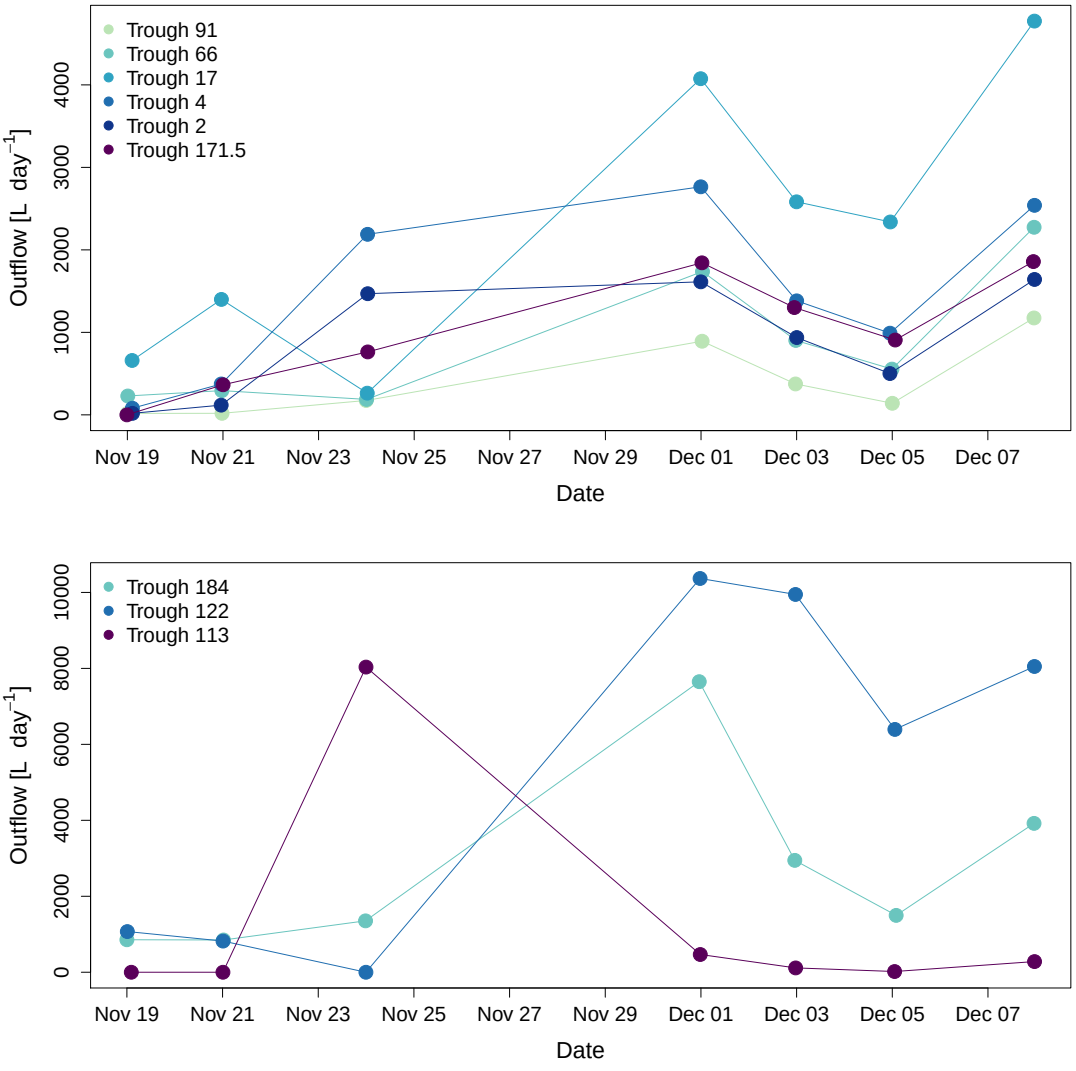

FIGURE A.13: Trough measurement time series of all measurements above 900 $Lday^{-1}$. The runoffs amounts were grouped, in order to provide clear view.

Bibliography

AR Anderson, D Ray, and DG Pyatt. Physical and hydrological impacts of blanket bog afforestation at bad a cheo, caithness: the first 5 years. *Forestry*, 73(5):467–478, 2000.

A Armstrong, J Holden, P Kay, M Foulger, S Gledhill, AT McDonald, and A Walker. Drain-blocking techniques on blanket peat: A framework for best practice. *Journal of Environmental Management*, 90(11):3512–3519, 2009.

TC Atkinson. Techniques for measuring subsurface flow on hillslopes. *Hillslope hydrology*, pages 73–120, 1978.

AJ Baird. Continuity in hydrological systems. *Contemporary hydrology: towards holistic environmental science (ed. R. Wilby)*, pages 25–58, 1997.

AJ Baird and SW Gaffney. A partial explanation of the dependency of hydraulic conductivity on positive pore water pressure in peat soils. *Earth Surface Processes and Landforms*, 20(6):561–566, 1995.

AJ Baird, PA Eades, and BWJ Surridge. The hydraulic structure of a raised bog and its implications for ecohydrological modelling of bog development. *Ecohydrology*, 1 (4):289–298, 2008.

J Balfour and L Banack. Burns bog ecosystem review - water chemistry, 2000.

CW Beckwith and AJ Baird. Effect of biogenic gas bubbles on water flow through poorly decomposed blanket peat. *Water Resources Research*, 37(3):551–558, 2001.

CW Beckwith, AJ Baird, and AL Heathwaite. Anisotropy and depth-related heterogeneity of hydraulic conductivity in a bog peat. i: laboratory measurements. *Hydrological processes*, 17(1):89–101, 2003.

I Blackwell. A hydrological study of the lagg zone of clara bog, county offaly, ireland. Master's thesis, 1992.

C Blodau and TR Moore. Macroporosity affects water movement and pore water sampling in peat soils. *Soil Science*, 167(2):98–109, 2002.

RA Bourbonniere. Review of water chemistry research in natural and disturbed peatlands. *Canadian water resources journal*, 34(4):393–414, 2009.

GEP Box and DR Cox. An analysis of transformations. *Journal of the Royal Statistical Society. Series B (Methodological)*, pages 211–252, 1964.

GEP Box and PW Tidwell. Transformation of the independent variables. *Technometrics*, 4(4):531–550, 1962.

OM Bragg. Hydrology of peat-forming wetlands in scotland. *Science of the Total Environment*, 294(1):111–129, 2002.

J Bromley, M Robinson, and JA Barker. Scale-dependency of hydraulic conductivity: an example from thorne moor, a raised mire in south yorkshire, uk. *Hydrological Processes*, 18(5):973–985, 2004.

TP Burt. *The hydrology of headwater catchments*, volume 1. Blackwell, 1992.

RH Byrd, P Lu, J Nocedal, and C Zhu. A limited memory algorithm for bound constrained optimization. *SIAM Journal on Scientific Computing*, 16(5):1190–1208, 1995.

YC Cheng. The ins and outs of burns bog: A water balance study. Master's thesis, 2011.

C. Chestnutt. For peat's sake: A comparison of the eddy covariance technique and semi-empirical calculation to determine summer evapotranspiration in burns bog, british columbia. Master's thesis, The University of Edinburgh, 2015.

TL Chow, HW Rees, I Ghanem, and R Cormier. Compactibility of cultivated sphagnum peat material and its influence on hydrologic characteristics. *Soil Science*, 153(4):300–306, 1992.

JJ Clague, JL Luternauer, PA Monahan, KA Edwardson, SR Dallimore, and JA Hunter. Quaternary stratigraphy and evolution of the fraser delta. *Bulletin - Geological Survey Of Canada*, pages 57–90, 1998.

RS Clymo. The limits to peat bog growth. *Philosophical Transactions of the Royal Society of London B: Biological Sciences*, 303(1117):605–654, 1984.

AM Cunliffe, AJ Baird, and J Holden. Hydrological hotspots in blanket peatlands: Spatial variation in peat permeability around a natural soil pipe. *Water Resources Research*, 49(9):5342–5354, 2013.

AWH Damman. Hydrology, development, and biogeochemistry of ombrogenous peat bogs with special reference to nutrient relocation in a western newfoundland bog. *Canadian Journal of Botany*, 64(2):384–394, 1986.

SM Daniels, CT Agnew, TEH Allott, and MG Evans. Water table variability and runoff generation in an eroded peatland, south pennines, uk. *Journal of Hydrology*, 361(1): 214–226, 2008.

DataflowSystems. *Odyssey Capacitive Water Level Logger*. Dataflow Systems PTY Ltd, 2013.

LA Emili and JS Price. Hydrological processes controlling ground and surface water flow from a hypermaritime forest–peatland complex, diana lake provincial park, british columbia, canada. *Hydrological processes*, 20(13):2819–2837, 2006.

EnvironmentCanada. Daily data report for 2014, richmond nature park, british columbia, accessed, July 2014. URL `http://climate.weather.gc.ca/climateData/dailydata_e.html?timeframe=2&Prov=BC&StationID=837&dlyRange=1977-03-01|2015-06-20&Year=2014&Month=6&cmdB1=Go#`.

MG Evans, TP Burt, J Holden, and JK Adamson. Runoff generation and water table fluctuations in blanket peat: evidence from uk data spanning the dry summer of 1995. *Journal of Hydrology*, 221(3):141–160, 1999.

E Fay and C Lavoie. The impact of birch seedlings on evapotranspiration from a mined peatland: an experimental study in southern quebec, canada. *Mires and Peat*, 5:1–7, 2009.

CJD Fraser, NT Roulet, and M Lafleur. Groundwater flow patterns in a large peatland. *Journal of Hydrology*, 246(1):142–154, 2001.

F Freléchoux, A Buttler, FH Schweingruber, and JM Gobat. Stand structure, invasion, and growth dynamics of bog pine (pinus uncinata var. rotundata) in relation to peat

cutting and drainage in the jura mountains, switzerland. *Canadian Journal of Forest Research*, 30(7):1114–1126, 2000.

RO Gilbert. *Statistical methods for environmental pollution monitoring*. John Wiley & Sons, 1987.

PH Glaser, DI Siegel, EA Romanowicz, and YP Shen. Regional linkages between raised bogs and the climate, groundwater, and landscape of north-western minnesota. *Journal of Ecology*, pages 3–16, 1997.

GK Golinksi. *Mires of Vancouver Island, British Columbia: vegetation classification and differences between disturbed and undistrubed mires*. PhD thesis, 2004.

JW Harvey, SL Krupa, CJ Gefvert, C Jungyill, RH Mooney, and JB Giddings. Interaction between ground water and surface water in the northern everglades and relation to water budget and mercury cycling; study methods and appendixes. Technical report, US Department of the Interior, US Geological Survey; Branch of Information Services [distributor],, 2000.

RJ Hebda, K Gustavson, K Golinski, and Calder AM. Burns bog ecosystem review, 2000.

Heron. *Dipper-T Water Level Meter*. Heron Instruments Inc., 2015.

P Hiemstra. *Automatic interpolation package*, 2013.

NB Hobbs. Mire morphology and the properties and behaviour of some british and foreign peats. *Quarterly Journal of Engineering Geology and Hydrogeology*, 19(1): 7–80, 1986.

J Holden. Peatland hydrology and carbon release: why small-scale process matters. *Philosophical Transactions of the Royal Society of London A: Mathematical, Physical and Engineering Sciences*, 363(1837):2891–2913, 2005a.

J Holden. Controls of soil pipe frequency in upland blanket peat. *Journal of Geophysical Research: Earth Surface (2003–2012)*, 110(F1), 2005b.

J Holden. Flow through macropores of different size classes in blanket peat. *Journal of Hydrology*, 364(3):342–348, 2009.

J Holden and TP Burt. Piping and pipeflow in a deep peat catchment. *Catena*, 48(3): 163–199, 2002a.

J Holden and TP Burt. Laboratory experiments on drought and runoff in blanket peat. *European Journal of Soil Science*, 53(4):675–690, 2002b.

J Holden and TP Burt. Hydrological studies on blanket peat: the significance of the acrotelm-catotelm model. *Journal of Ecology*, 91(1):86–102, 2003a.

J Holden and TP Burt. Hydraulic conductivity in upland blanket peat: measurement and variability. *Hydrological Processes*, 17(6):1227–1237, 2003b.

J Holden and TP Burt. Runoff production in blanket peat covered catchments. *Water Resources Research*, 39(7), 2003c.

J Holden, TP Burt, and NJ Cox. Macroporosity and infiltration in blanket peat: the implications of tension disc infiltrometer measurements. *Hydrological Processes*, 15 (2):289–303, 2001.

J Holden, PJ Chapman, and JC Labadz. Artificial drainage of peatlands: hydrological and hydrochemical process and wetland restoration. *Progress in Physical Geography*, 28(1):95–123, 2004.

SA Howie and HJ van Meerveld. The essential role of the lagg in raised bog function and restoration: a review. *Wetlands*, 31(3):613–622, 2011.

SA Howie and HJ van Meerveld. Temporal variation in depth to water table and hydrochemistry in three raised bogs and their laggs in coastal british columbia, canada. *Hydrology and Earth System Sciences Discussions*, 9(12):14065–14107, 2012.

SA Howie and HJ van Meerveld. Regional and local patterns in depth to water table, hydrochemistry and peat properties of bogs and their laggs in coastal british columbia. *Hydrology and Earth System Sciences*, 17(9):3421–3435, 2013.

SA Howie, Whitfield PH, Hebda RJ, Dakin RA, and Jeglum JK. Can analysis of historic lagg forms be of use in the restoration of highly altered raised bogs? examples from burns bog, british columbia. *Canadian Water Resources Journal*, 34(4):427–440, 2009a.

SA Howie, PH Whitfield, RJ Hebda, TG Munson, RA Dakin, and JK Jeglum. Water table and vegetation response to ditch blocking: restoration of a raised bog in southwestern british columbia. *Canadian Water Resources Journal*, 34(4):381–392, 2009b.

PDM Hughes and KE Barber. Mire development across the fen–bog transition on the teifi floodplain at tregaron bog, ceredigion, wales, and a comparison with 13 other raised bogs. *Journal of Ecology*, 91(2):253–264, 2003.

DG Hutchinson and RD Moore. Throughflow variability on a forested hillslope underlain by compacted glacial till. *Hydrological processes*, 14(10):1751–1766, 2000.

JN Hutchinson. The record of peat wastage in the east anglian fenlands at holme post, 1848-1978 ad. *The Journal of Ecology*, pages 229–249, 1980.

MJ Hvorslev. Time lag and soil permeability in ground-water observations. *Waterway Experiments*, 36:1–50, 1951.

HAP Ingram. *Hydrology: Ecosystems of the World 4A, Mires: Swamp, Bog, Fen and Moor*. Oxford: Elsevier, 1983.

KE Ivanov. Filtration in the top layer of convex mire massifs. *Meteorologiya. L Gidrologiya*, 2:46–59, 1948.

JK Jeglum, HM Kershaw, DM Morris, and DA Cameron. *Best forestry practices: a guide for the boreal forest in Ontario*. [Sault Ste. Marie, Ont.]: Canada-Ontario Memorandum of Understanding for Cooperation in Forestry, 2003.

AG Journel and ME Rossi. When do we need a trend model in kriging? *Mathematical Geology*, 21(7):715–739, 1989.

S Jutras, AP Plamondon, H Hökkä, and J Bégin. Water table changes following precommercial thinning on post-harvest drained wetlands. *Forest ecology and management*, 235(1):252–259, 2006.

S Jutras, AN Rousseau, and C Clerc. Implementation of a peatland-specific water budget algorithm in hydrotel. *Canadian Water Resources Journal*, 34(4):349–364, 2009.

CD Kennedy, LC Murdoch, DP Genereux, DR Corbett, K Stone, P Pham, and H Mitasova. Comparison of darcian flux calculations and seepage meter measurements in

a sandy streambed in north carolina, united states. *Water Resources Research*, 46(9), 2010.

JP Keough and Pippen RW. The movement of water from peatland into surrounding groundwater. *Canadian Journal of Botany*, 62:835–839, 1984.

BJ Kopp, JH Fleckenstein, NT Roulet, E Humphreys, J Talbot, and C Blodau. Impact of long-term drainage on summer groundwater flow patterns in the mer bleue peatland, ontario, canada. *Hydrology and Earth System Sciences*, 17(9):3485–3498, 2013.

SL Krupa, TV Belanger, HH Heck, JT Brock, and BJ Jones. Krupaseep—the next generation seepage meter. *Journal of Coastal Research*, pages 210–213, 1998.

J Kværner and B Kløve. Generation and regulation of summer runoff in a boreal flat fen. *Journal of Hydrology*, 360(1):15–30, 2008.

Matthew K Landon, David L Rus, and F Edwin Harvey. Comparison of instream methods for measuring hydraulic conductivity in sandy streambeds. *Groundwater*, 39 (6):870–885, 2001.

DR Lapen, JS Price, and R Gilbert. Modelling two-dimensional steady-state groundwater flow and flow sensitivity to boundary conditions in blanket peat complexes. *Hydrological Processes*, 19(2):371–386, 2005.

Leica. *Leica TPS 800 Series*. Leica Geosystems, 2015.

MG Letts, NT Roulet, NT Comer, MR Skarupa, and DL Verseghy. Parametrization of peatland hydraulic properties for the canadian land surface scheme. *Atmosphere-Ocean*, 38(1):141–160, 2000.

G Levrel, AN Rousseau, P Lafrance, S Jutras, C Clerc, PH Whitfield, G Kamp, and A St-Hilaire. Characterization of water retention and hydraulic conductivity in boreal soils of the james bay region: presentation of an experimental protocol and preliminary results. *Canadian Water Resources Journal*, 34(4):329–348, 2009.

John B Lewis. Measurements of groundwater seepage flux onto a coral reef: spatial and temporal variations. *Limnology and Oceanography*, 32(5):1165–1169, 1987.

Maurice A Lock and Peter H John. The measurement of groundwater discharge into a lake by a direct method. *Internationale Revue der gesamten Hydrobiologie und Hydrographie*, 63(2):271–275, 1978.

D R Maidment et al. *Handbook of hydrology.* McGraw-Hill Inc., 1992.

N Malmer. Vegetational gradients in relation to environmental conditions in northwestern european mires. *Canadian Journal of Botany*, 64(2):375–383, 1986.

McElhanney. Topographic map of burns bog, 1999.

J Muller, RAJ Wüst, D Weiss, and Y Hu. Geochemical and stratigraphic evidence of environmental change at lynch's crater, queensland, australia. *Global and planetary change*, 53(4):269–277, 2006.

National Wetlands Working Group NWWG. *Wetlands of Canada, Ecological Land Classification Series, No. 24, Sustainable Development Branch.* Environment Canada, Ottawa, Ontario and Polyscience Publications Inc. Montréal, QC, 1988.

RH Økland, T Økland, and K Rydgren. A scandinavian perspective on ecological gradients in north-west european mires: reply to wheeler and proctor. *Journal of Ecology*, 89(3):481–486, 2001.

H Osvald. Vegetation of the pacific coast bogs of north america. *Acta Phytogeogr Suec*, pages 1–32, 1933.

RJ Paulsen, CF Smith, D O'Rourke, and T-F Wong. Development and evaluation of an ultrasonic ground water seepage meter. *Groundwater*, 39(6):904–911, 2001.

E Pebesma and B Graeler. *Spatial and Spatio-Temporal Geostatistical Modelling, Prediction and Simulation*, 2015.

E Pebesma, R Biwand, B Rowlingson, V Gomez-Rubio, R Hijmans, M Sumner, D MacQueen, and J O'Brien. *Classes and Methods for Spatial Data*, 2015.

JS Price. Blanket bog in newfoundland. part 2. hydrological processes. *Journal of Hydrology*, 135(1):103–119, 1992.

JS Price. Role and character of seasonal peat soil deformation on the hydrology of undisturbed and cutover peatlands. *Water Resources Research*, 39(9), 2003.

JS Price, AL Heathwaite, and AJ Baird. Hydrological processes in abandoned and restored peatlands: an overview of management approaches. *Wetlands Ecology and Management*, 11(1-2):65–83, 2003.

Random.org. True random number service, accessed, August 2014. URL `https://www.random.org/`.

AS Reeve, DI Siegel, and PH Glaser. Simulating vertical flow in large peatlands. *Journal of Hydrology*, 227(1):207–217, 2000.

AS Reeve, R Evensen, PH Glaser, DI Siegel, and D Rosenberry. Flow path oscillations in transient ground-water simulations of large peatland systems. *Journal of hydrology*, 316(1):313–324, 2006.

DO Rosenberry and RH Morin. Use of an electromagnetic seepage meter to investigate temporal variability in lake seepage. *Groundwater*, 42(1):68–77, 2004.

DO Rosenberry, JW LaBaugh, and RJ Hunt. Use of monitoring wells, portable piezometers, and seepage meters to quantify flow between surface water and ground water. *Field techniques for estimating water fluxes between surface water and ground water. US Geological Survey Techniques and Methods*, pages 4–D2, 2008.

V Roy, AP Plamondon, and P-Y Bernier. Influence of vegetation removal and regrowth on interception and water table level on wetlands. *International Peat Journal*, 10: 3–12, 2000.

JA Ryan and Ulrich JM. *eXtensible Time Series*, 2013.

H Rydin and JK Jeglum. *The biology of peatlands*. Oxford university press, 2013.

H Rydin, H Sjörs, and M. Lofroth. *Swedish Plant Geography*, volume 84. Acta Phztogeogr. Suec., 1999.

MGC Schouten. *Conservation and restoration of raised bogs: geological, hydrological and ecological studies*. The Government Stationary Office, 2002.

W Shotyk. Peat bog archives of atmospheric metal deposition: geochemical evaluation of peat profiles, natural variations in metal concentrations, and metal enrichment factors. *Environmental Reviews*, 4(2):149–183, 1996.

T Tahvanainen. Water chemistry of mires in relation to the poor-rich vegetation gradient and contrasting geochemical zones of the north-eastern fennoscandian shield. *Folia Geobotanica*, 39(4):353–369, 2004.

M Taniguchi and Y Fukuo. Continuous measurements of ground-water seepage using an automatic seepage meter. *Groundwater*, 31(4):675–679, 1993.

C Tarnocai, IM Kettles, and Lacelle B. Peatlands of canada database. agriculture and agri-food canada, research branch, ottawa, canada, 2005.

L vonPost. Das genetische system der organogenen bildungen schwedens. *Memoires sur la nomenclature et la classification des sols*, pages 287–304, 1924.

ZE Wallage and J Holden. Near-surface macropore flow and saturated hydraulic conductivity in drained and restored blanket peatlands. *Soil Use and Management*, 27 (2):247–254, 2011.

BD Wheeler and Shaw SC. Resoration of damaged peatlands with particular reference to lowland raised bogs affected by peat extraction. *HMSO, London*, 1995.

PH Whitfield, RJ Hebda, JK Jeglum, and SA Howie. Restoring the natural hydrology of burns bog, delta, british columbia - the key to the bog's ecological revcovery. In *Water under Pressure*, pages 58–70. Chantler A., 2006.

PH Whitfield, G van der Kamp, and A St-Hilaire. Introduction to peatlands special issue: improving hydrological prediction in canadian peatlands. *Canadian Water Resources Journal*, 34(4):303–310, 2009.

WTW. *TetraCon 325 - Standard conductivity cell.* WTW - Wissenschaftlich-Technische Werkstaetten GmbH, 2005.

WTW. *Handheld meter Cond 340i - Conductivity measuring instrument.* WTW - Wissenschaftlich-Technische Werkstaetten GmbH, 2008.

Ryan J.A. Andrews F. Zeileis A., Grothendieck G. *S3 Infrastructure for Regular and Irregular Time Series (Z's Ordered Obsercations)*, 2015.